IDENTIFICATION AND CHARACTERIZATION OF NOVEL MECHANISMS OF FUNCTIONAL AND STRUCTURAL SYNAPSE REMODELING: FOCUS ON VAV GUANINE NUCLEOTIDE EXCHANGE FACTORS AND MEF2 TRANSCRIPTION FACTORS

APPROVED BY SUPERVISORY COMMITTEE

Christopher W. Cowan, Ph.D. (Supervisor)

Carla B. Green, Ph.D.

Kimberly M. Huber, Ph.D. (Chair)

Tae-Kyung Kim, Ph.D.

DEDICATION

For Luke and William.

IDENTIFICATION AND CHARACTERIZATION OF NOVEL MECHANISMS OF FUNCTIONAL AND STRUCTURAL SYNAPSE REMODELING: FOCUS ON VAV GUANINE NUCLEOTIDE EXCHANGE FACTORS AND MEF2 TRANSCRIPTION FACTORS

by

CARLY FENWICK HALE

DISSERTATION

Presented to the Faculty of the Graduate School of Biomedical Sciences

The University of Texas Southwestern Medical Center at Dallas

In Partial Fulfillment of the Requirements

For the Degree of

DOCTOR OF PHILOSOPHY

The University of Texas Southwestern Medical Center

Dallas, Texas

August, 2014

IDENTIFICATION AND CHARACTERIZATION OF NOVEL MECHANISMS OF FUNCTIONAL AND STRUCTURAL SYNAPSE REMODELING: FOCUS ON VAV GUANINE NUCLEOTIDE EXCHANCE FACTORS AND MEF2 TRANSCRIPTION FACTORS

CARLY FENWICK HALE, Ph.D.

The University of Texas Southwestern Medical Center at Dallas, 2014

CHRISTOPHER W. COWAN, Ph.D.

Proper development of synaptic connectivity is a dynamic process requiring formation, elimination, maintenance, and plasticity of synapses. During early postnatal development, excess synapses are formed in most neural circuits, which are subsequently pruned during adolescence in a sensory- and activity-dependent mechanism. The brain also exhibits experience-dependent synaptic modifications that may enhance or weaken functional synapse strength.

Investigation of numerous neurodevelopmental and psychiatric disorders reveals dysfunctions in synapse formation and function; however, underlying molecular mechanisms remain poorly understood.

In Part One of this study, I identify a novel role for Vav guanine nucleotide exchange factors (GEFs) in brain-derived neurotrophic factor (BDNF)-dependent synapse plasticity. BNDF and its receptor, TrkB, are well-established positive modulators of hippocampal long-term potentiation (LTP), and increasing evidence suggests that BDNF/TrkB facilitates LTP in part through the stimulation of Rho GTPases and subsequent F-actin remodeling and dendritic spine structural dynamics. I report that Vav-family GEFs are activated by BDNF/TrkB signaling, and are required for BDNF-induced Rac-GTP formation. Vav GEFs, which are enriched at hippocampal glutamatergic synapses, are necessary for rapid BDNF-induced dendritic spine growth and CA3-CA1 LTP. Furthermore, Vav2/3-deficient mice have impaired contextual fear conditioning, as well as reduced anxiety. Together, findings support a role for Vav-dependent F-actin dynamics in BDNF-stimulated dendritic spine head enlargement and LTP, and normal hippocampal-dependent learning and memory and anxiety in mice.

Part Two of this study reports the identification of common MEF2 and FMRP mRNA targets that are required for MEF2-induced synapse elimination. The activity-dependent transcription factor myocyte enhancer factor 2 (MEF2) is a key negative regulator of excitatory synapse number, promoting synapse

removal in neurons through a complex program of gene expression. The RNA binding protein and translational regulator fragile X mental retardation protein (FMRP) was recently identified as an essential downstream component of MEF2-induced synapse elimination, suggesting that these autism-linked proteins coordinate transcriptional and translational control of common transcripts to mediate proper synaptic connectivity. Using high throughput sequencing of RNA isolated by cross-linking immunoprecipitation (HITS-CLIP) of FMRP, I find a large overlap of MEF2-induced transcripts and FMRP-associated mRNAs, consistent with their shared roles in synapse elimination. More specifically, protocadherin 17 (Pcdh17) mRNA is induced by MEF2 and exhibits differential binding to FMRP following MEF2 activation. Reducing Pcdh17 alone does not alter basal synapse number, but reducing Pcdh17 levels blocks MEF2-induced dendritic spine elimination of hippocampal neurons. These data suggest that MEF2-induced synapse elimination requires Pcdh17 – a MEF2 target gene and FMRP-associated transcript.

TABLE OF CONTENTS

PRIOR PUBLICATIONS

Smith, L.N., Jedynak, J.P., Fontenot, M.R., **Hale, C.F.**, Dietz, K.C., Taniguchi, M. Thomas, F.S., Zirlin, B.C., Birnbaum, S.G., Huber, K.M., Thomas, M.J., and Cowan, C.W. (2014). Fragile X mental retardation protein regulates synaptic and behavioral plasticity to repeated cocaine administration. Neuron *82*, 645-658.

Hale, C.F., Dietz, K.C., Varela, J.A., Wood, C.B., Zirlin, B.C., Leverich, L.S., Greene, R.W., and Cowan, C.W. (2011). Essential role for Vav guanine nucleotide exchange factors in brain-derived neurotrophic factor-induced dendritic spine growth and synapse plasticity. J Neurosci *31*, 12426-12436.

Meyer, D.A., Richer, E., Benkovic, S.A., Hayashi, K., Kansy, J.W., **Hale, C.F.**, Moy, L.Y., Kim, Y., O'Callaghan, J.P., Tsai, L.H., Greengard, P., Nairn, A.C., Cowan, C.W., Miller, D.B., Antich, P., and Bibb, J.A. (2008). Striatal dysregulation of Cdk5 alters locomotor responses to cocaine, motor learning, and dendritic morphology. Proc Natl Acad Sci U S A *105*, 18561-18566.

Cowan, C.W., Taniguchi, M., and **Hale, C.F.** (2008). Regulation of synaptic connectivity with chronic cocaine. Am J Psychiatry *165*, 1393.

Pulipparacharuvil, S., Renthal, **Hale, C.F.**, Taniguchi, M., Xiao, G., Kumar, A., Russo, S.J., Sikder, D., Dewey, C.M., Davis, M.M., Greengard, P., Nairn, A.C., Nestler, E.J., and Cowan, C.W. (2008). Cocaine regulates MEF2 to control synaptic and behavioral plasticity. Neuron *59*, 621-633.

LIST OF FIGURES

LIST OF TABLES

LIST OF ABBREVIATIONS

AMPA – α-amino-3-hydroxy-5-methyl-4-isoxazolepropionic acid

BDNF – brain-derived neurotrophic factor

CaMK – calcium/calmodulin-dependent protein kinase

CBP – CREB-binding protein

Cdk5 – cyclin-dependent kinase 5

cDNA – complementary DNA

CPP – condition placed preference

CREB – cAMP response element-binding protein

CtBP – C-terminal binding protein

DH – Dibble homology

DIV – days *in vitro*

DKO – double knockout

DNA – deoxyribonucleic acid

EPSC – excitatory postsynaptic current

EPSP – excitatory postsynaptic potential

ERK – extracellular signal-related kinase

F-actin – filamentous actin

fEPSP – field excitatory postsynaptic potential

FGF – fibroblast growth factor

FMRP – fragile X mental retardation protein

FXS – fragile X syndrome

GAP – GTPase activating protein

GEF – guanine nucleotide exchange factor

GFP – green fluorescent protein

GST-PBD – glutathione S-transferase PAK1 p21-binding domain

GWAS – genome wide association study

HAT – histone acetyl transferase

HDAC – histone deacetylase

HITS-CLIP – high throughput sequencing of RNA isolated by cross-linking immunoprecipitation

HP1 – heterochromatin protein 1

IEI – inter-event interval

IP3 – inositol 1,4,5-triphosphate

IPSC – inhibitory postsynaptic current

KH – K homology

KO – knockout

LTP – long-term potentiation

MADS – minichromosome maintenance 1-agamous-deficiens-serum

MAPK – mitogen-activated protein kinase

MEF2 – myocyte enhancer factor 2

MeCP2 – methyl-CpG binding protein 2

mEPSC – miniature excitatory postsynaptic current

mGluR – metabotropic glutamate receptor

MSN – medium spiny neuron

NAc – nucleus accumbens

NMDA – N-methyl-D-aspartate

PCDH - protocadherin

PCR – polymerase chain reaction

PH – pleckstrin homology

PI3-K – phosphatidylinositol 3-kinase

PLC – phospholipase C

PPI – prepulse inhibition

PSD – postsynaptic density

qRT-PCR – quantitative real-time reverse transcription PCR

RNA – ribonucleic acid

RNAi – RNA interference

SH2 – Src homology 2

SH3 – Src homology 3

SNP – single nucleotide polymorphism

SUMO – small ubiquitin-like modifier

TAD – transcriptional activation domain

TBS – theta burst stimulus

TrkA – tropomyosin-related kinase A

TrkB – tropomyosin-related kinase B

VTA – ventral tegmental area

WAVE – WASP family verprolin homologous protein

WIRS – WRC interacting receptor sequence

WRC – WAVE regulatory complex

WT – wild-type

ZF – zinc finger

CHAPTER ONE

Introduction

PART ONE: Brain-derived Neurotrophic Factor (BDNF) Regulates Synapse and Behavioral Plasticity through a Complex Signaling Network

The neurotrophin brain-derived neurotrophic factor (BDNF) is a well-established regulator of dendritic spine structural and functional synapse plasticity, as well as behavioral plasticity in animal models. Several studies reveal a complex and incompletely understood network of signaling mechanisms by which BDNF and its high affinity receptor, tropomycin-related kinase B (TrkB) control these plasticity events. As BDNF has been implicated in numerous neurodevelopmental disorders, as well as in diseases characterized by long-lasting behavioral changes, including anxiety, schizophrenia, and addiction to drugs of abuse, understanding the many aspects of BDNF/TrkB's functions in neurons will be of significant importance towards gaining insight into understanding the molecular and cellular underpinnings of these and related disorders.

BDNF/TrkB controls synapse plasticity through the activation of prominent signaling cascades in neurons

The neurotrophin BDNF and its cognate receptor TrkB are well-established regulators of critical synapse plasticity events, including long-term potentiation (LTP), dendritic spine number, and dendritic spine size. BDNF/TrkB signaling regulates these processes through the activation of four major signaling cascades: the PLCγ (phospholipase C γ), MAPK (mitogen-activated protein kinase), PI3-K (phosphoinositide 3-kinase), and Rho GTPase pathways (Kaplan and Miller, 2000). *In vivo*, BDNF exists as a non-covalent homodimer, and binding of the neurotrophin to the TrkB receptor induces receptor dimerization, following by activation of TrkB's intrinsic kinase activity (Cunningham and Greene, 1998). The receptors then phosphorylate each other in *trans*, which has the effect of enhancing their kinase activities.

The TrkB receptor has several conserved autophosphorylated tyrosines, three of which are found in the activation loop of the kinase domain and are critical for full kinase activity (Y670, Y674, and Y675) (Kaplan and Miller, 2000). Well-studied autophosphorylated tyrosines that are required for the activation of specific downstream pathways and have critical functional roles include Y785, the site at which PLCγ binds, and Y490, the Shc/Frs2 binding site leading to downstream activation of PI3-K and MAPK pathways (Kaplan and Miller, 2000). A fourth pathway activated by BDNF/TrkB signaling is Rho

GTPase family members, critical regulators of the actin cytoskeleton (Kaplan and Miller, 2000; Luo, 2002; Tashiro and Yuste, 2004). BDNF/TrkB induces activation of the Rho GTPases Rac and Cdc42, proteins that are associated with the formation of dendritic spines, as well as in growth of existing dendritic spines (Nakayama et al., 2000; Tashiro et al., 2000).

BDNF/TrkB regulates hippocampal CA3-CA1 LTP

Numerous studies link BDNF/TrkB with regulation of hippocampal CA3-CA1 early (E)- and late (L)-phases of LTP, the widely hypothesized functional correlate of learning and memory. *Trkb*- and *Bdnf*-null and conditional knockout mice have dramatically reduced theta burst- and tetanus-induced hippocampal CA3-CA1 LTP (Korte et al., 1995; Minichiello et al., 1999; Pozzo-Miller et al., 1999). Consistent with these observations, stimulation of hippocampal neurons with exogenous BDNF results in enhanced tetanus-induced LTP in a TrkB kinase-dependent manner (Rex et al., 2007). Furthermore, LTP deficits observed in BDNF knockout mice can be rescued by prolonged incubation with exogenous BDNF (2-4 hours) (Patterson et al., 1996), or by infection with a BDNF-expressing adenovirus (Korte et al., 1996), indicating that the absence of BDNF, and not cumulative deficits formed developmentally, is likely responsible for reduced LTP. It is important to note that several groups observe that exogenous BDNF is not sufficient to induce LTP (Gartner and Staiger, 2002; Hale et al.,

2011), suggesting a permissive action in allowing for LTP induction and maintenance, but indicating an absolute requirement for activity-dependent events for normal LTP.

BDNF/TrkB facilitates LTP through pre- and postsynaptic mechanisms

A considerable debate in the BDNF/TrkB field has been the uncertainty of the site of BDNF's action and whether TrkB functions pre- or postsynaptically to modulate E- or L-LTP in the hippocampus. Most findings from studies aimed at addressing this question have concluded that a combination of pre- and postsynaptic TrkB together mediate effects on synaptic plasticity. Presynaptically, BDNF/TrkB-stimulated MAPK induces the phosphorylation of synapsin-1, causing vesicle detachment and an increased probability of exocytosis (Jovanovic et al., 1996; Jovanovic et al., 2000). Additionally, BDNF/TrkB enhances neurotransmitter release by triggering the ERK2-dependent phosphorylation of RIM1α, a protein necessary for L-LTP (Huang et al., 2005; Simsek-Duran and Lonart, 2008).

At the complementary postsynaptic site, BDNF stimulates the phosphorylation of N-methyl-D-aspartate (NMDA) receptor subunits NR1 and NR2B, which has been demonstrated to potentiate NMDA receptor currents (Suen et al., 1997; Wang and Salter, 1994). AMPA (α-amino-3-hydroxy-5-methyl-4-isoxazolepropionic acid) receptor trafficking into the synaptic plasma membrane

is also essential for LTP, and there is evidence that BDNF promotes the delivery of the GluA1 subunit to synapses in a mechanism that remains to be determined (Caldeira et al., 2007; Minichiello, 2009).

Application of exogenous BDNF in hippocampal slices facilitates L-LTP, a plasticity event that requires local protein synthesis in dendrites (Kang and Schuman, 1996). Investigations into mechanisms underlying BDNF/TrkB-regulated L-LTP find that BDNF can stimulate the synthesis of several dendritic proteins by facilitating trafficking of dendritic mRNAs (Righi et al., 2000). Additionally, BDNF increases the translation of existing dendritic mRNAs by de-repressing RNA granules, activating translation initiation factors, and modulating elongation factors (Kanhema et al., 2006; Shiina et al., 2005; Takei et al., 2001; Zeitelhofer et al., 2008). Numerous BDNF-induced proteins involved in L-LTP have already been identified, and include Arc, CaMKIIα, and CREB (Shiina et al., 2005; Yin et al., 2002).

Together, these data indicate that BDNF/TrkB regulates LTP via pre- and post-synaptic mechanisms that promote both fast-acting and long-lasting synaptic transmission. Furthermore, these studies provide some important, although limited insight into the TrkB-dependent signaling cascades through which the receptor potently regulates LTP. Additional pharmacological and genetic analyses offer more detailed information regarding the downstream signaling mechanisms effecting plasticity changes.

Analysis of BDNF/TrkB-dependent signaling cascades that mediate LTP

Although BDNF/TrkB are well-established positive modulators of hippocampal CA3-CA1 LTP, the downstream signaling mechanisms mediating this functional plasticity event are not clearly understood. Pharmacological analyses describe an essential role for BDNF-induced CaMKII activation in LTP, which in turn phosphorylates AMPA receptors, leading to increased channel conductance of GluA1 subunits (Adams and Sweatt, 2002; Citri and Malenka, 2008; Ying et al., 2002). CaMKII also has a role in stimulating the exocytosis of AMPA receptors, increasing the number of receptors at the synapse (Lisman et al., 2012). Additional studies implicate the MAPK pathway that results in activation of ERK1-ERK2, as the presence of MEK (MAPK/ERK kinase) inhibitors abolished induction of LTP induced by exogenous BDNF (Adams and Sweatt, 2002; Ying et al., 2002). Mechanistically, these studies speculate that LTP is facilitated by the ERK-induced activation of cAMP response element binding protein, CREB, a well-documented transcription factor that effects durable synaptic changes.

Minichiello and colleagues utilized a genetic approach to investigate the requirement of specific BDNF/TrkB-induced signaling pathways, by generating mice with targeted mutations in the Shc/Frs2 docking site (Y490) or PLCγ docking site (Y785), and examining effects on hippocampal LTP (Minichiello et

al., 2002). Findings reveal that the PLCγ mutation resulted in dramatically reduced theta burst or tetanus-induced early- and late-LTP. In correlation with this finding, CREB and CaMKIV phosphorylation was impaired in PLCγ mutant mice, suggesting that BDNF/TrkB-dependent recruitment of PLCγ mediates hippocampal LTP in a mechanism involving CREB and CaMKIV regulation. Interestingly, in contrast to the previously described pharmacological studies, mutation of the Shc/Frs2 docking site had no effect on LTP, illustrating that ERK activation is dispensable for this durable plasticity event (Minichiello et al., 2002). Subsequent investigations later determined that the TrkB-PLCγ site, but not the Shc docking site, is also necessary for associative learning in mice (Gruart et al., 2007), supporting the hypothesis that the PLCγ pathway underlies both CA3-CA1 LTP and associative learning.

In line with the report by Minichiello and colleagues, a more recent examination suggests that hippocampal CA3-CA1 LTP is supported by TrkB-induced PLCγ signaling at both pre- and postsynaptic sites (Gartner et al., 2006). In this study, it was found that blockade of PLCγ signaling was required in both pre- and postsynaptic neurons to lead to reduction of LTP similar to that observed by knocking out TrkB and BDNF. No effect on LTP was observed if PLCγ signaling was blocked in either CA3 or CA1 of the hippocampus. The authors hypothesize that recruitment of Ca^{2+} from inositol 1,4,5-triphosphate (IP3)-sensitive intracellular stores plays a key role in PLCγ-dependent LTP.

BDNF/TrkB regulates dendritic spine number

Many of the earliest inquiries into BDNF's functions report that the neurotrophin regulates the number of dendritic spine protrusions, the structural site of the vast majority of excitatory synapses formed onto a neuron. Specifically, many reports describe that the addition of exogenous BDNF to hippocampal and cortical pyramidal neurons, dentate granule neurons, and olfactory bulb granule cells in culture leads to increases in dendritic spine density (Matsutani and Yamamoto, 2004; Tyler and Pozzo-Miller, 2003; Tyler and Pozzo-Miller, 2001). Consistent with these findings, mice with conditional deletion of TrkB induced prior to synapse formation have decreased spine and synapse density in hippocampal pyramidal neurons; however, *in vivo* deletion of TrkB after synapse formation has occurred mediates no effect on spine or synapse density, indicating that regulation of synapse number by BDNF/TrkB may occur only during a specific period of synaptogenesis (Luikart et al., 2005).

As *Bdnf*-null mice die postnatally before BDNF reaches its activity-induced adult levels, examination of *in vivo* postnatal roles for the neurotrophin proved difficult until the generation of conditional BDNF knockout mice. Interestingly, mice with conditional knockout of BDNF in postmitotic neurons throughout the CNS shortly after birth display no deficit in hippocampal CA1 neuron dendritic spine density (Rauskolb et al., 2010), demonstrating that the

TrkB receptor may regulate dendritic spine/synapse formation in a BDNF-independent manner in the CA1 region of the hippocampus. CA1 neurons, however, were found to display a slight reduction and increase in mushroom and thin spines, respectively, indicating that BDNF deficiency may impede spine maturation. The authors also investigated CA3-CA1 hippocampal LTP induced by high-frequency stimulation of Schaffer collaterals, and found LTP to be reduced in the conditional BDNF knockouts, consistent with previous reports describing impaired LTP in *Bdnf*-null and –heterozygous mice. In contrast to the dendritic spine density findings in the hippocampus, medium spiny neurons in the striatum of the same mice have significantly reduced dendritic spine density (Rauskolb et al., 2010), indicating the importance of BDNF/TrkB signaling in the postnatal development of striatal neuron spine number. In the future, it will be interesting to investigate the differences between these two neuronal populations, which may account for their sensitivity to regulation by BDNF/TrkB.

BDNF/TrkB facilitates synaptogenesis through pre- and postsynaptic mechanisms

In 2005, Luikart and colleagues sought to determine whether TrkB controls hippocampal structural synapse formation pre- or postsynaptically by examining properties of CA1 synapses in which TrkB was conditionally knocked out in presynaptic, or in both pre- and postsynaptic cells during early development or post-developmentally (Luikart et al., 2005). TrkB was ablated in presynaptic

DG, CA2, and CA3 neurons at E12.5 using a synapsin-1-cre line, while CaMKII-cre and hGFAP-cre lines were utilized to ablate TrkB in both pre- and postsynaptic Schaffer collateral terminals after and before synapse formation occurs, respectively. Authors discovered that TrkB has a role at both pre- and postsynaptic sites during development, as no synaptic aberrations were observed when the receptor was knocked out after synapse formation had occurred. Specifically, as a result of presynaptic deletion, reductions in synaptophysin staining in CA1 were observed, as well as a reduced density of axon varicosities projecting to CA1, observations that were accompanied by an increase in the number of multi-synapse boutons. No aberrations in dendritic spine density or PSD-95 staining were observed in these neurons. As a result of developmental TrkB deletion at both pre- and postsynaptic sites and in addition to the previously specified deficits, CA1 neurons displayed reductions in both dendritic spine density and postsynaptic puncta. Together, data from this study suggest that the TrkB receptor possesses cell-autonomous roles in the development of synaptic components in pre- and postsynaptic neurons. Future experiments are necessary to delineate the functional consequences of these cell-autonomous roles for the TrkB receptor, particularly with respect to effects on LTP.

Role of the PI3-K/MAPK pathway in BDNF/TrkB-dependent regulation of dendritic spine number

Following the discovery that TrkB deficiency in neurons results in decreased synapse and dendritic spine density, a focus of interest turned to the identification of specific BDNF/TrkB-induced signaling pathways controlling normal synaptogenesis/dendritogenesis. In 2008, Luikart *et al.* reported that synapse density is significantly reduced in hippocampal neurons expressing kinase-dead (K538N) or Y490F (Shc/Frs2) mutant forms of the TrkB receptor (Luikart et al., 2008). Expression of Y785F (PLCγ), however, had no effect on synapse density in these neurons. In correlation with these observations, treatment of wild-type neurons with BDNF or overexpression of wild-type TrkB augmented the motility of dendritic filopodia. Furthermore, expression of a Y490F mutant (Shc/Frs2) blocked the enhancement of filopodial motility, while Y795F (PLCγ) had no effect. This supports the hypothesis that TrkB-mediated dendritic filopodial motility may be an important event in the establishment of appropriate synaptic contacts, and that additionally, TrkB signaling through the PI3-K or ERK pathways is critical for both events. Further characterization identified that PI3-K mediates the TrkB-dependent motility of dendritic filopodia.

BDNF/TrkB regulates dendritic spine growth

Emerging evidence is correlating structural synapse plasticity with functional plasticity, especially for durable events, including LTP, which is associated with dendritic spine head growth, and LTD, an event accompanied by a reduction in spine head size (Cingolani and Goda, 2008; Dillon and Goda, 2005; Yuste and Bonhoeffer, 2001). Numerous lines of evidence suggest that structural dendritic spine dynamics contribute to LTP, including (1) spine enlargement triggered by glutamate uncaging occurs rapidly, in the same time course as LTP induction, (2) spine volume correlates with the number of functional AMPA receptors, and (3) spine enlargement is protein synthesis-dependent, like L-LTP and long-term memory (Kasai et al., 2010; Takumi et al., 1999; Tanaka et al., 2008).

In addition to its well-characterized role in regulating synaptogenesis/dendritic spine formation, BDNF/TrkB has more recently been implicated in promoting LTP-associated structural dendritic spine changes, specifically dendritic spine head enlargement. Several studies have uncovered a role for BDNF in mediating activity-induced, long-lasting increases in dendritic spine head area/volume, an effect found to require new protein synthesis (Bramham, 2008; Kasai et al., 2010; Tanaka et al., 2008). Additionally, other reports have implicated the involvement of F-actin remodeling enzymes in

BDNF-dependent dendritic spine growth (Schwechter and Tolias, 2013; Yuste and Bonhoeffer, 2001).

Requirement for new protein synthesis in activity-induced BDNF/TrkB-dependent dendritic spine head enlargement

Numerous investigations are specifying a requirement for new protein synthesis in BDNF/TrkB-dependent dendritic spine structural plasticity. Recently, miR-134, a microRNA localized at the synapto-dendritic compartment, was reported to regulate BDNF-induced dendritic spine plasticity by controlling the protein synthesis of Lim kinase (Limk), a regulator of F-actin dynamics (Schratt et al., 2006). miR-134 is known to repress the translation of Limk through binding at the 3' UTR of its mRNA. The study found that BDNF led to increased expression of dendritic Limk through an unknown mechanism involving the suppression of miR-134 function. Authors therefore hypothesized that synaptic plasticity may be regulated by the BDNF-dependent relief of Limk translational inhibition by miR-134.

An additional study reveals a requirement for BDNF-induced protein synthesis in dendritic spine head enlargement elicited by the pairing of postsynaptic spikes and two-photon glutamate uncaging (spike-timing). The spike-timing protocol induced a long-term enlargement of the dendritic spine head in CA1 pyramidal neurons (Tanaka et al., 2008). This effect was dependent on

BDNF/TrkB signaling and protein synthesis, as incubation with BDNF scavengers, or anisomycin or cycloheximide, almost completely abolished the growth of the spine head. Stimulation with exogenous BDNF in the presence of glutamate uncaging without spikes also led to robust dendritic spine growth, both immediately and in a gradual long-lasting phase. Co-stimulation with anisomycin, however, caused a significant reduction in spine head size observed during the gradual long-term phase, indicating that BDNF's actions during this phase require protein synthesis.

Requirement for F-actin remodeling in BDNF/TrkB-dependent dendritic spine head enlargement

While several studies demonstrate a requirement for new protein synthesis in BDNF/TrkB-dependent dendritic spine growth, an additional mechanism by which BDNF/TrkB signaling has been widely hypothesized to mediate its effects is through the regulation of F-actin remodeling enzymes. Indeed, F-actin polymerization is required for hippocampal CA3-CA1 TBS-LTP, illustrating that enzymes that control F-actin dynamics are likely critical for normal LTP (Fukazawa et al., 2003; Kim and Lisman, 1999; Krucker et al., 2000). BDNF also promotes theta burst-induced increases in dendritic spine F-actin levels, and sequestering BDNF impairs CA3-CA1 TBS-LTP, suggesting that BDNF may

facilitate LTP by stimulating F-actin remodeling in dendritic spines (Rex et al., 2007).

BDNF/TrkB is a strong activator of the Rho GTPase Rac1, a regulator of F-actin remodeling dynamics that is highly correlated with dendritic spine formation and enlargement. Activation of Rac1 in particular induces spine morphology changes associated with LTP, specifically dendritic spine enlargement (Tashiro and Yuste, 2004), and furthermore, its overexpression leads to strengthening of synapses by promoting AMPA receptor clustering in spines (Wiens et al., 2005). Additionally, pharmacological inhibition of Rac1 activation or actin dynamics blocks LTP induction, suggesting that Rac-dependent cytoskeletal remodeling events are necessary for LTP (Kim and Lisman, 1999; Wiens et al., 2005). Numerous groups have thus speculated that BDNF/TrkB mediates its effects on synapse plasticity through the regulation of F-actin remodeling enzymes, including Rac1. However, the specific signaling mechanisms by which BDNF/TrkB-induced activation of these Rho GTPases occurs, as well as potential roles for this pathway in synapse plasticity, are poorly understood.

Vav guanine nucleotide exchange factors (GEFs) mediate activation of Rho-family GTPases

The Vav family of GEFs consists of three distinct genes, *Vav1-3*, encoding multi-domain cell signaling molecules that are evolutionarily conserved from nematodes to mammals (Bustelo, 2001). Vav GEFs were first identified in hematopoietic cells, and a bulk of information regarding its functional roles and signaling properties has been identified in these blood stem cells. However, numerous neuronal duties for the GEFs, including in axon guidance and synapse plasticity, have recently emerged.

While expression of Vav1 is limited to hematopoietic cells, Vav2 and Vav3 proteins are highly expressed in the brain from embryonic development through adulthood (Cowan et al., 2005; Hale et al., 2011; Turner and Billadeau, 2002). Vav proteins possess multiple domains that have been identified or are hypothesized to function in cell signaling events, including calponin homology, acidic, Dbl homology, pleckstrin homology, zinc finger, and proline-rich regions, as well as two Src homology type 3 (SH3) domains flanking a Src homology type 2 (SH2) domain. Functionally, the Dbl homology domain confers GEF activity, and regulatory tyrosines that modulate this function can be found within the acidic-rich region (Aghazadeh et al., 2000). In general, calponin homology domains have been demonstrated to bind actin, while pleckstrin homology regions are lipid-binding targeting domains. Additional critical structural features of Vav

GEFs include the presence of the tandem SH3-SH2-SH3 domains, sequence-specific phosphotyrosine-binding modules involved in substrate recruitment.

The crucial molecular function of GEF proteins is to activate members of the Rho GTPase family by facilitating the exchange of GDP for GTP. Rho GTPases act as molecular switches, cycling between GDP-bound inactive and GTP-bound active states. GEFs activate GTPases by facilitating the exchange of GDP for GTP, while GAPs (GTPase activating proteins) render GTPases inactive by accelerating the hydrolysis of GTP (Cerione and Zheng, 1996). Studies suggest that Vav proteins specifically activate Rac1 and Cdc42 (Abe et al., 2000; Liu and Burridge, 2000; Marignani and Carpenter, 2001), Rho GTPases that promote spine formation and enlargement (Nakayama et al., 2000; Tashiro et al., 2000). Furthermore, it has recently been demonstrated that Vav exhibits a preference for activating Rac1 over Cdc42 (Kawakatsu et al., 2005; Marignani and Carpenter, 2001).

Vav's GEF activity is regulated by an auto-inhibitory arm, which occludes the GEF activity-conferring Dbl homology domain in the inactive state. Upon phosphorylation of tyrosine residues, specifically Y172 or Y174 in Vav2 and Vav3, respectively, the N-terminal inhibitory arm is released, thus exposing the GEF-conferring Dbl homology region (Aghazadeh et al., 2000). Signaling mechanisms regulating Vav tyrosine phosphorylation and activation have been identified in both lymphocyte and neuronal cells, and include phosphorylation by

Src and Syk family kinases and receptor tyrosine kinases, including EGF, PDGF, and EphB (Aghazadeh et al., 2000; Bustelo, 2001; Cowan et al., 2005; Crespo et al., 1997; Servitja et al., 2003; Tamas et al., 2003).

Vav GEFs have critical roles in neuronal development

A neuron-specific function for Vav was first identified in 2005, with the discovery that Vav2 mediates Eph receptor-dependent growth cone collapse and axon guidance (Cowan et al., 2005). Specifically, the study reports that ephrin stimulation of neurons induces the recruitment of Vav2 to the Eph receptor, upon which Vav2 is then tyrosine phosphorylated and activated. Vav2 was demonstrated to be required for ephrin-Eph endocytosis and ephrin-induced growth cone collapse *in vitro*, suggesting that Vav-stimulated F-actin dynamics are critical for these molecular and cellular processes. Importantly, Vav deficiency in mice resulted in aberrant axonal projections from the retina to the thalamus, revealing a necessary role for Vav-dependent Eph signaling in proper axon guidance *in vivo*.

Since this initial discovery, additional studies are linking Vav-induced Rac-GTP activation and F-actin dynamics in other aspects of neuron development. Specifically, a recent investigation discovered that Vav2 regulates neurite outgrowth and branching in *Xenopus* spinal neurons (Moon and Gomez, 2010). Authors identified that loss or gain of Vav2 function reduces the rate of

neurite extension, demonstrating that balanced Vav2 activity is critical for appropriate neurite formation. Effects of Vav2 on branching of processes were also examined, and indicated that Vav2 overexpression promotes neurite branching *in vitro* and *in vivo* in a process requiring Vav GEF-dependent Rac1 activation.

Finally, Vav has also been implicated in regulation of proper cerebellar development. Using *Vav3*$^{-/-}$ mice, Quevedo and colleagues discovered that Vav3 deficiency leads to impaired Purkinje cell dendritic arborization *in vivo*, as well as reduced survival and aberrant migration of cerebellar granule cells in the internal and external granule layers (Quevedo et al., 2010). As Vav2 and Vav3 proteins have redundant functions as exchange factors in neurons, the authors speculated that Vav2 might also contribute to cerebellar neuron development. However, neurons lacking Vav2 exhibited no changes in the examined cerebellar properties, suggesting that Vav3 specifically controls these functions. Because a primary function of the cerebellum is in controlling motor coordination, the authors next investigated possible effects of Vav3 deficiency on motor control. Analyses revealed that at five weeks of age, *Vav3*$^{-/-}$ mice have impaired motor coordination on the rotarod accelerating test, in addition to an abnormal hind/forepaw overlap pattern. At four months of age, the mice were re-examined for any persistence or improvement of the observed deficiencies. At this time, the motor coordination deficits were largely ameliorated, and the abnormal pattern of paw overlap was no

longer discernible. Together, this study uncovers important roles for Vav3 in regulating cellular and functional development of the cerebellum.

Because numerous roles for Vav proteins in regulating aspects of brain development and plasticity have now been identified, we may also expect emerging studies to link the GEF with human disorders characterized by abnormal neuronal development and synapse function. Indeed, a recent genome wide association study (GWAS) of schizophrenia in a Japanese population was the first study to report a strong association signal in a region of *VAV3*, rs1410403 (Ikeda et al., 2011). Following this discovery, a separate study sought to examine whether rs1410403 is associated with altered brain structure in healthy and schizophrenic individuals, and also performed exon resequencing for further mutation analysis (Aleksic et al., 2013). Previously published studies utilizing voxel-based morphometry (VBM) have reported the observation of smaller volumes in the temporal gyrus of schizophrenic individuals, a brain region that promotes the formation of language and semantic memory processing, visual perception, and multimodal sensory integration, cognitive processes that are deficient in patients with schizophrenia (Onitsuka et al., 2004). Interestingly, Vav3 is more highly expressed than Vav2 in the left superior and medial temporal gyri, suggesting that Vav3 may be more likely to impinge on the identified region-specific functions. VBM revealed that rs1410403 is associated with a reduction in the volume of the left superior and middle temporal gyri in patients

with schizophrenia. As a result of mutation analysis, four rare novel missense mutations in *VAV3* were also detected, one of which, Glu741Gly was found to be significantly associated with schizophrenia in a large independent sample (P=0.02). In the future, it will be necessary to explore the mechanism by which Glu741Gly, located within the SH2 domain of Vav3, affects the pathogenesis of schizophrenia.

BDNF/TrkB regulates molecular and behavioral aspects of learning and memory, anxiety, and disease-associated behaviors in humans and mice

In addition to the well-documented roles of BDNF/TrkB in regulating LTP and structural synapse plasticity, molecular and behavioral analyses are implicating the neurotrophin and its receptor in devastating neurological disorders, including depression, anxiety, addiction to drugs of abuse, schizophrenia, and fragile X syndrome.

Roles for BDNF/TrkB in mediating learning and memory behaviors in mice have been studied extensively, which is not surprising since BDNF/TrkB are well-established regulators of LTP, a widely hypothesized cellular substrate of learning and memory. Mice in which BDNF or TrkB has been conditionally knocked out display deficits in learning the Morris water maze, a hippocampal-dependent spatial navigation task that requires mice to use visual cues to locate a hidden platform in a pool of water (Gorski et al., 2003; Minichiello et al., 1999).

BDNF- or TrkB-deficient mice have also been examined for their responses in contextual and cued fear conditioning, which measure the ability of a mouse to form and remember an association between an aversive experience and environmental cues. Lesion studies indicate that while cue-dependent conditioning relies primarily on the amygdala, the context-dependent counterpart additionally requires the hippocampus, as damage of the formation leads to impaired context-dependent but not auditory cue fear conditioning (Rudy et al., 2004; Rudy and O'Reilly, 1999). BDNF heterozygote mice exhibit impaired context-dependent fear conditioning, without a change in cue-dependent conditioning (Liu et al., 2004), while TrkB conditional knockouts show impaired context- and cue-dependent conditioning (Minichiello et al., 1999). Together, these data describe critical functions for BDNF and TrkB in mediating hippocampal-dependent learning and memory tasks in mice.

Reports also present an association between BDNF/TrkB and anxiety. A V66M SNP in BDNF, which results in a defect in activity-regulated release of BDNF, is associated with enhanced anxiety in human patients (Montag et al., 2010), and furthermore, carriers of the V66M allele have impairments in fear extinction (Soliman et al., 2010). Consistent with these findings, homozygous V66M mice have elevated anxiety in open field and elevated plus maze tests (Chen et al., 2006). Additional behavior investigations in mice also implicate

BDNF in anxiety, as heterozygous BDNF mice show increased anxiety in open field and elevated plus maze tests (Chen et al., 2006).

Major depressive disorder is a leading cause of disability characterized by anxiety, loss of pleasure, guilt, and sleep disturbances. Individuals with MDD have decreased BDNF and TrkB levels in the hippocampus and prefrontal cortex, regions that also exhibit reduced volumes in patients with MDD (Bremner et al., 2000; Castren, 2004; Castren and Rantamaki, 2010; Thompson Ray et al., 2011). Interestingly, MDD leads to enhanced BDNF levels in other regions of the brain, including the nucleus accumbens (NAc) and amygdala, illustrating complex and incompletely understood circuitry through which BDNF regulates depression (Krishnan et al., 2007; Tebartz van Elst et al., 2000). Importantly, studies in humans and mice suggest that BDNF is necessary for antidepressant responses. Specifically, various antidepressant treatments lead to increased BDNF levels in corticolimbic regions, and importantly, experiments in animal models indicate that BDNF and TrkB are required for the effects of antidepressants (Adachi et al., 2008; Monteggia et al., 2004; Monteggia et al., 2007; Saarelainen et al., 2003). Finally, additional behavioral tests in mice connect BDNF with the regulation of depression-like responses. Forebrain deletion of BDNF in female mice leads to increased depression-like responses in sucrose preference and Porsolt forced swim tests (Monteggia et al., 2007). In contrast, deleting BDNF in the ventral tegmental area (VTA) produces an anxiolytic response in mice, suggesting that

region-specific BDNF may have differential influences on depression-like behaviors (Berton et al., 2006; Krishnan et al., 2007).

Schizophrenia is a devastating and complex disorder characterized by positive and negative symptoms, including hallucinations, disordered thoughts and speech, and social deficits. Numerous studies describe aberrations in BDNF levels in brain tissue from individuals with schizophrenia; however, the reported directions of the regulation are inconsistent. While some studies observe increased BDNF expression in frontal cortical and hippocampal regions (Takahashi et al., 2000), others cite decreased BDNF and TrkB levels in these brain regions (Hashimoto et al., 2005; Weickert et al., 2003). Assessment of serum levels of BDNF in live patients report similarly inconsistent findings, signifying the possibility that the variable effects result from antipsychotic therapy, which has been reported to alter BDNF levels. Studies with heterozygous BDNF mice also connect the neurotrophin with regulation of behavioral aspects of schizophrenia. BDNF heterozygotes have deficient sensorimotor gating, consistent with human studies, and the mice also show enhanced locomotor responses to amphetamines, which may imply a lower threshold for psychosis-associated behavior (Dluzen et al., 2001; Saylor and McGinty, 2008).

BDNF/TrkB-dependent signaling and synapse plasticity is widely hypothesized to contribute to behavioral alterations associated with addiction to drugs of abuse. In mice, cocaine administration causes increased BDNF

expression and TrkB phosphorylation in the nucleus accumbens (NAc), a critical locus within the brain reward pathway (Graham et al., 2007; Graham et al., 2009; Russo et al., 2009). These findings are correlated with increased dendritic arborization and spine density in the reward circuitry, suggestive of a potential role for BDNF in regulating cocaine-induced structural modifications of the synapse (Robinson and Kolb, 1999). Knocking down BDNF or TrkB in the NAc in mice reduces cocaine conditioned place preference, a test based on association of the reward produced by the drug and neutral environmental cues (Graham et al., 2007; Graham et al., 2009). Together, these data suggest that reducing levels of BDNF in the reward pathway blunts the rewarding effects of cocaine use.

Finally, BDNF may have a role in mechanisms underlying neurodevelopmental disorders, including fragile X syndrome (FXS) and Rett syndrome, autism-related disorders. In *Fmr1* KO mice, a mouse model for FXS, BDNF protein levels are altered in the hippocampus. Whereas BDNF levels are initially enhanced in the hippocampus during the first two postnatal months, they are reduced in comparison to controls after four months of age (Uutela et al., 2012). Critical findings that suggest additional links between BDNF and FXS include that BDNF application can rescue hippocampal CA3-CA1 LTP deficits in *Fmr1* KO mice (Lauterborn et al., 2007). Interestingly, however, genetically reducing BDNF levels in *Fmr1* KOs ameliorated several behaviors in the FXS model mice, including locomotor, sensorimotor learning, and auditory responses,

thus demonstrating a complex interaction between these two genes that may be dependent on regional expression differences and functions (Uutela et al., 2012). Rett syndrome (RTT) is also a neurodevelopmental autism-related disorder, and results from loss of function mutations in MeCP2, a methyl-CpG-binding domain protein. Interestingly, BDNF is a target of MeCP2, and its expression in MeCP2 null mice is reduced (Chang et al., 2006; Chen et al., 2003). Deleting BDNF in MeCP2-deficient mice triggered an earlier onset of RTT symptoms, and conversely, increasing BDNF levels in these mice rescued locomotor and electrophysiological impairments observed in *MeCP2* KO mice (Chang et al., 2006).

The studies described above convincingly link BDNF/TrkB with numerous neurobiological disease pathologies; however, results can sometimes be inconsistent and often fail to provide insight into the BDNF/TrkB-dependent signaling mechanisms controlling these pathologies. As BDNF/TrkB are critical regulators of multiple molecular and behavioral disease pathologies, it will be of paramount importance to continue the expansion of our knowledge of mechanisms by which BDNF/TrkB controls brain function at the molecular, cellular, and systems levels.

Motivation for studies and summary of research

Increasing evidence suggests a coupling of functional plasticity and dendritic spine structural dynamics, particular in long-lasting forms of plasticity such as LTP, which is associated with dendritic spine head enlargement, and LTD, an event linked with contraction of the dendritic spine head (Cingolani and Goda, 2008; Dillon and Goda, 2005; Yuste and Bonhoeffer, 2001). BDNF and its cognate receptor, TrkB, are critical positive modulators of hippocampal CA3-CA1 TBS-LTP, and emerging evidence suggests that BDNF/TrkB may facilitate LTP in part through modulation of F-actin remodeling enzymes and dendritic spine dynamics. Several lines of evidence support this hypothesis, including (1) F-actin polymerization is required for hippocampal CA3-CA1 TBS-LTP (Chen et al., 1999; Kim and Lisman, 1999; Krucker et al., 2000), (2) Rho-GTPases, critical regulators of F-actin formation and cytoskeletal dynamics, are activated by BDNF-stimulated TrkB signaling (Huang and Reichardt, 2003), (3) BDNF promotes the formation of TBS-induced F-actin assembly in dendritic spines (Rex et al., 2007), and (4) pairing local glutamate uncaging with postsynaptic spikes leads to long-lasting increases in dendritic spine head size through a mechanism that requires TrkB kinase-dependent signaling (Tanaka et al., 2008).

A likely mechanism by which BDNF/TrkB signaling facilitates functional and structural synapse plasticity events is through the activation of Rho-family GTPases, which are critical regulators of F-actin formation and cytoskeletal

dynamics (Luo, 2002; Tashiro and Yuste, 2004). GTPases act as molecular switches, cycling between GDP-bound inactive and GTP-bound active states. GEFs activate GTPases by facilitating the exchange of GDP for GTP, while GAPs render GTPases inactive by accelerating the hydrolysis of GTP. The BDNF/TrkB-induced activation of the Rac1 and Cdc42 GTPases, which are associated with dendritic spine formation and enlargement, is a well-documented signaling event (Huang and Reichardt, 2003). However, the molecular events that link BDNF/TrkB signaling with the activation of GTPases and subsequent downstream consequences on synapse plasticity are poorly understood.

In Chapter Two, we report that Vav-family GEFs are tyrosine phosphorylated and activated by BDNF/TrkB signaling, and are required for BDNF-induced Rac-GTP formation. We observe that Vav GEFs, which are enriched at hippocampal glutamatergic synapses, are dispensable for normal synapse number in CA1 pyramidal neurons. However, we find that they are necessary for rapid BDNF-induced dendritic spine growth and CA3-CA1 TBS-LTP. Together, findings from this study suggest that Vav-dependent F-actin dynamics are critical for BDNF-stimulated dendritic spine head enlargement and LTP, thus providing a novel molecular event linking Vav GEFs with BDNF/TrkB-dependent synapse plasticity.

The emergence of these critical synaptic roles for Vav proteins prompts the hypothesis that the GEFs may be important for regulating appropriate

behavioral responses, including in behaviors mediated by proper BDNF/TrkB signaling. Numerous studies in rodents report requirements for BDNF/TrkB in a wide range of behaviors, including learning and memory, anxiety, and depression. Because Vav GEFs mediate BDNF/TrkB-dependent spine plasticity and LTP, it is important to understand whether the GEF also modulates behaviors, dependently or independently of BDNF/TrkB function. In Chapter Three, I present detailed results from a behavioral analysis of *Vav2*$^{-/-}$*3*$^{-/-}$, *Vav2*$^{-/-}$, and *Vav3*$^{-/-}$ mice. In summary, Vav2/3-deficient mice have impaired contextual but not cued fear conditioning, as well as reduced anxiety in elevated plus maze and open field tests. Analysis of Vav single KO mice indicated that Vav2 and Vav3 are each required for associative learning in mice, while only Vav2 controls anxiety-related responses.

PART TWO: Autism-linked Genes Myocyte Enhancer Factor 2 (MEF2) and Fragile X Mental Retardation Protein (FMRP) are Critical Regulators of Structural and Functional Synapse Plasticity

Deficits in proper synapse formation, elimination, and maintenance, are hypothesized to underlie numerous neurological disorders, including autism, intellectual disability, schizophrenia, and addiction to drugs of abuse. Synapses are formed during early brain development, but neuronal activity also promotes the elimination of synapses to either prune excess synapses or to homeostatically maintain a steady-state number of synaptic connections. The transcription factor myocyte enhancer factor 2 (MEF2) is a critical activity-dependent regulator of excitatory synapse elimination in developing and adult brains. However, the molecular and cellular mechanisms by which MEF2 controls synapse number are not well understood.

Recently, the RNA-binding protein, fragile X mental retardation protein (FMRP), was identified as an essential downstream component of MEF2-induced synapse elimination, suggesting that these two proteins work together to mediate proper synaptic connectivity and brain function. Specifically, findings support the hypothesis that MEF2 and FMRP coordinate transcriptional and translational control of common mRNAs to confer proper experience-dependent synapse refinement, and that dysfunction of this process may contribute to neurological

disorders, including autism, intellectual disability, and addiction to drugs of abuse. Further investigation into the mechanisms by which MEF2 and FMRP coordinate the formation of proper synaptic connections will have broad implications for understanding these and related disorders.

MEF2 transcription factors are activity-dependent regulators of gene expression

MEF2 proteins are members of the minichromosome maintenance 1-agamous-deficiens-serum (MADS) response factor box family of transcription factors. While initially identified for their role in regulating muscle differentiation, critical functions for the MEF2 family of transcription factors in the nervous system have recently emerged. One well-described role for MEF2 is in the control of neuronal survival and apoptosis in response to extracellular stimuli. The transcription factor also controls synapse number and function in several brain regions *in vitro* and *in vivo*, and importantly, is being increasingly implicated in diseases, including addiction to drugs of abuse, intellectual disability, and autism.

The MEF2 family comprises four distinct genes, MEF2A-D, which are expressed in unique, but overlapping patterns in both developing and adult brains (Heidenreich and Linseman, 2004; Ikeshima et al., 1995; Leifer et al., 1993; Lin et al., 1996; Lyons et al., 1995; Lyons et al., 2012; Pulipparacharuvil et al., 2008).

Expression of all four proteins can be found in the cortex, but evidence suggests that MEF2C is the predominant MEF2 protein expressed in this region. In the hippocampus, expression of MEF2C is restricted to the dentate gyrus, whereas MEF2A and MEF2D are expressed throughout the formation. In the cerebellum, MEF2C mRNA exhibits the strongest expression in Purkinje cells, while MEF2C and MEFD show preferential expression in the granule cell layer. Also, in the striatum, the primary MEF2 subtypes expressed are MEF2A and D.

Structurally, the MEF2 proteins have three domains: (1) a MADS box, (2) a MEF2 domain, and (3) a transcriptional activation domain. All MEF2 proteins possess a highly conserved MADS domain, which confers dimerization and DNA binding, targeting the proteins to A/T-rich sequences in gene regulatory regions (West et al., 1997). The transcription factors also have a conserved MEF2 domain, which mediates homo- and heterodimerization of MEF2 proteins, as well as provides binding sites for co-factor interactions (Molkentin et al., 1996; Yu et al., 1992). The third prominent domain shared by all MEF2 proteins is a C-terminal transactivation domain (TAD) that diverges significantly between the family members, and has diverse consequences on transcriptional activity of MEF2 (Black and Olson, 1998).

Mechanisms of MEF2 regulation and effects on neuronal functions

MEF2 transcriptional activity is controlled by several mechanisms, including interactions with co-repressors and -activators, posttranslational modifications of MEF2, and differential splicing.

In the absence of transactivating stimuli, genes targeted by MEF2 exist in a repressed state due to MEF2's interaction with class IIa histone deacetylases (HDACs) (McKinsey et al., 2002). HDACs associate with MEF2 through binding to its MADS and MEF2 domains, and interestingly, they exert a repressive function on MEF2 target genes independently of their deacetylase activity (Bertos et al., 2001; Verdin et al., 2003). Rather, they repress transcription by recruiting additional transcriptional co-repressors, including class I HDACs, C-terminal binding protein (CtBP), and histone methyltransferase binding protein heterochromatin protein 1 (HP1) (Chan et al., 2003; Dressel et al., 2001; Zhang et al., 2001). HDACs are released from MEF2 upon their phosphorylation by activated calmodulin (CaM)-dependent protein kinases (CaMKs) at conserved N-terminal serine and threonine residues. Phosphorylation at these amino acids creates binding sites for 14-3-3 proteins, which trigger the nuclear export of HDAC proteins, thus allowing for association of MEF2 with transcriptional co-activators (Grozinger and Schreiber, 2000; Kao et al., 2001; McKinsey et al., 2001; Wang and Yang, 2001; Zhao et al., 2001). The identities, mechanisms, and consequences of co-activator association with MEF2 are less well-studied, but are

known to include the histone acetyl transferases (HATs), cAMP response element binding protein (CREB)-binding protein (CBP) and p300. Association of these co-activators with MEF2 has been demonstrated to increase lysine acetylation of chromatin at MEF2 target genes, which is linked with transcriptional activation (Zhang et al., 2002).

MEF2's transcriptional activation domain possesses several phosphorylation sites that are targeted by kinases and phosphatases, and mediate activation of targeted genes. An additional calcium-dependent mechanism that regulates MEF2 transcriptional activity is its dephosphorylation by calcineurin, a serine-threonine phosphatase activated by calcium signals. In the absence of calcium signaling, calcineurin is an inactive dimer, comprised of a regulatory and catalytic chain (Aramburu et al., 2004; Aramburu et al., 2000). Upon calcium entry, the protein calmodulin binds to calcineurin's catalytic chain and interrupts its interaction with the regulatory chain, thus allowing for dephosphorylation of targeted proteins. Evidence reveals that calcineurin exerts strong control over MEF2's depolarization-stimulated dephosphorylation and enhanced activity levels in neurons, as the use of the specific calcineurin inhibitors cyclosporin A and FK506 almost completely blocked MEF2A and D dephosphorylation and MEF2 reporter activity in hippocampal neurons (Flavell et al., 2006).

MEF2A and MEF2C are phosphorylated by p38MAPK in their transcriptional activation domain, which has the effect of enhancing their

transcriptional activity. p38MAPK-dependent phosphorylation of MEF2 occurs in response to osmotic stress or inflammatory stimuli, a mechanism speculated to contribute to a pro-survival function for MEF2 in neurons in response to sustained activity (Han et al., 1997; Marinissen et al., 1999). In support of this hypothesis, activation of p38MAPK is required for MEF2-dependent survival following calcium influx induced by depolarization (Mao and Wiedmann, 1999). Furthermore, MEF2A is required for the survival of primary cerebellar granule neurons in response to activity (Gaudilliere et al., 2002). MEF2 phosphorylation by ERK5 may also confer a pro-survival function of MEF2 in response to oxidative stress. Activation of ERK5 in response to oxidative stress enhances DNA binding of MEF2C in PC12 cells (Suzaki et al., 2002). Blocking ERK5 activity pharmacologically causes an increase in stress-induced apoptosis, revealing that ERK5-dependent activation of MEF2C may provide a neuroprotective role in the presence of oxidative stress (Suzaki et al., 2002).

In addition to facilitating pro-survival pathways, MEF2 is also a target of survival-inhibiting pathways induced by excitotoxic stress. One such pathway is the phosphorylation of MEF2 by Cdk5, a cyclin-dependent kinase that is activated in response to oxidative stress (Gong et al., 2003). MEF2's phosphorylation by Cdk5 results in inhibition of its transcriptional regulation (Zhao et al., 2001), though the mechanism is unknown. Candidate theories include that phosphorylation of the Cdk5 site induces the recruitment of negative

transcriptional regulators to MEF2 (Zhu and Gulick, 2004). Additionally, evidence in neurons lends support that Cdk5 phosphorylation of MEF2 induces caspase-dependent cleavage of MEF2, resulting in truncation of MEF2 that generates a dominant negative consisting of a DNA-binding domain without a TAD (Okamoto et al., 2002). In this model, overexpression of constitutively active MEF2 is thought to protect neurons against NMDA-induced apoptosis, an effect that is blunted by co-expression of caspase-cleaved MEF2 fragments. Together, these findings present a potential mechanism through which oxidative stress reduces the pro-survival function of MEF2.

MEF2 can also be regulated by attachment of small ubiquitin-like modifier (SUMO) proteins, which alters the activity of many transcription factors. In cerebellar granule cells, the majority of MEF2A is SUMOylated, resulting in repressed transcriptional activity (Shalizi et al., 2006). Activity-dependent calcium signaling stimulates the dephosphorylation of MEF2A's S408 by calcineurin, triggering a switch from SUMOylation to acetylation at K403. This mechanism is hypothesized to underlie the regulation of dendritic claw differentation in cerebellar granule neurons.

Finally, differential splicing of MEF2's transcriptional activation domain also modulates its transcriptional activity. As mentioned previously, MEF2 proteins have C-terminal transcriptional activation domains that diverge significantly and have diverse consequences on transcriptional activity. While all

MEF2 subtypes experience alternative splicing of α and β domains, only MEF2C exhibits alternative splicing of the γ domain, a major regulatory site governing transcriptional activity of MEF2 (Shalizi et al., 2006). Variants of MEF2C lacking the γ domain have enhanced sensitivity to depolarization-induced activation in cortical neurons, and specific knockdown of MEF2C results in significant impairment of depolarization-dependent expression of *Bdnf* exon IV in rat cortical neurons (Lyons et al., 2012). In contrast, knockdown of MEF2D does not alter expression of *Bdnf* exon IV, but instead causes a significant increase in expression of *Bdnf* exon I. Together, this study reveals that MEF2 subtypes exert differential regulation of genes and that expression of different MEF2 variants has specific consequences on transcriptional inducibility of important activity-regulated genes.

MEF2 controls functional and structural synapse properties in vitro and in vivo

MEF2 is a critical negative regulator of excitatory synapse number in vitro and in vivo

MEF2 proteins have recently emerged as crucial negative regulators of excitatory synapse number in neurons. In 2006, Flavell and colleagues observed that knocking down MEF2A and MEF2D proteins using RNAi in dissociated hippocampal neuron cultures elicits a robust increase in co-cluster density of PSD-95 and synapsin-1, and a concomitant increase in mEPSC frequency,

suggesting that MEF2 restricts the number of excitatory synapses that a neuron receives (Flavell et al., 2006). A constitutively active form of MEF2 in which the DNA binding and dimerization domains are fused to the potent transcriptional activator domain of VP16, MEF2-VP16, is sufficient to restrict structural synapse density, while a mutant in which the DNA binding domain is deleted produces no changes in synapse number. Importantly, findings report that MEF2-induced synapse elimination requires NMDA receptor activation, L-type calcium channel function, and calcineurin activity, indicating that activity is necessary for MEF2's effects on synapse number.

Since this first report, additional *in vitro* studies corroborate the hypothesis that MEF2 mediates synapse elimination. In organotypic hippocampal slices, active MEF2 reduces dendritic spine density, as well as mEPSC frequency and evoked EPSC amplitude in CA1 pyramidal neurons, findings that are consistent with a decrease in functional synapse number (Pfeiffer et al., 2010; Tsai et al., 2012; Wilkerson et al., 2014). Conversely, a dominant negative form of MEF2 in which the DNA and dimerization domains are fused to the strong transcriptional repressor domain of Engrailed, MEF2-Engrailed, produces an increase in mEPSC and evoked EPSC amplitude, indicative of an increase in functional synapse number (Pfeiffer et al., 2010).

Together, findings from these *in vitro* studies illustrate that MEF2 controls synapse pruning, an activity-dependent process that refines synapses and

reinforces the maintained connections. *In vivo* studies also link the transcription factor with negative regulation of synapse number (Barbosa et al., 2008). Specifically, in the hippocampus, MEF2C deletion causes an increase in dendritic spine density of dentate gyrus neurons, and its overexpression in postsynaptic cells leads to a reduction in density of dendritic spines, accompanied by a decrease in mEPSC frequency, suggestive that MEF2 limits synapse number in the hippocampus. In the striatum, knockdown of MEF2A and MEF2D subtypes using RNAi produces an increase in dendritic spine density of medium spiny neurons (MSNs), revealing that reducing MEF2A and MEF2D in NAc MSNs is sufficient to increase dendritic spine density, and thus describing a critical role for MEF2A and MEF2D in regulating basal spine density in the NAc *in vivo* (Pulipparacharuvil et al., 2008).

MEF2 regulates basal synaptic transmission in vivo

Since these initial findings linking MEF2 with the control of synapse number, a study reported by Akhtar and colleagues identifies additional functions for MEF2 subtypes in the hippocampus *in vivo* (Akhtar et al., 2012). The study reports that brain-specific MEF2A/D knockouts have normal CA1 pyramidal neuron spine density, as well as unaltered CA3-CA1 LTP. In contrast, paired pulse facilitation is enhanced in the knockout mice, indicating that presynaptic release probability is decreased in the absence of MEF2A and D proteins *in vivo*.

The authors next turned to *in vitro* experiments using dissociated neuron cultures to more closely examine a role for MEF2 in regulating unitary spontaneous transmission. In MEF2A/D knockout neuron cultures, no changes in mEPSC frequency were observed, indicating that spontaneous excitatory synaptic transmission is unchanged in MEF2A/D-deficient neuron cultures. Additional experiments examined synaptic effects resulting from MEF2A, C, and D deletion, as MEF2C has previously been reported to control functional and structural excitatory synapse number *in vivo*. In MEF2A/C/D KO mice, CA1 pyramidal neuron dendritic spine density is unchanged, while neurotransmitter release probability is reduced, similar to findings in the MEF2A/D knockouts. Together, these data suggest that MEF2A, C, and D proteins control short-term synapse plasticity *in vivo*.

MEF2A regulates synapse maturation in cerebellar neurons

The previously described studies suggest that MEF2 is a regulator of synapse number and transmission, and find that the transcription factor does not appear to affect synapse maturation. However, Shalizi and colleagues present evidence that MEF2 has a role in controlling synapse maturation in cerebellar granule neurons (Shalizi et al., 2006). During cerebellar development, granule neuron dendritic tips differentiate from a long, tapered structure to a mature dendritic claw. In the absence of MEF2, dendritic claw formation is impaired, in a

mechanism hypothesized to involve de-repression of MEF2A targets. In the study, authors found that the majority of MEF2A was in cerebellar granule neurons was SUMOylated, resulting in repressed transcriptional activity. Expressing MEF2-EN in neurons triggered increased dendritic claw formation, supporting the hypothesis that SUMOylated, and therefore transcriptionally repressing, MEF2 promotes claw differentiation.

MEF2C controls cortical maturation and organization

Finally, MEF2C has also been linked with neuronal differentiation and maturation in the developing cortex. Brain-specific MEF2C conditional deletion causes aberrant cortical plate compaction, resultant of impaired differentiation of neurons that are characterized by more immature network properties (Li et al., 2008). In correlation with these findings, MEF2C null mice in the study exhibit enhanced anxiety, working memory deficits, and enhanced paw clasping, behaviors that are reminiscent of Rett syndrome, an autism-related disorder.

Transcriptional programs controlled by MEF2

As described above, MEF2 controls numerous aspects of synapse development and behavioral plasticity; however, the gene program through which MEF2 facilitates these events has remained poorly understood. To gain knowledge of the MEF2-dependent transcriptional program, genome-wide

approaches were implemented, and numerous experimental manipulations of MEF2, including loss- and gain-of-function, were used to identify MEF2 target genes in neurons (Flavell et al., 2008). Using this approach, 182 activity-dependent MEF2 target genes were identified, which have wide-ranging roles in the regulation of excitatory synapse weakening, excitatory synapse maturation, inhibitory synapse development, and presynaptic vesicle release. Intriguingly, several of the targeted MEF2 genes have identified mutations that are implicated in neurological disorders, including autism and epilepsy, supporting the hypothesis that MEF2 controls critical activity-dependent networks that support appropriate synapse development and function.

MEF2 controls learning and memory behaviors, and behaviors associated with autism and addiction to drugs of abuse

MEF2 proteins are critical regulators of functional and structural synapse plasticity, and profound alterations in synapse properties are observed following changes in MEF2 activity and protein levels. Because MEF2 has important roles in regulating proper brain function, it is likely that behavioral consequences may result from altered MEF2 function.

MEF2C was first reported to regulate behavior responses in mice in 2008. Specifically, Barbosa and colleagues observed that mice with conditional brain deletion of MEF2C have impaired hippocampal-dependent contextual fear

conditioning, with no changes in cued fear conditioning (Barbosa et al., 2008). In the same year, a separate study reported behavioral alterations in MEF2C brain null mutant mice (Li et al., 2008). In a Y maze task, a paradigm used to study working memory, MEF2C knockouts exhibited a reduction in spontaneous alterations, suggestive of deficient spatial working memory. In the elevated plus maze, an assay used to measure anxiety, MEF2-deficient mice displayed reduced anxiety by spending more time in the open arms of the maze. Additionally, MEF2C knockout mice exhibited an enhanced paw clasping phenotype, which may model hand clasping in humans, a behavior that is increased in Rett syndrome, an autism-related disorder. Together, these studies describe critical roles for MEF2C in regulating cognition and memory, anxiety, and paw clasping behaviors.

An additional study also links MEF2 with appropriate memory formation; however, findings contrast with previously reported observations. The study reports that increasing MEF2 expression in the dentate gyrus using viral injection blocked the formation of spatial memory in a water maze task, in a mechanism hypothesized to involve MEF2-dependent facilitation of AMPA receptor endocytosis (Cole et al., 2012). Overexpression of MEF2 in the dentate gyrus impaired hippocampal-dependent contextual fear conditioning, and increasing MEF2 levels in the amygdala obstructed contextual and cued fear conditioning. Conversely, reducing MEF2 levels in the dentate gyrus and amygdala promoted

the formation of spatial and associative fear memory. Together, these findings suggest that MEF2 inhibits memory formation in mice, and furthermore, reveal disparities in the role of MEF2 in memory, which may be attributed to developmental differences.

Other MEF2 isoforms have been analyzed for contributions to behavioral responses in mice. MEF2A/D-deficient mice have impaired motor coordination on the rotarod test, and display unaltered contextual and cued fear conditioning, suggestive of normal associative learning in these mice (Akhtar et al., 2012). Interestingly, MEF2A and D proteins mediate responses to cocaine in mice, as knocking down MEF2A and D in the NAc delayed acquisition of cocaine-induced locomotor senstization and reduced the behavioral response to a cocaine challenge dose following two weeks of withdrawal (Pulipparacharuvil et al., 2008). In contrast, overexpressing constitutively active MEF2, MEF2-VP16, in the NAc enhanced cocaine locomotor sensitization in mice. Furthermore, consistent with the locomotor sensitization phenotype, mice expressing MEF2-VP16 have increased cocaine condition placed preference (CPP), indicative that the mice experience enhanced rewarding effects of cocaine in comparison to their WT counterparts.

Molecular and genetic studies link MEF2 with autism and intellectual disability

As described above, studies in mice link MEF2 with regulation of behaviors associated with autism and intellectual disability, including cognition and memory, anxiety, and paw clasping. Interestingly, important recent molecular and genetic studies in mice and humans connect MEF2 in the modulation of molecular and behavior aspects of these neurocognitive disorders. MEF2 controls the expression of numerous autism-linked genes, including *DIA-1* (deleted in autism-1), *PCDH10* (protocadherin 10), and *SLC9A6* (solute carrier family 9, subfamily A, member 6) (Flavell et al., 2008; Morrow et al., 2008). Interestingly, the *MEF2C* gene is also repressed by methyl-CpG binding protein 2 (MeCP2), the gene mutated in Rett syndrome, an autism spectrum disorder (Chahrour et al., 2008). Importantly, recent studies in humans are also implicating *MEF2C* in these prevalent neurodevelopmental disorders, as several patients with autism and mental retardation are reported to have deletions in the *MEF2C* gene. Described as *MEF2C* haploinsufficiency syndrome, specific symptoms of the disorder include 1) profound language deficits, 2) abnormal movements (dyskinesias), 3) abnormalities in reciprocity (e.g., eye contact/tracking), 4) epilepsy, and 5) intellectual disability (Novara et al., 2010; Novara et al., 2013; Paciorkowski et al., 2013; Zweier et al., 2010; Zweier and Rauch, 2012).

FMRP is required for MEF2-induced synapse elimination

MEF2 is a well-established negative regulator of excitatory synapse number; however, the molecular and cellular mechanisms of MEF2-induced synapse pruning remain poorly understood. A recent study discovered that fragile X mental retardation protein (FMRP), an RNA binding protein with roles in the transport and translation of neuronal mRNAs, is required for MEF2-induced synapse elimination (Pfeiffer et al., 2010). Specifically, the study reports that MEF2 activation fails to elicit functional or structural synapse elimination in FMRP-deficient mice, *Fmr1* KO mice. In the converse experiment, inhibition of MEF2 does not generate an increase in excitatory synapse number in neurons lacking FMRP. Together, these data suggest that MEF2 and FMRP function in a common pathway to control synapse pruning.

FMRP is an RNA binding protein with over 800 identified targets comprising approximately four percent of mRNA transcripts in the mammalian brain (Brown et al., 2001; Darnell et al., 2011). Structurally, FMRP has three binding motifs that confer association with mRNAs: two KH domains referred to as KH1 and KH2, and one RGG domain (Darnell et al., 2001; Siomi et al., 1994). The KH2 domain recognizes a loop structure in the RNA described as a "kissing complex," and evidence suggests that this binding motif is critical for FMRP functions, as inclusion of a point mutation (I304N) disrupting RNA interactions results in a severe form of FXS (De Boulle et al., 1993). The RGG box also

mediates association with RNAs, specifically through a common tertiary mRNA structure known as a G-quartet, but is not required for prominent FMRP functions, including regulation of synapse number (Darnell et al., 2001; Pfeiffer and Huber, 2007).

Extensive evidence indicates that FMRP regulates the translation of its targeted transcripts, and furthermore, that it controls local dendritic translation at the synapse. Studies primarily suggest that FMRP acts to repress the translation of bound mRNAs by stalling ribosomal translocation along the transcript (Bassell and Warren, 2008; Darnell et al., 2011). Indeed, exaggerated translation of several proteins, including the synaptic proteins CaMKIIα, Arc, EF1α, and PCDH10, is observed in the absence of FMRP (Bassell and Warren, 2008; Niere et al., 2012; Tsai et al., 2012). However, reports also describe that FMRP can act as a translational switch, and furthermore, suggest that this may depend on FMRP's phosphorylation state, with dephosphorylated FMRP suppressing translation, and phosphorylated FMRP activating translation of its target mRNAs (Ceman et al., 2003).

FMRP controls functional and structural synapse plasticity

While brains from individuals with FXS exhibit no gross anatomical changes, alterations in structural morphology can be observed at the level of the synapse (O'Donnell and Warren, 2002). In particular, patients with FXS, as well

as the mouse model of the disease, *Fmr1* KO mice, have an increased density of spines across several regions of the cortex (Comery et al., 1997; Grossman et al., 2010; Grossman et al., 2006; Irwin et al., 2002; Irwin et al., 2001). An additional prominent characteristic of dendritic spines in FXS and the *Fmr1* KO mouse is a long and tortuous, generally immature appearance (Comery et al., 1997; Dolen et al., 2007). Together, the observation that FMRP-deficient neurons have an increased number of filopodial-like spines provokes the question of whether FMRP functions to regulate pruning or maturation of dendritic spines.

In testing this question, it was observed that FMRP appears to control spine pruning. In the study, authors found that *Fmr1* KO hippocampal neurons have an increased mEPSC frequency, and a decrease in synaptic failures in response to minimal stimulation (Pfeiffer and Huber, 2007). These findings are indicative of the presence of an increased number of functional synapses, and are therefore consistent with the enhanced dendritic spine density findings. Reintroduction of FMRP containing a functional KH2 domain reduced structural and functional synapse number, but did not affect percentage of silent synapses, indicative of a role for FMRP in mediating pruning, and not maturation of synapses.

FMRP was recently implicated in the regulation of local connection pruning in layer 5A pyramidal neurons in the neocortex (Patel et al., 2013). Patel and colleagues obtained simultaneous recordings in the L5A neocortical network

of WT or *Fmr1* KO mice to measure cell-to-cell connections in isolation. It was observed that connection frequency among pyramidal neurons in WT mice decreases between the third and fifth postnatal weeks. In contrast, connection frequency in the *Fmr1* KO does not change during this time period, and is therefore elevated compared to the WT condition by the conclusion of the fifth week, resulting in hyperconnectivity in the FMRP-deficient L5A network. The deficit in connection pruning was determined to be due to loss of postsynaptic FMRP. Together, findings from this study demonstrate an *in vivo* and cell-autonomous role for FMRP in the connectivity pruning of L5A pyramidal neurons in the neocortex, and provide an important system for the examination of altered pruning in FXS.

Emerging evidence describes a critical role for FMRP in controlling neuronal circuit properties. A robust phenotype in the *Fmr1* KO mouse are alterations in UP states, spontaneous and rhythmic episodes of neuronal depolarization with simultaneous onset in local neuronal networks (Hays et al., 2011; Ronesi et al., 2012). Generally, UP states are indicators of network excitability and spontaneous dynamics of the network. In *Fmr1* KO mice, UP states in the somatosensory cortex are significantly longer than in WT mice (Hays et al., 2011; Ronesi et al., 2012). Furthermore, FMRP deficiency in only excitatory, and not inhibitory, neurons is sufficient to produce the prolonged UP state effects (Hays et al., 2011). Together, these data illustrate the presence of a

hyperexcitable neocortical network in FXS. Indeed, circuit hyperexcitability in FXS is a longstanding hypothesis, due to observations of increased epilepsy, abnormal EEGs, and enhanced sensitivity to sensory stimuli in individuals with FXS.

An additional well-documented function for FMRP is the regulation of mGluR-dependent long-term depression (LTD), a form of LTD that is induced by stimulation of group 1 (Gp1) metabotropic glutamate receptors (mGluRs) and relies on the synthesis of new proteins at the synapse (Huber et al., 2000). *Fmr1* KO mice exhibit enhanced mGluR-dependent LTD, and furthermore, LTD in FMRP-lacking mice does not require protein synthesis (Huber et al., 2002). Together, these findings suggest that FMRP inhibits synthesis of proteins that mediate LTD, and that in the absence of FMRP, these proteins are highly expressed and lead to enhanced mGluR-LTD.

Fragile X syndrome (FXS) is the most prevalent inherited form of autism and mental retardation

FXS, which results from loss of function of FMRP, is the most common inherited form of autism, a prevalent neurological disorder affecting approximately 1 in 68 individuals (Bassell and Warren, 2008). Characterized by reduced social interaction, impaired communication, and stereotyped behavior, the neurobiological underpinnings of autism remain poorly understood, and

current treatment for the disorder is limited, relying on coordinated behavioral intervention and medication to alleviate only specific symptoms.

FXS affects 1:4000 males and 1:8000 females, accounting for 1-2% of all autism diagnoses (Bassell and Warren, 2008; Garber et al., 2008). Furthermore, 30-50% of individuals with FXS are diagnosed with autism, with severity ranging across cases (Hagerman et al., 2005; Kaufmann et al., 2004). Deficits in FXS include (1) mental retardation, with IQs varying between 40-70 (Merenstein et al., 1996), (2) deficits in social interaction, (3) repetitive behavior, (4) hypersensitivity to sensory stimuli, especially to auditory and tactile inputs, (5) epilepsy, affecting approximately 15% of patients, and (6) alterations in physical characteristics, including prolonged face and hyperflexible joints.

In most cases, FXS results from a CGG trinucleotide repeat expansion in the promoter of the X-linked gene, *FMR1*, which encodes FMRP. In individuals with the full mutation, in which there are over 200 CGG repeats, hypermethylation of the repeat expansion occurs, leading to transcriptional silencing of the gene (O'Donnell and Warren, 2002). Additionally, investigators have identified a single mutation in FMRP protein that results in a severe form of FXS (De Boulle et al., 1993). The mutation occurs in the KH2 domain of the protein, in which an isoleucine in mutated to an asparagine (I304N), suggesting that FMRP-dependent RNA binding and synapse plasticity, is critical in the pathogenesis of FXS.

A FXS mouse model, the Fmr1 KO mouse, phenocopies synaptic and behavioral characteristics of FXS

Two decades ago, investigators developed the *Fmr1* KO mouse, a model of FXS to study molecular and cellular underpinnings of the disorder (1994). The mouse harbors a neomycin cassette in exon 5 of *Fmr1*, which results in loss of FMRP expression. As mentioned previously, analysis of the mouse indicates that it phenocopies many aspects of FXS in humans on both synaptic and behavioral levels. Synaptically, similar to human patients, the *Fmr1* KO mouse has an increased number of dendritic spines in several cortical regions (Comery et al., 1997; Grossman et al., 2010). Furthermore, like in FXS, the dendritic spines are thin and filopodial in structure, suggestive of a potentially immature state (Comery et al., 1997; Grossman et al., 2006).

The *Fmr1* KO mouse also phenocopies several behavioral characteristics of FXS. One of the most consistently observed phenotypes is an alteration in prepulse inhibition (PPI), a sensorimotor gating task that reflects ability to process and prioritize incoming sensory information (Chen and Toth, 2001). In the PPI test, the presentation of a weak stimulus tone will inhibit the response to a subsequent stronger startle stimulus. FMRP-deficient mice have an increased percent prepulse inhibition (Zhu and Gulick, 2004). As prepulse inhibition of acoustic startle triggers activation of forebrain gating circuitry to allow pre-

stimulus processing, while subsequently interfering with processing of the second stimulus, these findings may signify changes in *Fmr1* KO mice in network circuitry and sensitivity to acoustic stimuli.

An additional non-cognitive phenotype in the *Fmr1* KO mouse is the presence of increased sensitivity to seizure modalities. A common phenotype in FMRP-deficient mice is susceptibility to audiogenic seizures, seizures triggered by exposure to a loud sound. While WT mice will not seize in response to the prolonged high frequency tone, approximately 60% of *Fmr1* KOs seize as a result of the sound (Dolen et al., 2007; Musumeci et al., 2000; Yan et al., 2005). Additionally, in FMRP-lacking mice, there is a reduced threshold for limbic seizures, as reduced electrical stimulation of the amygdala is sufficient to induce a seizure (Qiu et al., 2009). Together, the observation that *Fmr1* KO mice have an increased propensity to seizures is suggestive of a hyperexcitable circuit, one of the widely hypothesized core deficits in FXS.

Because cognitive deficits are a primary symptom of FXS, studies have investigated performance of the *Fmr1* KO mouse in cognitive tasks, including the Morris water maze, fear conditioning, and a visual discrimination task. In the visual discrimination task, mice were first trained to nose poke illuminated holes to receive a food reward (Krueger et al., 2011). During the testing phase, only one of the five holes was lit and generated a reward, and mice were required to learn this criterion. While FMRP-deficient mice generally acquired the task and met

established criteria, they made significantly more mistakes than their WT counterparts, revealing that *Fmr1* KOs have subtle deficits in visual discrimination tasks. Other behavioral paradigms have been used to examine cognitive dysfunction in *Fmr1* KOs, including Morris water maze and fear conditioning. Reports from Morris water maze studies are often inconsistent, generating varied conclusions. Some reports state that *Fmr1* KO mice have no deficits in learning the task, while others describe that the mice have deficits in the acquisition phase of the test (Van Dam et al., 2000). A more consistent finding is that *Fmr1* KOs are impaired in Morris water maze reversal learning, in which mice are required to learn a new platform location; however, additional studies report no deficits in this task (Eadie et al., 2009; Paradee et al., 1999; Van Dam et al., 2000). The inconsistencies between studies examining these paradigms may be due to differences in background strain, as performance of FMRP-deficient mice is believed to be highly sensitive to genetic background. In another hippocampal-dependent task, contextual fear conditioning, mice lacking FMRP exhibit no alterations in freezing responses (Peier et al., 2000; Smith et al., 2014).

An additional core symptom of FXS is deficiency in social interaction. Similar to human patients, the *Fmr1* KO mouse exhibits deficits in preference for social novelty, as well as reduced social investigation, indicative of autistic-like behaviors (Pietropaolo et al., 2011). Additionally, mice lacking FMRP display aggressive tendencies, as mice were observed to have an increased propensity to

attack a juvenile stimulus mouse (Pietropaolo et al., 2011). This finding also phenocopies FXS, in which patients commonly exhibit aggressive behaviors.

A recent study reports critical roles for FMRP in regulating behaviors associated with addiction to drugs of abuse. Interestingly, absence of FMRP in mice reduces locomotor sensitization to cocaine, as well as cocaine conditioned place preference, suggesting that the mice experience reduced rewarding effects of cocaine in comparison to controls (Smith et al., 2014). These behavioral findings were correlated with cocaine-induced dendritic and spine structural changes. Specifically, cocaine administration in FMRP-deficient mice elicited significant increases in dendritic branch number and length in medium spiny neurons (MSNs) in the NAc core, as well as an increase in spine density of NAc shell MSNs compared to WT. Functionally, *Fmr1* KO shell MSNs exhibited an increase in mEPSC frequency in response to cocaine with no change in paired pulse ratio, suggesting an increase in functional synapse number, a finding that is consistent with structural spine observations. Furthermore, cocaine-treated *Fmr1* KO mice had increases in both mEPSC amplitude and AMPAR/NMDAR ratio, supporting the hypothesis that FMRP reduces AMPA receptor-mediated transmission in response to cocaine. Together, findings from this study delineate a critical role for FMRP in regulating cocaine-induced synaptic and behavioral plasticity, suggesting that FMRP facilitates behavioral plasticity to cocaine by promoting synapse elimination and weakening.

δ2 non-clustered protocadherins regulate synapse properties and are implicated in neurodevelopmental disorders

Findings described above suggest that MEF2 and FMRP function in the same pathway to control synapse elimination, regulating the transcription and translation of common targeted transcripts to induce elimination of excitatory synapses. To examine this hypothesis, we performed experiments to identify shared target(s) of MEF2 and FMRP, and have begun experiments to test their requirement for MEF2-dependent synapse pruning.

In our studies, we found that MEF2 and FMRP both target several members of a specific family of non-clustered protocadherins (Pcdh), the δ2 subfamily, consisting of *Pcdh8*, *10*, *12*, *17*, *18*, and *19* (Yasuda et al., 2011). The δ2 protocadherins are members of the superfamily of cadherins, calcium-dependent cell adhesion molecules with broad functions in neuronal and non-neuronal tissues (Kim et al., 2011). While δ2 protocadherins share many structural features with classical cadherins, they exhibit weaker homo- and heterophilic binding, and also possess a diverse C-terminal region with several hypothesized signaling-related motifs for which few effectors have yet been identified (Kim et al., 2011; Yasuda et al., 2007). Intriguingly, several δ2 protocadherins, including *Pcdh8*, *10*, and *19*, have been linked with autism, and *Pcdh17* has been implicated in schizophrenia and language delay (Dean et al.,

2007; Kim et al., 2011; Morrow et al., 2008; Piton et al., 2011; Prasad et al., 2012). Additionally, *Pcdh8* and *10* have identified roles in controlling activity-dependent synapse elimination, suggesting that protocadherin-dependent synapse regulation in neurons may contribute to behaviors associated with neurodevelopmental disorders (Tsai et al., 2012; Yasuda et al., 2007).

My studies are focused on the investigation of a requirement for Pcdh17 in MEF2-induced synapse elimination. Below, I describe known information regarding functions of Pcdh17 and other δ2 protocadherins in neurons; detailed experimental procedures and results are presented in Chapter Four.

Pcdh17 regulates synaptic transmission in the striatum

Neuronal functions for Pcdh17, a highly brain-expressed and synaptically localized δ2 protocadherin, are poorly understood (Hoshina et al., 2013; Kim et al., 2011). A recent report identifies a role for the protocadherin in regulating synaptic properties of striatal neurons, as well as in behavioral plasticity in mice (Hoshina et al., 2013). Pcdh17 is highly perisynaptically localized at excitatory and inhibitory neurons in the basal ganglia, and mediates homophilic intercellular interactions at synapses in striatal neurons. Unlike *Pcdh10*$^{-/-}$ mice, *Pcdh17*$^{-/-}$ mice do not have deficits in topographic map formation, but instead have an increased number of docked synaptic vesicles in the anterior striatum. Following identification of this presynaptic function for Pcdh17, synaptic transmission

efficacy in corticoanterior striatal synapses was examined in *Pcdh17*-deficient mice. Results indicate that basic AMPA and NMDA receptor properties are normal, but that paired pulse ratios for both EPSCs and IPSCs exhibit trending and significant increases, respectively, suggesting that Pcdh17 may regulate presynaptic release probability at these synapses. Repetitive stimulation-induced depression of the EPSC amplitude was found to be weaker in *Pcdh17*$^{-/-}$ mice compared to WT controls, which is hypothesized to be a consequence of the Pcdh17-induced increase in number of docked synaptic vesicles available for release. Authors also examined consequences of Pcdh17 deficiency in behaviors in mice, and report that *Pcdh17*$^{-/-}$ mice display anti-depressant-like behaviors in tail suspension and forced swim tests, and no changes in open field, elevated plus maze, and contextual and cued fear conditioning tests. Together, these findings demonstrate critical presynaptic roles for Pcdh17 in corticobasal ganglia circuits, which may underlie anti-depressant-like behaviors in Pcdh17-deficient mice. In the future, it will be necessary to investigate functional roles for Pcdh17 in other regions of the brain where it is also highly expressed. In Chapter Four, I describe findings from a study in which I am investigating a requirement for Pcdh17 in MEF2-induced synapse pruning in the hippocampus.

Pcdh8 and Pcdh10 mediate activity-dependent synapse elimination in neurons

While studies have not yet implicated Pcdh17 in the control of synapse number, reports have identified two closely related family members of Pcdh17, Pcdh8 and Pcdh10, as important participants in the process of activity-dependent synapse elimination.

Pcdh8, also known as arcadlin, interacts with and is required for the endocytosis of N-cadherin that occurs in response to depolarization or increased cAMP levels (Yasuda et al., 2007). Pcdh8-dependent N-cadherin endocytosis relies on the homophilic binding of Pcdh8, which recruits p38MAPK to its C-terminus. p38MAPK, in turn, induces the phosphorylation of thousand and one amino acid protein kinase 2β (TAO2β), triggering internalization of N-cadherin at the synapse. To test the consequences of deficient Pcdh8-stimulated N-cadherin endocytosis, authors examined hippocampal neurons from *Pcdh8*$^{-/-}$ mice, discovering that Pcdh8-deficient neurons have an enhanced dendritic spine density, which is rescued by knocking down N-cadherin using siRNA. In summary, these findings reveal an interesting mechanism by which Pcdh8 mediates depolarization-induced internalization of N-cadherin, resulting in synapse loss.

Pcdh10 was also recently linked with the process of activity-dependent synapse elimination, in a study reporting a requirement for Pcdh10 in MEF2-induced pruning of excitatory synapses (Tsai et al., 2012). Like Pcdh8, Pcdh10 is

an autism-linked member of the δ2 subfamily of non-clustered protocadherins. Tsai and colleagues determined that MEF2 activity stimulates the ubiquitination of PSD-95 by the ubiquitin E3 ligase murine double minute 2 (Mdm2), and that Pcdh10 subsequently links PSD-95 to the proteasome for degradation. MEF2-induced decreases in both mEPSC frequency and evoked EPSC amplitude were blocked in neurons transfected with the Pcdh10 shRNA, suggestive that Pcdh10 is required for MEF2-triggered decreases in functional synapse number. Manipulation of Pcdh10 levels through overexpression or knockdown did not alter functional synapse number, indicating that it is required, but not sufficient, for regulating MEF2-induced synapse elimination. Together, these findings describe a role for Pcdh10 in controlling the MEF2-induced degradation of PSD-95 and subsequent synapse loss.

δ2 protocadherins interact with the WAVE regulatory complex

While the above studies provide insight into the molecular and cellular mechanisms underlying the neuronal functions for δ2 protocadherins, recent studies also present evidence that two δ2 protocadherins, Pcdh10 and Pcdh19, interact with the WAVE (WASP family verprolin homologous protein) regulatory complex, or WRC (Chen et al., 2014). The WRC, a complex consisting of five components, critically regulates actin cytoskeletal dynamics by inducing the actin-nucleating activity of the Arp2/3 complex. Until recently, the factors that

mediate recruitment of the WRC to specific membrane locations have remained poorly understood. However, several current studies have identified numerous potential WRC ligands, including PCDH10 and PCDH19, and furthermore, Chen and colleagues have identified a novel conserved peptide motif, WRC interacting receptor sequence (WIRS), that binds the WRC and is possessed by all δ2 protocadherins (Chen et al., 2014; Nakao et al., 2008; Tai et al., 2010). Interestingly, authors find that mutation of the WIRS in flies impairs actin cytoskeletal organization and egg morphology during oogenesis. Together, these findings reveal an intriguing mechanism through which δ2 protocadherins may regulate the actin cytoskeleton to effect changes in synapse plasticity.

Motivation for studies and summary of research

Aberrant synapse number, structure, function, and plasticity are widely hypothesized to underlie autism, mental retardation, and other neurological disorders. Activity-dependent MEF2 transcription factors are critical negative regulators of excitatory synapse number, eliciting synapse removal in neurons through the stimulation of a complex program of gene expression (Barbosa et al., 2008; Flavell et al., 2006; Flavell et al., 2008; Pfeiffer et al., 2010; Pulipparacharuvil et al., 2008; Tsai et al., 2012; Wilkerson et al., 2014). Molecular and behavioral studies increasingly associate MEF2 with neurological disorders, including autism and intellectual disability, suggestive that

dysfunctional MEF2-dependent gene transcription and synapse plasticity may underlie these disorders. Molecular evidence links MEF2 with the gene regulation of numerous candidate autism genes, including *DIA1* (deleted in autism-1) and *PCDH10* (protocadherin 10) (Flavell et al., 2008; Morrow et al., 2008). Recent studies in humans are also implicating *MEF2C* in these prevalent neurodevelopmental disorders, as several patients with autism, mental retardation, and epilepsy are reported to have deletions in the *MEF2C* gene (Novara et al., 2010; Novara et al., 2013; Paciorkowski et al., 2013; Zweier et al., 2010; Zweier and Rauch, 2012).

Fragile X mental retardation protein (FMRP) was recently identified as an essential downstream component of MEF2-induced synapse elimination (Pfeiffer et al., 2010). FMRP is an RNA-binding protein that controls synapse plasticity through translational regulation of its targeted transcripts, likely acting as a translational switch to suppress or permit mRNA translation (Bassell and Warren, 2008). Studies indicate that one-third of the synaptic proteome are FMRP targets, and approximately 50% of identified autism gene candidates are targets of FMRP, supporting the hypothesis that dysfunction in FMRP-dependent translation increases the risk of synapse dysfunction and autism (Darnell et al., 2011). Indeed, FXS, which results from loss-of-function mutations in the *FMR1* gene, is the single most common inherited form of autism, and numerous reports describe critical synaptic functions for FMRP, including regulation of appropriate synapse

number (Bassell and Warren, 2008). The finding that FMRP is required for MEF2-dependent synapse elimination lends evidence that these two autism-linked proteins work together to mediate proper synaptic connectivity and brain function (Pfeiffer et al., 2010). Specifically, we hypothesize that MEF2 and FMRP coordinate transcriptional and translational control of common mRNAs to confer proper experience-dependent synapse refinement, and that dysfunction of this coordinated process leads to autism.

To test this hypothesis, we utilized high throughput sequencing of RNA isolated by cross-linking immunoprecipitation (HITS-CLIP) of FMRP to identify common targets of MEF2 and FMRP in neurons. We find a strong overlap of MEF2-induced transcripts and FMRP-associated mRNAs, and observe that a majority of one specific family of non-clustered protocadherins, the δ2 subfamily, are targets of both MEF2 and FMRP. Several of the δ2 protocadherins, including *Pcdh8*, *9*, *10* and *19* have been implicated in autism, and *Pcdh17* is linked with schizophrenia and language delay (Dean et al., 2007; Kim et al., 2011; Morrow et al., 2008; Piton et al., 2011; Prasad et al., 2012). Using shRNA-mediated RNA interference, we find that Pcdh17 is required for MEF2-induced dendritic spine elimination of hippocampal CA1 pyramidal neurons. However, reducing Pcdh17 levels in the absence of MEF2 activation does not alter structural or functional glutamatergic synapses, suggesting that regulation of Pcdh17 is necessary, but not sufficient, for regulating MEF2-induced synapse elimination. Critical future

experiments are necessary to examine key molecular and cellular mechanisms by which Pcdh17 mediates MEF2- and FMRP-dependent synapse elimination.

CHAPTER TWO: Essential Role for Vav Guanine Nucleotide Exchange Factors (GEFs) in Brain-derived Neurotrophic Factor (BDNF)-induced Dendritic Spine Growth and Synapse Plasticity

Summary

Brain-derived neurotrophic factor (BDNF) and its cognate receptor, TrkB, regulate a wide range of cellular processes, including dendritic spine formation and functional synapse plasticity. However, the signaling mechanisms that link BDNF-activated TrkB to F-actin remodeling enzymes and dendritic spine morphological plasticity remain poorly understood. We report here that BDNF/TrkB signaling in neurons activates the Vav family of Rac/RhoA guanine nucleotide exchange factors (GEFs) through a novel TrkB kinase-dependent mechanism. We find that Vav is required for BDNF-stimulated Rac-GTP production in cortical and hippocampal neurons. Vav is partially enriched at excitatory synapses in the postnatal hippocampus, but does not appear to be required for normal dendritic spine density. Rather, we observe significant reductions in both BDNF-induced, rapid dendritic spine head growth and in CA3-CA1 theta burst stimulated (TBS) long-term potentiation (LTP) in Vav-deficient mouse hippocampal slices, suggesting that Vav-dependent regulation of dendritic spine morphological plasticity facilitates normal functional synapse plasticity.

Introduction

A vast majority of excitatory synapses in the mature brain are formed onto dendritic spines (Harris and Kater, 1994). The structure of a dendritic spine is highly dynamic, exhibiting morphological plasticity under both basal and activity-induced conditions (Dillon and Goda, 2005). Increasing evidence suggests that dendritic spine structural dynamics are coupled with functional synapse plasticity, particularly for durable plasticity events such as long-term potentiation (LTP), which is correlated with dendritic spine head enlargement, and long-term depression (LTD), a phenomenon accompanied by a reduction in spine head size (Yuste and Bonhoeffer, 2001; Dillon and Goda, 2005; Cingolani and Goda, 2008). Brain-derived neurotrophic factor (BDNF) and its high-affinity receptor, TrkB, are well-established positive modulators of LTP. BDNF- or TrkB-deficient mice exhibit impaired hippocampal LTP, and addition of exogenous BDNF enhances tetanus and theta burst stimulation (TBS)-induced hippocampal LTP in a Trk kinase-dependent manner (Shen and Cowan, 2010). Recent work in hippocampal slices suggests that BDNF/TrkB facilitates TBS-LTP, at least in part, through regulation of F-actin remodeling and dendritic spine structural dynamics (Rex et al., 2007). Furthermore, pairing local glutamate uncaging with postsynaptic spikes induces long-lasting dendritic spine enlargement through a mechanism that requires BDNF/TrkB kinase-dependent signaling (Tanaka et al., 2008). While several studies describe a requirement for new protein synthesis in

BDNF-induced long-lasting functional and structural synapse plasticity (Bramham, 2008), an additional likely mechanism by which BDNF/TrkB regulates plasticity is through activation of Rho-family GTPases. These are critical regulators of the actin cytoskeleton and have documented roles in dendritic spine formation, motility, and morphology (Luo, 2002; Tashiro and Yuste, 2004). Activation of Rac and Cdc42 GTPases promote spine formation and enlargement, while activation of RhoA promotes dendritic spine instability (Nakayama et al., 2000; Tashiro et al., 2000). Guanine-nucleotide exchange factors (GEFs) render GTPases active by accelerating the exchange of GDP for GTP (Cerione and Zheng, 1996). However, the molecular link(s) between BDNF/TrkB receptors and activation of Rho-family GTPases, and a potential role for this pathway in synapse plasticity, are poorly understood.

The Vav-family GEFs comprise 3 distinct genes (Vav1-3) in vertebrates (Bustelo, 2001). While Vav1 expression occurs nearly exclusively in hematopoietic cells, Vav2 and Vav3 exhibit a more ubiquitous pattern of expression, and are highly expressed in the brain during embryonic and early postnatal development (Turner and Billadeau, 2002; Cowan et al., 2005). Vav GEFs are activated upon phosphorylation of conserved acidic domain tyrosines (Y142, Y159, and Y172) that disrupt an autoinhibitory interaction between the acidic domain and the GEF catalytic DH (Dibble homology) domain (Aghazadeh et al., 2000).

We report here a novel functional interaction between BDNF/TrkB signaling and Vav GEFs. Vav is partially enriched in developing hippocampal synapses and is regulated by BDNF and TrkB kinase activity. We show that Vav is required for BDNF-induced Rac-GTP induction and rapid dendritic spine growth of hippocampal CA1 pyramidal neurons. Finally, we show that hippocampal CA1 LTP is impaired in Vav-deficient neurons, suggesting a functional link between actin remodeling enzymes, dendritic spine growth and activity-dependent functional synapse plasticity in the hippocampus.

Materials and Methods

DNA constructs

Full-length and point mutant forms of Vav2 were generated as described previously (Cowan et al., 2005). Deletion constructs were generated using PCR-based cloning strategies. All Vav2 deletion plasmids contain a T7-epitope tag at the C-terminus. Detailed plasmid maps are available upon request. Full-length and mutant rat TrkB receptors are subcloned into pcDNA3 vectors and contain an N-terminal Flag epitope tag that begins after the signal sequence cleavage site. The Flag-TrkB (rat) Y490F, Y670F, Y674/675F, Y670/674/675F, Y785F, and K571N (amino acid positions refer to homologous positions on TrkA) were generated using modified quick-change mutagenesis (Stratagene).

Protein reagents

The anti-Vav2 total antibody (1:1000 dilution) was described previously (Cowan et al., 2005). Anti-P-Y172 Vav2, 1:1000 (1 μg/ml), was generated in rabbits using KLH-coupling using the following synthesized phosphorylated peptide (C-AEGDEIYEDLMRL) and affinity purified by standard procedures using a Pierce Sulfo-link resin and 100 mM glycine, pH 2.3 elution. The following are commercial antibodies: anti-phosphotyrosine (clone 4G10®, general anti-phosphotyrosine antibody), 1:1000, Upstate; anti-Rac1 (clone 23A8), 1:1000, Millipore; anti-TrkB, 1:1000, BD Biosciences Pharmingen; anti-P-TrkA (Y490), 1:1000, Cell Signaling; anti-Flag (clone M2), 1:2000, Millipore; anti-T7, 1:10,000, Novagen; anti-MAPK, 1:1000, Cell Signaling; anti-P-MAPK (T202/Y204), 1:1000, Cell Signaling, anti-P-Src (Y418), 1:1000, Invitrogen; anti-Src, 1:1000, Cell Signaling. BDNF (Peprotech) was dissolved in 0.1% (w/v) BSA in 10 mM Tris-HCl (pH 7.4).

Dissociated cortical cultures

Embryonic cortical neurons were cultured from embryonic day 16.5 (E16.5) mice or E18 rats. The cortices were dissected and treated with 100 U papain (Worthington) for 3 min. The digestion was terminated by the addition of trypsin inhibitor (Sigma). The tissue was washed for a total of 3X with trypsin inhibitor, followed by 3 washes with plating medium consisting of DMEM

(Invitrogen) supplemented with 10% fetal bovine serum (Invitrogen), 1% L-glutamine (Sigma), and 1% penicillin-streptomycin (Sigma). Neurons were mechanically dissociated with a pipet and plated on polyornithine (Sigma)-coated 10 cm dishes at a density of 8 million cells per dish. The culture medium was replaced with Neurobasal medium (Invitrogen) supplemented with B-27 (Invitrogen), L-glutamine (Sigma), and 1% penicillin-streptomycin (Sigma) 24 hr after plating.

Organotypic slice cultures

Hippocampal organotypic slices were cultured from P6 mice of either sex following the protocol of (Stoppini et al., 1991). The mice were rapidly decapitated and the brains were extracted and placed in chilled dissection medium (1 mM $CaCl_2$, 5 mM $MgCl_2$, 10 mM glucose, 4 mM KCl, 26 mM $NaHCO_3$, and 40 mM sucrose) oxygenated with 95% O_2/5% CO_2. Hippocampi were dissected and sectioned coronally into 400 μm thick sections using a McIlwain tissue chopper. Slices were transferred onto porous Millicell membranes in a 6-well plate with 750 μL of medium (MEM (Gibco) with 25% horse serum, 13 mM glucose, 5 mM $NaHCO_3$, 30 mM HEPES, 1 mM $CaCl_2$, 2 mM $MgSO_4$, 1 mM L-glutamine, 0.00125% ascorbic acid, 1 μg/mL insulin, pH 7.28). Slices were maintained at this liquid-air interface at 37°C with 5% CO2.

Western blotting

Samples were run on SDS-PAGE gels and transferred to PVDF membrane (GE Healthcare). The membranes were blocked in 10% milk for 1 hr and probed with 1° antibody for 2 hr at room temperature or overnight at 4°C. The membranes were then incubated with 2° antibody (1:10,000 G∝R or G∝M, Jackson ImmunoResearch Labs) for 1 hr at room temperature and developed with a homemade enzymatic chemiluminescence (ECL) solution or Amersham™ ECL Plus Western Blotting Detection System (GE Healthcare).

GST-PBD assay

Dissociated cortical neurons (plated at a density of 8 million cells per dish in a 10 cm dish) or hippocampal organotypic slices, prepared as described above, were treated with BDNF (0.1 μg/mL and 0.25 μg/mL, respectively; Peprotech) over a time-course at 6 and 9 days in culture, respectively. The neurons were lysed in a buffer consisting of 50 mM Tris (pH 7.2), 1% Triton X-100, 250 mM NaCl, and 10 mM $MgCl_2$. Each time-point was incubated with 10 μg GST-PBD and 20 μL glutathione beads (50% slurry; GE Healthcare) for 1 hr at 4°C. The beads were washed 3 times with a wash buffer consisting of 50 mM Tris (pH 7.2), 1% Triton X-100, 150 mM NaCl, and 5 mM $MgCl_2$. Samples were loaded onto SDS-PAGE gels for western blotting.

RNA isolation and reverse transcription

Whole hippocampi were dissected from mice of either sex at various ages and processed immediately or snap frozen on ethanol/dry-ice. The samples were homogenized in TRIzol (Invitrogen) using a tissue homogenizer, and the RNA was precipitated with chloroform (Sigma). The remaining steps were carried out using the RNeasy® Micro kit (Qiagen). The RNA concentration of each sample was determined using a NanoDrop spectrophotometer and was reverse transcribed using the Superscript™ III First-Strand Synthesis System for RT-PCR (Invitrogen).

Quantitative real-time PCR

All primers were designed to amplify a 100-150 base-pair product. The primers used to amplify Vav2 RNA were 5'-GCTCTGAAGTCCACCTCTGG-3' (forward) and 5'-TCCTTGGTGCTCTGAATGTG-3' (reverse). The primers used to amplify Vav3 RNA were 5'-AAAAGAGGCTCATGCTCAGG-3' (forward) and 5'-CGAAATCACGAAAGCTGTGA-3' (reverse). The primers used to amplify cyclophilin were 5'-CATCTATGGTGAGCGCTTCCC-3' (forward) and 5'-GCCTGTGGAATGTGAGGGGTG-3' (reverse). The reactions were carried out using the SYBR Green PCR Master Mix (Ambion) and the ABI 7500 real-time PCR thermal cycler (ABI). Vav2 and Vav3 expression in the hippocampus were determined by running reactions of 50 ng of cDNA. Fold changes relative

to cyclophilin were determined using the ΔΔCt method, in which mean fold change ($2^{-\Delta\Delta CtAVE}$) and s.e.m. ($abs(((2^{-\Delta\Delta CtAVE} \times 2^{-\Delta\Delta CtSEM}) - (2^{-\Delta\Delta CtAVE} / 2^{-\Delta\Delta CtSEM})) / 2)$) were determined.

Synaptosome preparation

Whole hippocampi were dissected from P15 mice of either sex and homogenized in buffer consisting of 7 mM Tris-HCl (pH 7.5), 0.36 M sucrose, 0.5 mM EGTA, and 0.25 mM DTT using a Wheaton glass mortar and Teflon pestle homogenizer. The samples were spun at 3500 rpm for 2 min at 4°C to pellet nuclei. The supernatant was collected and spun at 23,000xg for 6 min at 4°C, resulting in the formation of a membrane fraction-containing pellet. The pellet was resuspended in homogenization buffer and layered onto a 5%/13% discontinuous Ficoll gradient. The sample was spun at 45,000xg for 45 min at 4°C. Synaptosomes were collected from the 5% and 13% Ficoll interface, washed in ice-cold PBS, spun at 23,000xg for 20 min at 4°C, and resuspended in ice-cold PBS. The post-synaptic density (PSD) was collected by homogenizing an aliquot of the synaptosome fraction in homogenization buffer with 0.5% Triton X-100. The sample was vortexed repeatedly during a 15-min incubation on ice, then spun at 33,000xg for 20 min at 4°C. The pellet that formed following the centrifugation was PSD.

Slice culture transfection and live-cell imaging

After 6 DIV, slices were transfected with GFP using the biolistic gene transfer method (Bio-Rad). All experiments, acquisition of images, and analyses were performed blind to genotype. GFP-positive pyramidal neurons were selected for time-lapse imaging after 72 h of gene expression. Time lapse images were collected from the secondary and tertiary basal dendrites of CA1 hippocampal neurons on a Zeiss LSM 510 inverted microscope using an Achroplan 40 × 0.8 NA water immersion objective. Hippocampal slices were maintained in the liquid-air interface environment for the duration of the imaging session with 5% CO_2 at 34°C. GFP was visualized at 900 nm with a Chameleon Ti:Sapphire 2 photon laser (Coherent). Images were collected in stacks at an interval of 0.5 μm with a resolution of 0.09 pixels/μm. Image stacks were collapsed into maximum projections and analyzed. Dendritic spine head fluorescence intensity was normalized to an adjacent area of dendrite. Spine head size was defined as the area of thresholded pixels and measured with ImageJ software. BDNF (250 ng/mL) was directly applied as a 1 μL drop to the top of the slice. Each sample represents an average of five randomly chosen, isolated dendritic spines from one dendritic length. One dendritic length per slice was imaged and averaged to give an average spine behavior per dendrite.

Intracellular recordings

Hippocampal organotypic cultures were prepared from *wild-type* and *Vav2*$^{-/-}$*3*$^{-/-}$ mice of either sex at P6, as described previously. At 9 DIV, slices were transferred to a recording chamber and perfused with artificial cerebrospinal fluid (aCSF) containing (in mM): 124 NaCl, 26 $NaHCO_3$, 10 glucose, 3 KCl, 2.6 NaH_2PO_4, 1.3 $MgCl_2$, and 2.5 $CaCl_2$ and saturated with 95%O_2/5%CO_2. Picrotoxin (100 μM, Sigma-Aldrich) and tetrodotoxin (0.2 μM, Ascent Scientific) were added to block $GABA_A$ receptors and Na channels, respectively. Neurons were voltage clamped at -60 mV through whole cell recording pipettes (4-6 MΩ) filled with internal solution containing (in mM): 130 K-gluconate, 10 KCl, 10 HEPES, 3 $MgCl_2$, 2 Mg-ATP, and 1 Na-GTP, pH 7.30, 280±4 mOsm. CA1 pyramidal neurons were visualized using a Zeiss Axoskop 2A equipped with infrared differential interference contrast optics and a contrast gradient light source. Whole-cell voltage-clamp recordings were obtained using a Multiclamp 700A amplifier (Molecular Devices). For all recordings, the first 10 min were discarded to allow the internal solution time to dialyze the neuron and reach equilibrium. The following 15 min were considered, and cells were discarded if less than 100 events were recorded. mEPSCs were detected and analyzed using an automatic detection program (MiniAnalysis; Synaptosoft Inc, Decatur, GA). Seventy-five events were randomly selected per recording and the average amplitude and inter-event interval (IEI) were calculated. Following mEPSC

collection, Schaffer collaterals were stimulated using custom-made stimulation electrodes, with constant current discovered by A.M.P.I. stimulus isolators. The stimulus intensity was adjusted to evoke a monosynaptic EPSC and the stimulus was delivered twice at 100 ms (10 Hz) intervals. This was repeated at least 7 times every 30 seconds. Off-line analysis was performed using scientific analysis software (Igor Pro, Wavemetrics). Significant differences between *wild-type* and *Vav2*$^{-/-}$*3*$^{-/-}$ slices were determined using a t-test.

Slice preparation and TBS-LTP electrophysiology

All studies used postnatal day 15 (P15) mice of either sex. For slice preparation, animals were rapidly decapitated and the brains were removed and placed in ice-cold, oxygenated aCSF containing the following: 25 mM NaCl, 2.5 mM KCl, 1.25 mM NaH_2PO_4, 1 mM $MgCl_2 \bullet 6H_2O$, 2 mM $CaCl_2 \bullet 2H_2O$, 25 mM $NaHCO_3$, and 25 mM dextrose. A Vibratome 1500 sectioning system was used to prepare transverse hippocampal slices of 300 μm thickness, and the slices were immediately transferred to a holding chamber containing room-temperature aCSF. Slices were allowed to recover for at least 1.5 hr before recording. Slices were transferred to a recording chamber perfused with aCSF maintained at 30°C. Field EPSPs (fEPSPs) were recorded from CA1 in response to stimulation of Schaffer collaterals. Pulses were delivered through the stimulation electrode at 0.05 Hz.

After establishment of a 10 min stable baseline, two theta bursts were delivered, with each burst consisting of four pulses at 100 Hz and separated by 200 ms.

HEK293 cell transfections and immunoprecipitations

HEK293T cells were transfected using a calcium phosphate method. After 24 hours, cells were lysed in RIPA buffer (50 mM Tris-HCl, pH 7.4, 150 mM NaCl, 1 mM EDTA, 1% Triton X-100, 0.5% DOC, 0.1% SDS). Flag-tagged TrkB protein was precipitated using 20 μL anti-FLAG agarose (50% slurry; Sigma).

Results

BDNF stimulates the transient activation of Vav in neurons

As Vav GEFs are activated by several receptor tyrosine kinases (Pandey et al., 2000; Cowan et al., 2005; Hunter et al., 2006; Garrett et al., 2007), we speculated that BDNF/TrkB signaling might regulate Vav. To test this possibility, we stimulated cultured primary neurons (E18+6 DIV, rat cortical) with recombinant BDNF (100 ng/ml) over a 1-hour time-course. Endogenous Vav2 was immunoprecipitated with specific antibodies (Fig. 2.1A) and western blotting was performed to detect Vav2 tyrosine phosphorylation. We found that BDNF induced a rapid and transient tyrosine phosphorylation of Vav2, with phosphorylation peaking at approximately 2 minutes and remaining elevated

above pre-stimulation levels through at least 30 minutes (Fig. 2.1B). Consistent with these observations, TrkB receptors also activate Vav GEFs in HEK293T cells (Fig. 2.1C). Under these conditions, transient expression of wild-type TrkB displays high basal activity without addition of exogenous BDNF as revealed by western blotting with the P-Y490 Trk receptor-specific antibody. Compared to Vav2 or Vav3 expressed alone, co-expression with wild-type TrkB dramatically increased tyrosine phosphorylation of Vav2 and Vav3 using either a general phospho-tyrosine antibody (4G10) or using a site-specific antibody that is specific for Vav2 P-Y172, which is a key GEF activity-regulating residue in the Vav acidic domain (Crespo et al., 1997; Han et al., 1997; Schuebel et al., 1998). In addition, the co-expression of kinase-active TrkB receptor with either Vav2 or Vav3 resulted in altered cell morphology of transfected HEK293T cells compared to cells expressing TrkB or Vav2/3 alone (data not shown), suggesting a functional interaction between TrkB and Vav in living cells.

In the immune system, Src-family kinases phosphorylate Vav1 at acidic domain tyrosines in response to T-cell receptor activation (Bustelo, 2000). However, incubating cortical neurons with the Src inhibitor, PP2, did not block BDNF-induced endogenous Vav2 tyrosine phosphorylation (Fig. 2.1D), indicating a Src kinase-independent mechanism. Taken together, these experiments indicate that BDNF/TrkB activation increases tyrosine

phosphorylation and activation of Vav2 and Vav3 GEFs, which suggests a potential role for this novel BDNF/TrkB signaling pathway in neurons.

BDNF stimulates Rac-GTP formation through a Vav-dependent mechanism

Since Vav GEFs are activated by BDNF/TrkB signaling (Fig. 2.1) and are strong activators of Rac (Abe et al., 2000; Heo et al., 2005), we speculated that Vav GEFs might contribute to the BDNF-induced activation of Rac-GTP in neurons. To test this idea, we treated *wild-type* (WT) or *Vav2*$^{-/-}$*3*$^{-/-}$ hippocampal slice cultures (P6 + 9 DIV), dissociated cortical neurons (E16.5 + 6 DIV), or acute hippocampal slices (adult) with recombinant BDNF for various periods of time and measured production of Rac-GTP (Fig. 2.2A,C-D). In wild-type hippocampal slices (Fig. 2.2A) or dissociated neuron cultures (Fig. 2.2C), we observed that exogenous BDNF addition induced a rapid and transient increase in Rac-GTP levels, with peak levels occurring ~2-5 minutes after stimulation (Fig. 2.2). The kinetics of Rac-GTP activation in were very similar to the kinetics of BDNF-induced Vav2 tyrosine phosphorylation (Fig. 2.1B compared to Fig. 2.2C). In contrast, BDNF stimulation of Vav-deficient neurons produced a dramatically reduced induction of Rac-GTP (Fig. 2.2A,C-D), indicating that Vav GEFs are required for normal activation of Rac in these neuronal populations. We observed normal induction of P-ERK1/2 in the Vav-deficient neurons (Fig. 2.2B), indicating that Vav GEFs are not required for all BDNF/TrkB forward signaling

events. While we observed a significant reduction in BDNF-induced Rac activation in Vav-deficient cortical cultures or hippocampal slice cultures, the BDNF-induction of Rac-GTP is not completely abolished. Two recent studies indicated that the Rac GEF, Tiam1, can be activated by BDNF/TrkB signaling and contribute to Rac-GTP levels in Cos-7 cells or in cerebellar granule neurons (Miyamoto et al., 2006; Zhou et al., 2007); therefore, the residual BDNF-induced Rac activation is likely accounted for by Tiam1 or a similar Rac GEF.

Vav GEFs in the hippocampus co-localize with excitatory synaptic proteins

Since BDNF/TrkB signaling activates Rac-GTP in large part through a Vav-dependent mechanism, we speculated that Vav GEFs might contribute to morphological or functional synaptic changes induced by BDNF/TrkB signaling in hippocampal neurons. Toward this end, we first analyzed expression levels of Vav2 and Vav3 during the postnatal time-frame in which robust synaptogenesis, dendritic spinogenesis and synaptic remodeling are occurring *in vivo* (P4-P21) and in adult hippocampus. Using reverse transcription and quantitative real-time PCR (qRT-PCR), we found that Vav2 mRNA levels are high during the early postnatal phase (P4-P7) and then slightly decline during the next two weeks (P14-P21) before stabilizing at their adult hippocampal levels, which are approximately 50% of peak levels (Fig. 2.3A). In comparison, hippocampal Vav3 mRNA levels do not change from P4 to adult (Fig. 2.3A). By relative comparison, Vav2 is

expressed at a level that is ~2-4-fold higher than Vav3 mRNA in the hippocampus, depending on the postnatal age (Fig. 2.3B). Taken together, these data reveal that Vav2 and Vav3 are both highly expressed in the developing hippocampus.

BDNF/TrkB signaling is an important modulator of synapse formation, and morphological (dendritic spine) and functional synapse plasticity in the hippocampus (Korte et al., 1995; Figurov et al., 1996; Patterson et al., 1996; Minichiello et al., 1999; Pozzo-Miller et al., 1999; Kossel et al., 2001; Luikart et al., 2005; Rex et al., 2007; Luikart et al., 2008; Tanaka et al., 2008). To test whether Vav GEFs are found near excitatory synapses, and therefore in a position to mediate BDNF-dependent synaptic effects, we used a biochemical fractionation procedure to isolate membranous fractions enriched for glutamatergic synaptic proteins (*i.e.* synaptosomes, (Rao and Steward, 1991)) from whole mouse hippocampi (P15) and then analyzed Vav2 protein co-fractionation in the various cellular fractions by western blotting with a highly-specific Vav2 antibody (Fig. 2.1A). Interestingly, Vav2 was strongly enriched in proteins associated with the non-nuclear cell membrane pellet (P2) and synaptosome (syn), similar to the fractionation profiles of TrkB, Rac1, and PSD-95 (Fig. 2.3C), despite the fact that Vav2 lacks known membrane spanning domains or membrane-anchoring posttranslational modifications. To determine whether Vav2 is a component of the postsynaptic density (PSD) in synaptosome preparations, we performed mild

detergent (1% Triton X-100) extraction of the synaptosomal fraction. Interestingly, Vav2 partially extracted from the synaptosomal fraction, indicating that a large amount of synaptosomal Vav2 is associated with the PSD (Fig. 2.3C). In comparison, TrkB was almost completely detergent-extracted from the synaptosome fraction, whereas PSD-95 was not extracted from synaptosomes under these conditions (Fig. 2.3C), as expected. Taken together, these data suggest that hippocampal Vav2 is largely membrane-associated in synapse-containing fractions, is a partial constituent of the PSD, and is thus in a position to mediate BDNF/TrkB-mediated morphological and/or functional plasticity at the excitatory synapse.

Vav GEFs are required for BDNF-induced dendritic spine head growth in hippocampal CA1 neurons

Several recent studies reveal an important role for BDNF/TrkB signaling in hippocampal dendritic spine growth, F-actin remodeling and functional synapse plasticity (Korte et al., 1995; Figurov et al., 1996; Luikart et al., 2005; Rex et al., 2007; Luikart et al., 2008; Tanaka et al., 2008). Since (1) Vav GEFs are activated by BDNF/TrkB signaling, (2) Vav GEFs are required for BDNF-induced Rac-GTP production, and (3) Vav2 is co-localized with TrkB in synapse-enriched fractions, we speculated that Vav GEFs might be involved in BDNF/TrkB-induced morphological synapse plasticity. To test this idea, we treated *wild-type*

(WT) and *Vav2*$^{-/-}$*3*$^{-/-}$ mouse organotypic hippocampal slice cultures (P6 + 9 DIV) with recombinant BDNF and monitored dendritic spines using 2-photon confocal live cell imaging (Fig. 2.4A). Based on the rapid kinetics of BDNF-induced Vav2 phosphorylation and Rac-GTP activation, we monitored randomly chosen dendritic regions on secondary branches for 10 minutes before and 15 minutes after the addition of exogenous BDNF (Fig. 2.4A). Analysis of CA1 dendritic spines revealed that the existing spines demonstrated highly dynamic behavior in the basal state, with individual spine heads enlarging and shrinking rapidly within minutes (data not shown). However, the mean dendritic spine head size was fairly stable over the 10 minutes of pre-BDNF treatment (Fig. 2.4A, bottom). Upon addition of BDNF to the wild-type hippocampal slice, we observed a significant increase in spine head area (Fig. 2.4A, bottom, $p<0.05$, two-way ANOVA) that peaked by 8 minutes and maintained an enlarged spine head area throughout the duration of the experiment (Fig. 2.4A). In contrast, analysis of hippocampal slices from the Vav-deficient mice showed no significant change in spine head area after addition of BDNF (Fig. 2.4A-B), indicating that Vav GEFs are required for BDNF-induced dendritic spine head growth.

Because initial spine head area may affect a dendritic spine's relative capacity to change (occlusion), we analyzed pre-BDNF dendritic spine area in WT and Vav2/3 KO slices, but observed no significant differences between the genotypes (Fig. 2.4C). Similarly, there were no differences in cumulative

dendritic spine length between wild-type and Vav-deficient neurons (Fig. 2.4D). We also did not observe evidence of new dendritic spines forming during the 15-minute BDNF treatment (data not shown), indicating that BDNF-induced synaptogenesis requires a longer time scale (*e.g.* 24-48 hrs) as reported by others (Tyler and Pozzo-Miller, 2001; Tyler and Pozzo-Miller, 2003).

BDNF and TrkB signaling are required for dendritic filopodial motility and synapse formation in early postnatal periods of hippocampal development in CA1 neurons (Luikart et al., 2005; Luikart et al., 2008). To test whether Vav GEFs are required for these TrkB-influenced processes, we investigated morphological and functional synapses in *wild-type* and Vav-deficient neurons in hippocampal slice cultures. However, we observed no significant differences in dendritic spine density between *wild-type* and Vav-deficient CA1 neurons from analysis of dendritic regions used for the live-cell imaging study above (Fig. 2.4E). Using whole-cell patch clamp recordings from WT and Vav-deficient CA1 pyramidal neurons in hippocampal slice cultures, we observed no significant differences in miniature excitatory postsynaptic current (mEPSC) frequency (Fig. 2.5A) or amplitude (Fig. 2.5B), and no differences in pre-synaptic vesicle release probability as determined from paired pulse ratio of evoked postsynaptic responses with a 100 ms stimulus interval (Fig. 2.5C). Therefore, while Vav GEFs are important for BDNF-induced rapid induction of Rac-GTP and morphological dendritic spine plasticity, they appear to be dispensable for early hippocampal

synaptogenesis or basal synaptic function. As such, we sought to test whether Vav might function in existing dendritic spines to modulate or facilitate functional synapse plasticity.

Vav GEFs mediate synaptic plasticity in the hippocampus

F-actin remodeling and BDNF/TrkB signaling are required for induction of TBS-LTP at CA1 glutamatergic synapses (Chen et al., 1999; Kim and Lisman, 1999; Krucker et al., 2000). To test whether Vav GEFs are required for TBS-LTP, we stimulated Schaffer collateral axons with a weak theta-burst stimulus (2 × TBS) and recorded field excitatory post-synaptic potentials (fEPSPs) from the CA1 region of *wild-type* or Vav-deficient acute hippocampal slices at postnatal day 15 (P15). Weak TBS stimulation of *wild-type* slices resulted in significant LTP as determined from evoked field responses during the last 10 minutes of a 50-minute post-tetanus recording period. TBS-LTP was also significantly generated in the Vav-deficient slices, but the LTP level was significantly reduced compared *to wild-type* slices (Fig. 2.5D, wild-type 43.5%±8.7, *Vav2*$^{-/-}$*3*$^{-/-}$ 15.9%±4.4, $p<0.05$, student's t-test). Taken together, these findings reveal a novel role for Vav GEFs in the process of functional synaptic plasticity, and suggest that Vav GEFs facilitate TBS-LTP by regulating structural dynamics at functional synapses.

Vav2 activation requires TrkB kinase activity, but not autophosphorylation of the Shc/Frs2 and PLCγ-interacting TrkB phosphotyrosines

To better define how BDNF/TrkB signaling regulates Vav GEF activity, we transiently transfected HEK293T cells with plasmids expressing Vav2 alone or together with wild-type or mutant TrkB receptors. As mentioned previously, co-expression of wild-type TrkB with Vav2 resulted in elevated tyrosine phosphorylation levels using either a general phosphotyrosine-specific antibody (Fig. 2.1B) or with a specific anti-P-Y172-specific antibody (Figs. 2.1C and 2.6A). However, the TrkB-dependent increase in P-Y172 Vav2 required TrkB kinase activity (Fig. 2.6A, wt vs. K571N (kinase dead; KD)). Interestingly, the TrkB kinase-dependent increase in Vav2 P-Y172 levels did not require tyrosine autophosphorylation at TrkB Y490 (Shc/Frs2 binding site) or Y785 (PLCγ binding site) (Fig. 2.6A). Similarly, mutating one TrkB kinase domain autophosphorylation site (Y670F) did not alter P-Y172 levels (Fig. 2.6A). However, mutating multiple TrkB kinase domain autophosphorylation sites, Y674/675F, did reduce Vav2 P-Y172 levels, but these TrkB mutations caused similar magnitude reductions of TrkB P-Y490 autophosphorylation (data not shown), suggesting that the decreased Vav2 phosphorylation was due to indirect effects of these mutations on intrinsic TrkB kinase activity. Finally, the TrkB kinase-dependent increase in P-Y172 Vav2 was largely independent of the Vav2 SH2 domain (Fig. 2.6A, right), which was previously shown to be important for

activation by Eph receptors (Cowan et al., 2005). Taken together, these data indicate that Vav GEFs are activated by a TrkB kinase-dependent mechanism that is independent of the two best-studied TrkB autophosphorylation sites (Y490 and Y785) and independent of the Vav SH2 domain.

To determine whether Vav GEFs physically interact with TrkB receptors, we expressed wild-type Vav2 or Vav3 alone or together with TrkB in HEK293T cells and performed co-immunoprecipitation (co-IP) assays. We found that TrkB specifically co-IPed with either Vav2 or Vav3 (Fig. 2.6B) under stringent detergent lysis/IP buffer conditions (*i.e.* RIPA buffer, see methods). Unlike the regulation of Vav2 P-Y172 levels, we found that this interaction occurred independently of TrkB kinase activity since Vav2 and kinase-inactive TrkB (K571N) co-IPed together to a similar extent (Fig. 2.6C). Similarly, TrkB autophosphorylation site mutants, Y490F and Y785F, also co-IPed with Vav2 at similar levels as wild-type TrkB (Fig. 2.6C).

To further define the nature of this novel TrkB/Vav2 interaction, we generated a series of deletion mutants of Vav2 lacking the N-terminal calponin homology and acidic domain regions, or lacking the C-terminal adaptor domain, which comprises two SH3 domains flanking the SH2 domain. We also analyzed Vav2 lacking both of these regions, which leaves only the core DH/PH/ZF regions intact (Fig. 2.6D). All of these Vav2 mutants interacted strongly with TrkB, indicating that the TrkB kinase-independent interaction between Vav2 and

TrkB is mediated by residues within the DH/PH/ZF region. Deletion of the TrkB kinase domain disrupted the interaction (Fig. 2.6E), suggesting that the Vav DH/PH/ZF region mediates the interaction with the TrkB kinase domain. These findings reveal a strong kinase-independent binding mechanism between Vav and TrkB in cells, and suggest that activation of TrkB kinase activity stimulates Vav2 tyrosine phosphorylation and GEF activity.

Discussion

In this study, we report an essential role for Vav GEFs as important mediators of BDNF/TrkB receptor-induced activation of Rac GTPases and morphological plasticity of hippocampal dendritic spines, and a novel role in functional synapse plasticity. Specifically, we report that BDNF/TrkB signaling increases Vav tyrosine phosphorylation, and that Vav GEFs are required for BDNF-induced production of Rac-GTP and spine head growth in hippocampal neurons. Vav2 co-purifies with biochemically-enriched excitatory postsynaptic proteins, and Vav2/3 are necessary for normal TBS-LTP, supporting a role for F-actin remodeling enzymes in functional synaptic plasticity. Together, these data suggest that Vav GEF-dependent regulation of Rac activity and F-actin assembly in existing dendritic spines is an important process for the establishment and maintenance of LTP.

While our findings link Vav GEFs to regulated F-actin dynamics in dendritic spines and functional synapses, and suggest a possible mechanism by which BDNF/TrkB signaling may contribute to establishment of stable LTP, there remain a number of important questions about the role of Vav GEFs in BDNF-dependent structural and functional synapse plasticity for future investigation. Our findings demonstrate an important role for Vav in the BDNF-induction of Rac-GTP, but there is clearly a significant residual activation of Rac that remains in the Vav-deficient mice. Two recent studies reported that BDNF/TrkB signaling activates Tiam1 in neurons and non-neuronal cells (Miyamoto et al., 2006; Zhou et al., 2007). Like Vav GEFs, Tiam1 is a member of the Dibble homology family of Rho GEFs and a potent regulator of Rac activity. In Cos-7 cells, BDNF/TrkB signaling stimulates tyrosine phosphorylation of Tiam1 and activation of Rac-GTP, and in dissociated cortical neurons, dominant negative Tiam1 expression reduced BDNF-induced neurite outgrowth (Miyamoto et al., 2006). Similarly, using an RNA interference-based approach, BDNF-regulated migration of cerebellar granule cell precursors was shown to require Tiam1-dependent activation of Rac (Zhou et al., 2007). As such, we speculate that Tiam1, which is expressed in the developing hippocampus (Ehler et al., 1997), likely contributes to the residual Rac-GTP activation in Vav2/3 null mice. Depending on the developmental stage and neuronal cell type, Vav and Tiam GEFs may serve in a functionally redundant pathway for Rac activation, but either alone is not

sufficient for full Rac activation. In the future, it will be important to study the relationship between these GEFs in BDNF-dependent F-actin dynamics and related biological processes.

The Segal group recently reported that PI3-K activity was not required for BDNF-induced activation of Rac in cerebellar GCPs (Zhou et al., 2007), which is consistent with the idea that Rac activation is not downstream of PI3-K activity, but is rather an essential parallel signaling process important for cell morphological changes. A recent study reported an important role for TrkB P-Y490 and PI3-K activity in the process of filopodial motility and hippocampal synaptogenesis (Luikart et al., 2008). In general, our findings are consistent with these observations in that Vav GEFs, while important for BDNF-induced Rac activation, are not required for early hippocampal dendritic spinogenesis through postnatal day 15 (Fig. 2.4E). Similarly, P-Y490 TrkB is not required for Vav2 activation in non-neuronal cells (Fig. 2.6A), nor is it required for LTP induction (Minichiello et al., 2002; Gruart et al., 2007), suggesting that TrkB-mediated enhancement of filopodial motility and synaptogenesis is a distinct process from BDNF/Vav-dependent Rac activation, spine head growth and maintenance of LTP. Interestingly, unlike TrkB receptor knockout mice, CA1 hippocampal neurons of conditional brain-specific BDNF knockout mice do not have a reduced dendritic spine density, but instead have fewer mushroom-type spines and more thin-type spines (Rauskolb et al., 2010), suggesting the possibility that TrkB

receptors may regulate CA1 hippocampal neuron dendritic spine density in a BDNF-independent manner *in vivo*.

Many previous studies have documented the importance of F-actin assembly/remodeling for LTP maintenance (Kim and Lisman, 1999; Krucker et al., 2000; Fukazawa et al., 2003; Rex et al., 2007), and a strong correlation has been established between spine head volume and functional synapse plasticity (Matsuzaki et al., 2004; Okamoto et al., 2004; Honkura et al., 2008; Tanaka et al., 2008). In addition, BDNF enhances TBS-induced F-actin content in dendritic spines and inhibition of endogenous BDNF reduces TBS-LTP (Rex et al., 2007), supporting the hypothesis that BDNF/TrkB signaling enhances TBS-LTP by facilitating F-actin assembly in stimulated glutamatergic spine synapses. Rac activation in particular seems to be important for dendritic spine enlargement and stabilization (Nakayama et al., 2000; Tashiro et al., 2000), and as a major effector of Vav GEFs (Crespo et al., 1997; Abe et al., 2000; Zeng et al., 2000), the dramatic reduction in BDNF-induced Rac-GTP levels in Vav-deficient neurons likely contributes to the defect in BDNF-induced spine head enlargement and TBS-LTP. In HEK293T cells, we observe that transient expression of Vav2 or Vav3 together with TrkB results in robust lamellipodia-like protrusions from the transfected cells (unpublished observations, C. W. Cowan), indicative of Rac-induced F-actin assembly in cells. A recent study reported that the inhibitor, NSC23766, which is a small molecule inhibitor of some Rac-GEFs, such as

Tiam1 and Trio, did not reduce TBS-LTP in hippocampal slices (Rex et al., 2009). However, this compound exhibits specificity for inhibiting Tiam1-Rac binding and was found to reduce Tiam1-stimulated, but not Vav-stimulated, cell growth, suggesting that the inhibitor does not affect Vav-mediated Rac1 activation (Gao et al., 2004). Consistent with this idea, the NSC compound only reduced TBS-induced Rac-GTP levels by ~30%, suggesting that a NSC-sensitive GEF, like Tiam1, accounts for only a subset of the Rac activation. Our data would suggest that Vav GEFs account for a majority of the Rac-GTP produced by BDNF/TrkB signaling (Fig. 2.2).

Despite our initial speculation that Vav GEFs would be recruited to tyrosine autophosphorylated TrkB via the SH2 phosphotyrosine binding domain, which is how Vav2 interacts with Eph Receptors in HEK293T cells (Cowan et al., 2005), our findings in heterologous cells reveal a novel interaction between Vav2 and TrkB involving a TrkB kinase-independent interaction between the Vav DH/PH/ZF core catalytic region and the TrkB kinase domain. A similar interaction mechanism was observed between Ephexin1, a DH-family GEF required for axonal outgrowth and repulsion, and two different receptor tyrosine kinases: EphA4 and FGF receptors. Ephexin's DH and PH domains interacted with the kinase domain of the EphA4 receptor (Shamah et al., 2001), and recently, a similar interaction was described between Ephexin and the fibroblast growth factor (FGF) receptor (Zhang et al., 2007). In the former case, addition of

ephrinA1 ligand stimulated tyrosine phosphorylation of endogenous Ephexin, which in turn stimulated its RhoA GEF activity and promoted axon growth cone collapse (Sahin et al., 2005).

While our results suggest that Vav-dependent F-actin dynamics in dendritic spines may regulate aspects of postsynaptic structural and functional synapse plasticity, it will be important to determine the downstream signaling events and cellular processes by which Vav GEFs elicit these changes. Our findings suggest a postsynaptic role for Vav GEFs, but as these are total knockout mice, we cannot rule out a potential pre-synaptic role that could indirectly mediate TBS-LTP or spine growth. Since Vav2 and Vav3 mRNAs (and Vav2 protein) are expressed at similar levels in both primary neuron and astrocyte cultures (data not shown), we also cannot rule out a possible glial role for Vav GEFs in mediating structural and functional synapse plasticity. Finally, there could also be a developmental role for Vav GEFs that occurs prior to the structural and functional synapse plasticity events analyzed at P15 (or its rough equivalent in slice culture). Analysis of conditional Vav knockout mice will be important for resolving these questions in the future. On a mechanistic note, Vav GEFs may be necessary for endocytosis of the BDNF/TrkB receptor complex, which is known to be critical for neuronal survival, as well as for migration of cerebellar granule cell precursors (Valdez et al., 2005; Zhou et al., 2007). Previously, we found that Vav GEFs are required for endocytosis of the

ephrinA1/Eph receptor complex in retinal ganglion cells (Cowan et al., 2005), which led us to speculate that Vav-dependent endocytosis, possibly through a Rho/Rac-dependent process, is a critical step in Eph receptor-mediated forward signaling during axon guidance. Similarly, endocytosis of the BDNF-bound TrkB receptor has been shown to be critical for promoting forward signaling processes necessary for BDNF-dependent neuronal survival and migration of cerebellar granule cell precursors (Valdez et al., 2005; Zhou et al., 2007), but in the latter case, this was shown to require Tiam1 (Zhou et al., 2007). In the future it will be interesting to determine whether Vav GEFs regulate TrkB receptor endocytosis, and whether internalization of the BDNF-activated TrkB receptor is important for TBS-LTP and dendritic spine plasticity.

Regulation of local protein synthesis in dendrites plays a critical role in stabilizing long-lasting changes in dendritic spine morphology and functional synapse plasticity (Tanaka et al., 2008; Yang et al., 2008). However, the mechanisms by which *de novo* protein synthesis regulates spine and synapse plasticity are poorly understood. Based on the transient nature of BDNF-induced Vav tyrosine phosphorylation and Rac-GTP production, we speculate that Vav GEFs signaling stimulates transient F-actin assembly, but an independent, protein synthesis-dependent molecular process likely stabilizes the F-actin cytoskeleton and maintenance of LTP. Consistent with this idea, we find that addition of exogenous BDNF to hippocampal slices is sufficient to induce rapid spine head

growth (Fig. 2.4). However, addition of exogenous BDNF, in the absence of presynaptic stimulation, does not by itself produce LTP, but coupling exogenous BDNF pre-incubation with TBS does enhance CA3-CA1 LTP (L. Leverich, unpublished observations). This suggests that BDNF-induced spine head growth may be permissive for functional synapse plasticity, but additional activity-dependent processes are required to induce and stabilize LTP. It is also important to note that addition of 20 ng/ml BDNF to hippocampal slices did not alter spine head size unless coupled with glutamate uncaging (Tanaka et al., 2008). In contrast, we found that addition of 250 ng/ml BNDF was sufficient for spine head growth (Fig. 2.4A,B), suggesting that there is a threshold BDNF concentration required to stimulate spine growth without strong, coupled glutamate release, which appears to stimulate endogenous BDNF release. Glutamate is also known to stimulate other Rac-GEFs, such as Tiam1 and Kalirin-7, via activation of ionotropic AMPA or NMDA glutamate receptors (Tolias et al., 2005; Xie et al., 2007), which may synergize with BDNF/TrkB signaling mechanisms to facilitate spine growth.

Taken together, the findings described here introduce a novel role for Vav GEFs in BDNF-induced Rac activation and dendritic spine head growth in neurons, as well as in TBS-induced hippocampal LTP. By regulating Rho GTPase activity in response to BDNF/TrkB signaling, Vav proteins may modulate F-actin

remodeling in dendritic spines to facilitate dendritic structural changes and activity-dependent synapse plasticity.

Figure 2.1. BDNF stimulates the transient activation of Vav2 in neurons.

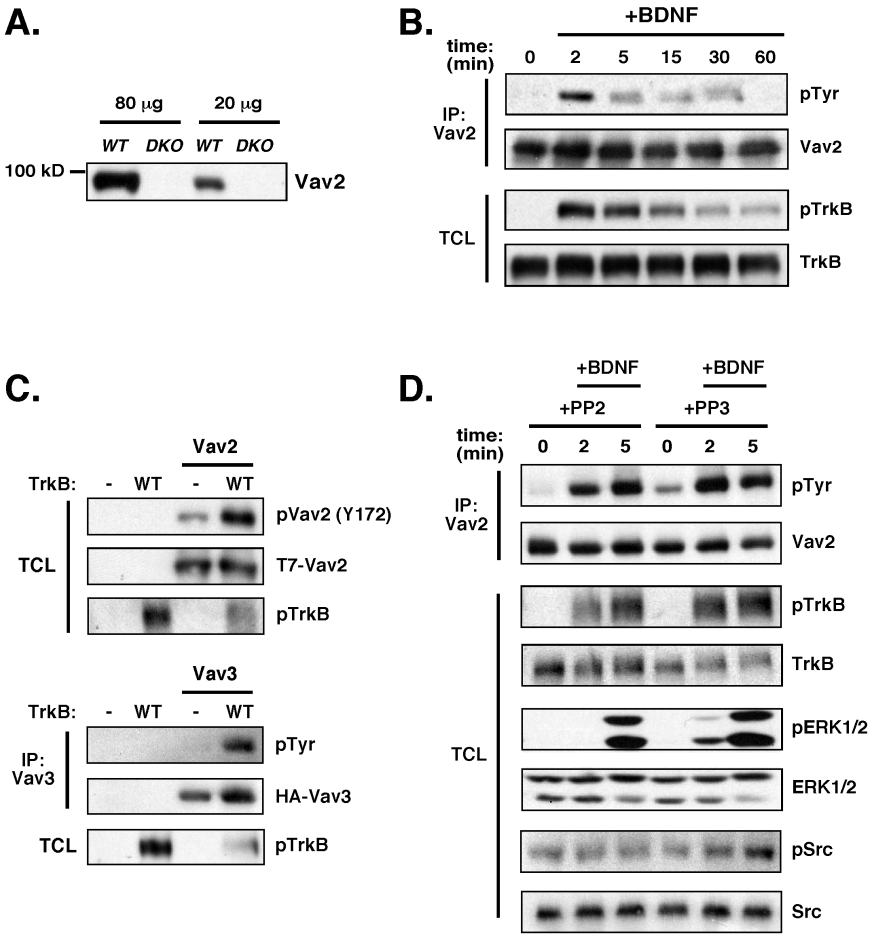

Figure 2.1. BDNF stimulates the transient activation of Vav2 in neurons. A, Vav2 antibodies are highly specific. Western blot of whole hippocampi from P15 *wild-type* (WT) or *Vav2*$^{-/-}$*3*$^{-/-}$ (*DKO*) mice with anti-Vav2 antibody (Cowan et al., 2005). **B**, E18 rat cortical neurons were cultured for 6 days and then stimulated with BDNF (100 ng/mL) over a time-course. Vav2 was immunoprecipitated and blotted with anti-phospho-tyrosine antibody (4G10). Total cell lysates (TCL) were blotted with anti-phospho-TrkB (Y490) and anti-TrkB antibodies. Result is a representative finding of five independent experiments. **C**, Co-expression of Vav2 or Vav3 and TrkB increases phospho-Vav in HEK293T cells. HEK293T cells were transfected with T7-tagged Vav2 or HA-tagged Vav3 and Flag-tagged TrkB. To examine Vav2 Y172 phosphorylation, whole cell lysates were blotted with anti-phospho-Vav2 (Y172) antibody. To examine Vav3 phosphorylation, total cell

lysates were immunoprecipitated with anti-HA antibody, then immunoblotted with anti-phospho-tyrosine (4G10) and anti-HA (Vav) antibodies. Total cell lysates were blotted with anti-pTrkB (Y490) antibody. Result is a representative finding of three independent experiments. **D**, BDNF stimulates activation of Vav2 independently of Src kinase activity. E18 cortical neurons were cultured for 6 days and then incubated with DMSO, PP2 (5 μM), or PP3 (5 μM) for 30 minutes prior to stimulation with BDNF (100 ng/mL) over a time-course. Vav2 was immunoprecipitated and blotted with anti-phospho-tyrosine antibody (4G10). Total cell lysates were blotted with anti-phospho-TrkB (Y490), anti-TrkB, anti-phospho-ERK1/2 (T202/Y204), anti-ERK1/2, anti-phospho-Src (Y418), and anti-Src antibodies. Result is a representative finding of two independent experiments.

Figure 2.2. BDNF stimulates Rac-GTP formation through a Vav-dependent mechanism.

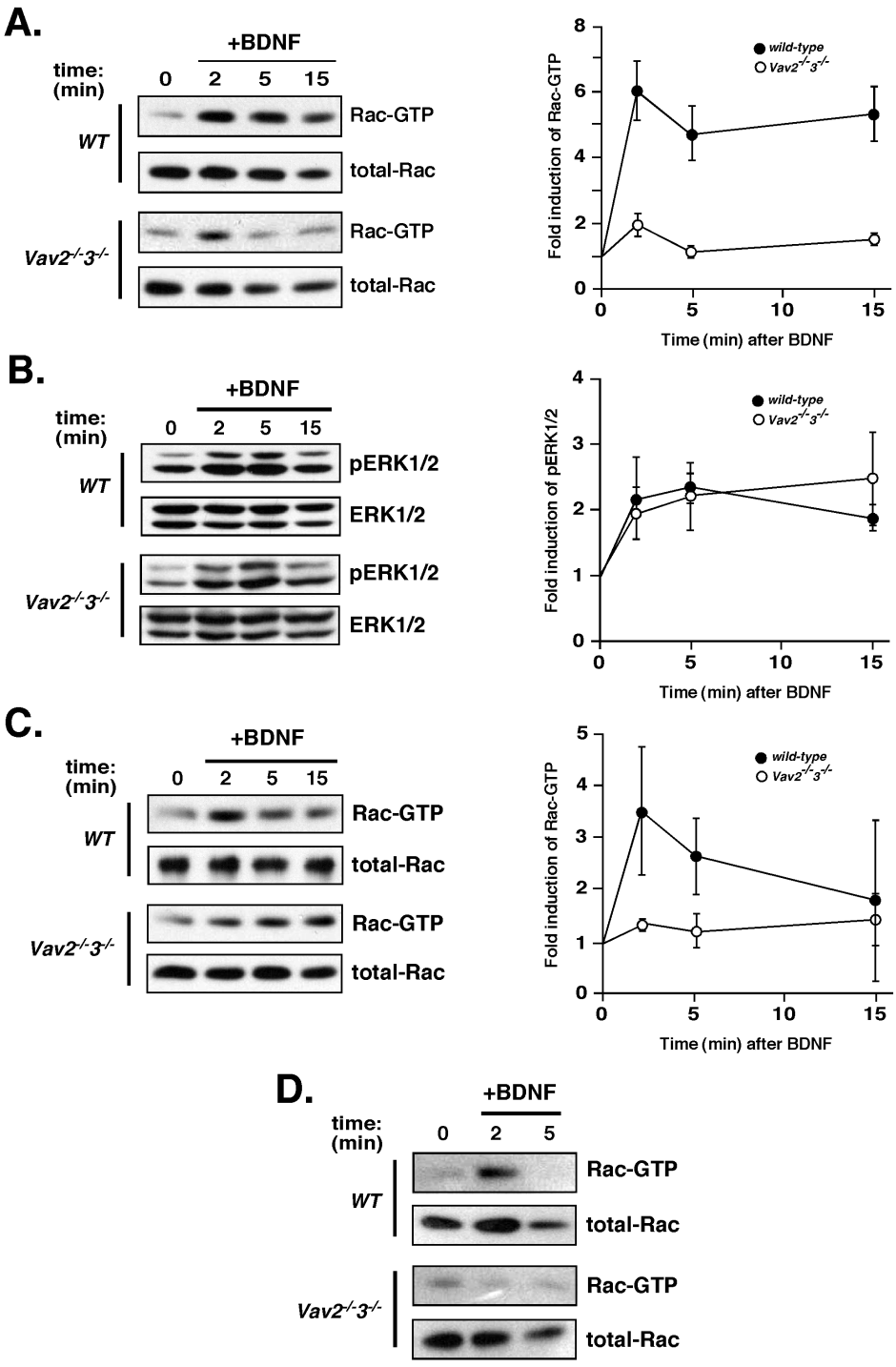

Figure 2.2. BDNF stimulates Rac-GTP formation through a Vav-dependent mechanism. A, Hippocampal organotypic slices (400 μm) were cultured from *wild-type* or *Vav2*$^{-/-}$*3*$^{-/-}$ mice at P6. At 9 DIV, slices were stimulated with BDNF (250 ng/mL) over a time-course. Rac1-GTP was precipitated using GST-PBD fusion protein and glutathione sepharose. Total cell lysates were blotted with anti-Rac1 antibody. Rac1-GTP was normalized to total Rac1 levels and expressed as fold change in comparison to the 0 minute time-point (***$p<0.001$, genotype by Two-way ANOVA). *Wild-type* and *Vav2*$^{-/-}$*3*$^{-/-}$ data are from four and five independent experiments, respectively. **B**, Erk1/2 pathway is activated normally in *Vav2*$^{-/-}$*3*$^{-/-}$ hippocampi (as in **A**) in response to BDNF stimulation. Total cell lysates were blotted with anti-phospho-ERK1/2 (T202/Y204) and anti-ERK1/2 antibodies. *Wild-type* and *Vav2*$^{-/-}$*3*$^{-/-}$ data are from three and four independent experiments, respectively. **C**, Rac1-GTP stimulation by BDNF as in (A), except using cultured primary cortical neurons (E16.5+6DIV) from either *wild-type* or *Vav2*$^{-/-}$*3*$^{-/-}$ mice and treatment with 100 ng/mL BDNF for indicated times. *Wild-type* and *Vav2*$^{-/-}$*3*$^{-/-}$ data are from four independent experiments. **D**, Acute hippocampal slices (300 μm) from adult (3 month) *wild-type* or *Vav2*$^{-/-}$*3*$^{-/-}$ mice were stimulated with BDNF (100 ng/mL) over a time-course. Rac1-GTP was precipitated using GST-PBD fusion protein and glutathione sepharose. *Wild-type* and *Vav2*$^{-/-}$*3*$^{-/-}$ results are representative findings from three independent experiments.

Figure 2.3. Vav GEFs co-localize with excitatory synaptic proteins in the hippocampus.

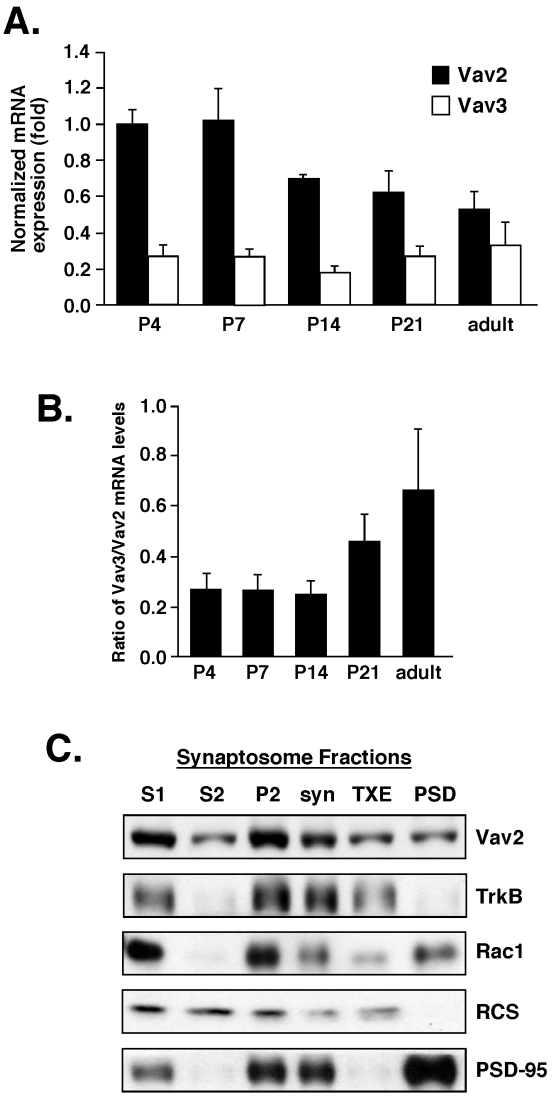

Figure 2.3. Vav GEFs co-localize with excitatory synaptic proteins in the hippocampus. A, Relative hippocampal expression of Vav2 and Vav3 mRNA at indicated time-points determined using real-time qPCR. Results were normalized to cyclophilin mRNA levels. For **A** and **B**, data are from three independent experiments, each of which was conducted in triplicate. **B**, Ratio of Vav3/Vav2 mRNA expression at indicated time-points. **C**, Synaptosomes were prepared from whole hippocampi of P15 mice. Vav2 localized to the membrane (P2) and

synaptosome (syn) fractions. S1, total hippocampal homogenate with nuclei removed. S2, cytosol. P2, crude membrane fraction. syn, synaptosomes collected following Ficoll gradient fractionation. TXE, 1% Triton X-100 soluble fraction of syn. PSD, pellet after 1% Triton X-100 extraction. Synaptosome fractions were blotted with anti-Vav2, anti-TrkB, anti-Rac, anti-RCS (regulator of calmodulin signaling; (Pulipparacharuvil et al., 2008), and anti-PSD-95 antibodies. Result is a representative finding of two independent experiments.

Figure 2.4. Vav GEFs are required for BDNF-induced dendritic spine head growth in hippocampal CA1 neurons.

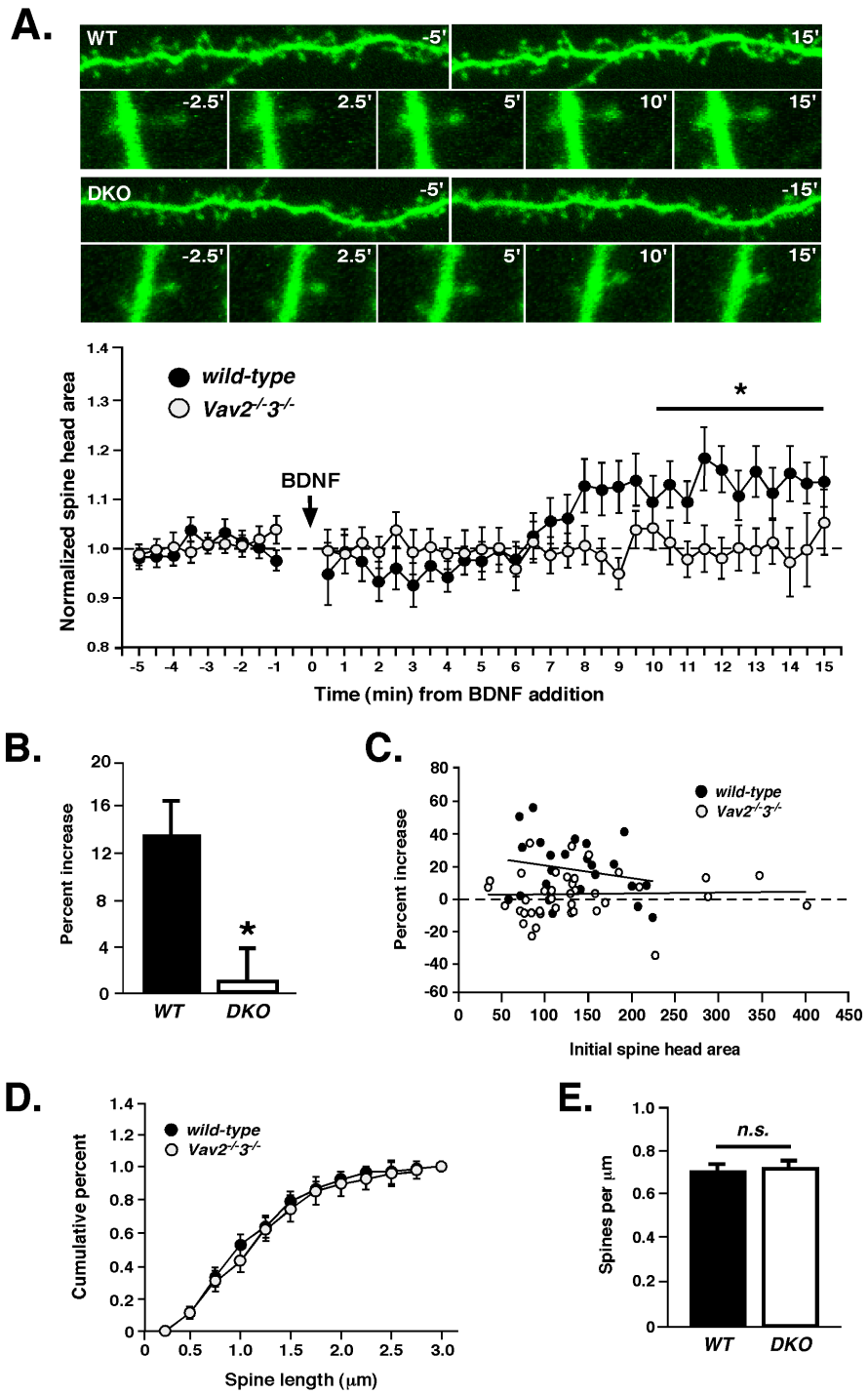

Figure 2.4. Vav GEFs are required for BDNF-induced dendritic spine head growth in hippocampal CA1 neurons. A, Top: Hippocampal organotypic slices (400 μm) were cultured from *wild-type* or *Vav2*$^{-/-}$*3*$^{-/-}$ mice at P6. At 9 DIV, slices were stimulated with BDNF (250 ng/mL) over a time-course and imaged using two-photon microscopy. Representative photomicrographs showing dendritic segments and dendritic spine heads from *wild-type* or *Vav2*$^{-/-}$*3*$^{-/-}$ mice at indicated times from BDNF stimulation. Data Plot: Normalized spine head areas from *wild-type* and *Vav2*$^{-/-}$*3*$^{-/-}$ mice at times before and after BDNF addition to slice. (*$p<0.05$, two-way ANOVA, genotype and time, n=6 (*wild-type)*, n=8 (*Vav2*$^{-/-}$*3*$^{-/-}$)). For all experiments (A-E), n=6 (*wild-type)* and n=8 (*Vav2*$^{-/-}$*3*$^{-/-}$). Each n represents an average of five randomly-chosen dendritic spines from one dendritic length. One dendritic length per slice was imaged and averaged to give an average spine behavior per dendrite. **B**, Percent increase of mean spine head size at 10-15 minutes post-BDNF compared to first 5 minutes after BDNF application (*$p<0.05$, student's t-test). **C**, Plot of the percent increase in spine head size vs. initial spine head area, demonstrating that similar range of spine heads were analyzed and that the failure of Vav KO spine head growth with BDNF treatment is not due to occlusion. **D**, Plot of cumulative dendritic spine length of *wild-type* and *Vav2*$^{-/-}$*3*$^{-/-}$ neurons from pre-BDNF treated spines in **A**. **E**, Dendritic spine densities of *wild-type* and *Vav2*$^{-/-}$*3*$^{-/-}$ neurons, cultured and imaged in **A**.

Figure 2.5. Vav GEFs mediate synaptic plasticity in the hippocampus.

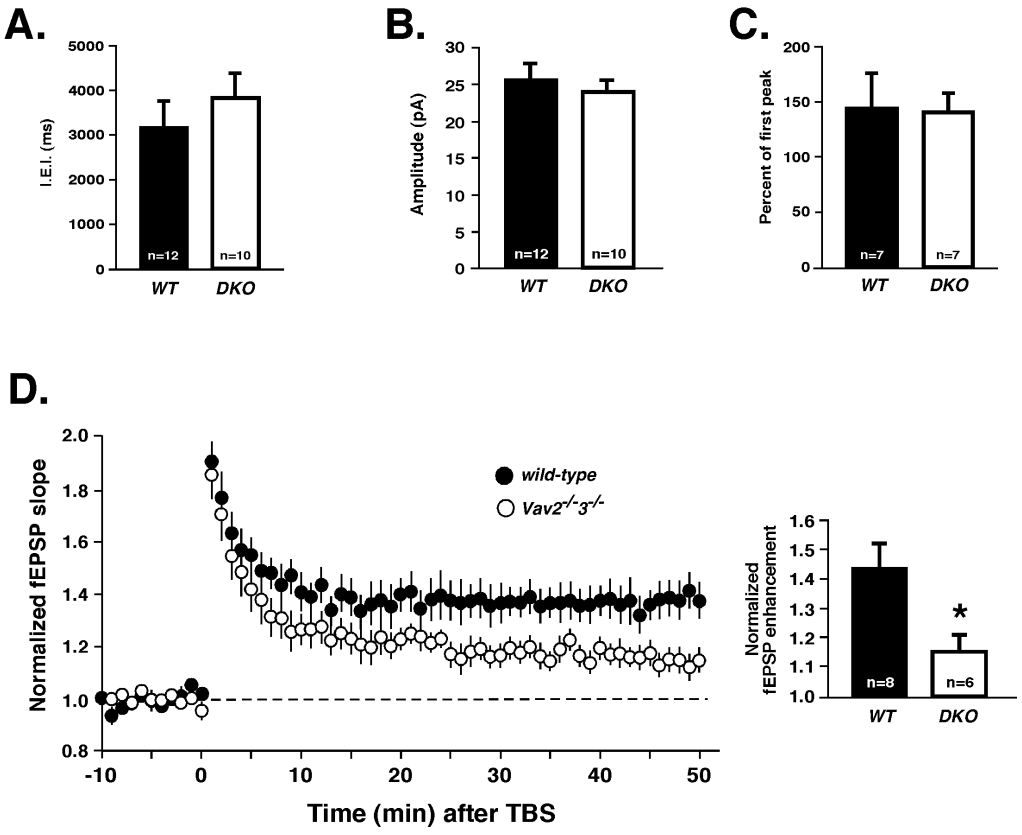

Figure 2.5. Vav GEFs mediate synaptic plasticity in the hippocampus. A, Average inter-event interval (IEI) per neuron from *wild-type* or *Vav2*$^{-/-}$*3*$^{-/-}$ CA1 pyramidal neurons (n.s., student's t-test). **B**, Average mEPSC amplitude per neuron from same recordings as in (B), (n.s., student's t-test). **C**, Paired-pulse stimulation (10 Hz). Average paired-pulse ratio measured as the percent of the second pulse relative to the first (n.s., student's t-test). **D**, Left: Field EPSPs (fEPSPs) were recorded from CA1 of P15 *wild-type* or *Vav2*$^{-/-}$*3*$^{-/-}$ acute hippocampal slices (300 μm) in response to two theta burst stimulation of Schaffer collaterals. Right: The fEPSP slopes were normalized for each genotype. Normalized fEPSP enhancement at 40-50 minutes is shown (*$p<0.05$, student's t-test).

Figure 2.6. Kinase-active TrkB activates Vav2 independently of the ERK/PI3K and PLCγ-interacting sites.

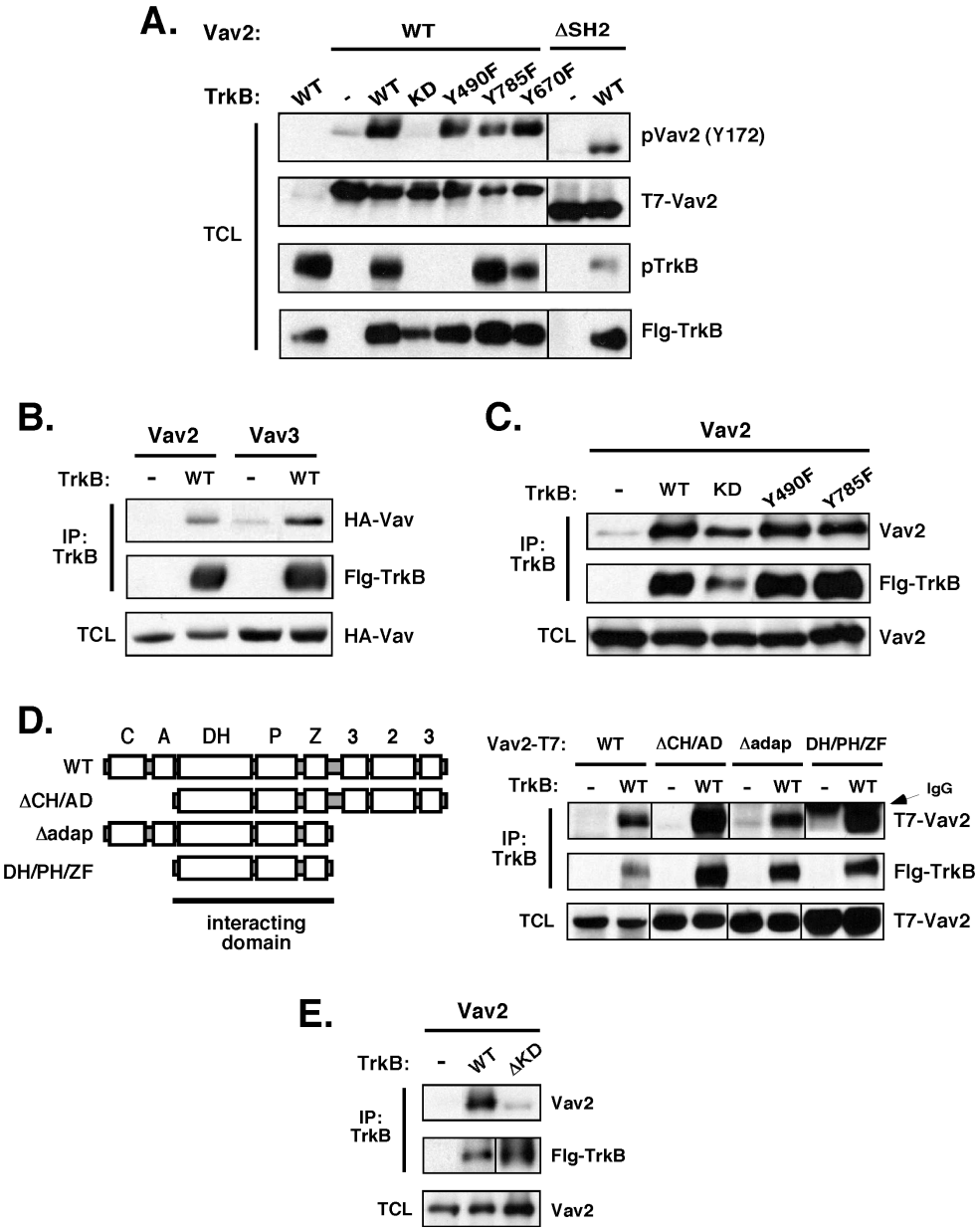

Figure 2.6. Kinase-active TrkB activates Vav2 independently of the ERK/PI3K and PLCγ-interacting sites. A, Co-expression of TrkB and Vav2 increases phospho-Vav2 (Y172) in HEK293T cells. HEK293T cells were

transfected with T7-tagged wild-type or ΔSH2 and Flag-tagged wild-type or mutant TrkB. Total cell lysates were blotted with anti-phospho-Vav2 (Y172), anti-T7 (Vav2), anti-phospho-TrkB (Y490), and anti-TrkB antibodies. KD, kinase-dead. For all panels (A-E), results are representative findings from three independent experiments. **B**, TrkB binds Vav2 and Vav3 in HEK293T cells. HEK293T cells were transfected with HA-tagged Vav2 or Vav3 and Flag-tagged TrkB. Total cell lysates were immunoprecipitated with anti-Flag antibody, then immunoblotted with anti-HA (Vav) and anti-Flag (TrkB) antibodies. Whole-cell lysates were blotted with anti-HA (Vav) antibody. **C**, TrkB binds Vav2 independently of TrkB kinase activity. T7-tagged Vav2 was coexpressed with Flag-tagged TrkB (wild-type), TrkB-KD (kinase dead: K571N), TrkB-Y490F, or TrkB-Y785F. Total cell lysates (TCL) were immunoprecipitated with anti-Flag antibody, then immunoblotted with anti-Vav2 and anti-Flag (TrkB) antibodies. Whole-cell lysates were blotted with anti-Vav2 antibody. **D**, Deletion analysis of Vav2 identifies the DH/PH/ZF region as sufficient to mediate co-association with TrkB. Domain composition of full-length and Vav2 deletion mutants that were generated. C, calponin homology domain; A, acidic domain; DH, Dbl homology domain; P, pleckstrin homology domain; Z, zinc finger domain; P, proline-rich domain; 3, Src homology type 3 domain (SH3); 2, Src homology type 2 domain (SH2). HEK293T cells were transfected with Flag-tagged TrkB (wild-type) and T7-tagged Vav2 (wild-type), Vav2-ΛCH/AD, Vav2-Λadaptor, or Vav2-DH/PH/ZF. Total cell lysates were immunoprecipitated with anti-Flag antibody and immunoblotted with anti-T7 (Vav2) and anti-Flag (TrkB) antibodies. Whole-cell lysate was blotted with anti-T7 (Vav2) antibody. **E**, TrkB's kinase domain is required for its interaction with Vav2. T7-tagged Vav2 was coexpressed with wild-type or Δ kinase domain (ΔKD)-TrkB. Total cell lysates were immunoprecipitated with anti-Flag antibody and immunoblotted with anti-Vav2 and anti-Flag (TrkB) antibodies. Whole-cell lysate was blotted with anti-Vav2 antibody.

Figure 2.7. Model for the role of Vav GEFs in BDNF/TrkB-induced dendritic spine growth and functional synapse plasticity.

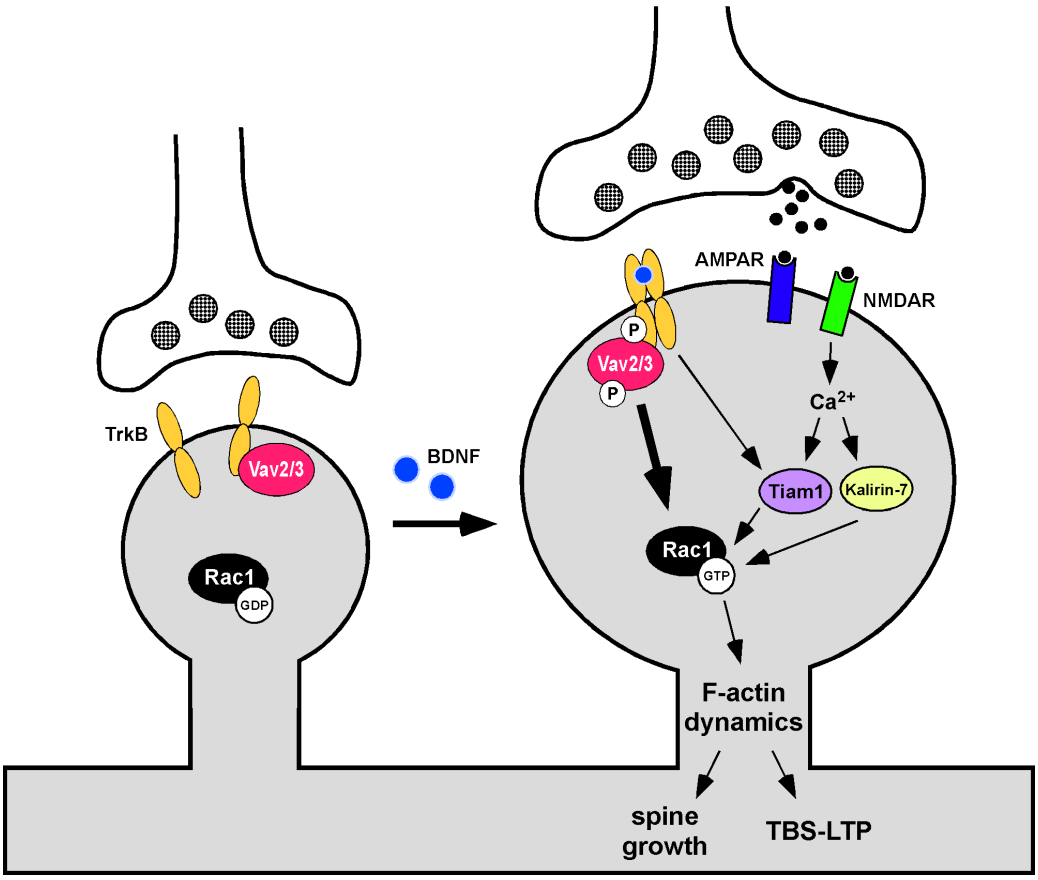

CHAPTER THREE: Vav Guanine Nucleotide Exchange Factors (GEFs) Mediate Learning and Memory and Anxiety Behaviors in Mice

Summary

Vav-family guanine nucleotide exchange factors (GEFs) have emerged as important modulators of neuronal development and function. Most recently, we discovered that Vav GEFs are localized at excitatory synapses and are required for BDNF-induced Rac-GTP formation in hippocampal slices. Importantly, Vav-deficient neurons have impaired brain-derived neurotrophic factor (BDNF)-induced dendritic spine growth and theta burst-stimulated CA3-CA1 long-term potentiation (LTP), suggesting that Vav-dependent F-actin dynamics are critical for these synapse plasticity events. Despite the emergence of these molecular and cellular functions for Vav proteins, a role for the GEFs in mediating animal behavior has not yet been investigated. Here, we report that *Vav2*$^{-/-}$*3*$^{-/-}$ mice have impaired context, but not cue-dependent, fear conditioning. *Vav2*$^{-/-}$*3*$^{-/-}$ mice also exhibit reduced anxiety-like behavior in elevated plus maze and open field tests. Further analysis of single Vav2 and Vav3 knockouts reveals that these genes are each necessary for normal contextual fear conditioning, while only Vav2 is required for normal anxiety-like behaviors. Together, these studies implicate Vav GEFs as critical regulators of normal learning and memory and anxiety behaviors

in mice, and furthermore, suggest that their molecular and cellular roles in neuronal development and synapse plasticity may underlie these behaviors.

Introduction

Initially identified as oncogenes and regulators of hematopoietic cell development and signaling, Vav GEFs now have numerous identified roles in regulating various aspects of brain development and function. The Vav family comprises three distinct genes, *Vav1-3*, in vertebrates (Bustelo, 2000). Of these, Vav2 and Vav3 are highly expressed in the brain from embryonic development through adulthood (Cowan et al., 2005; Hale et al., 2011; Turner and Billadeau, 2002), and are localized at excitatory synapses (Hale et al., 2011).

Vav GEFs regulate the activity of Rho-family GTPases, regulators of the actin cytoskeleton that have documented roles in dendritic spine formation and plasticity (Luo, 2002; Tashiro and Yuste, 2004). Rho-family GTPases, including Rho, Rac, and Cdc42, act as molecular switches, cycling between inactive GDP-bound and active GTP-bound states. GEFs activate GTPases by facilitating the exchange of GDP for GTP, while GAPs (GTPase activating proteins) render GTPases inactive by accelerating GTP hydrolysis (Cerione and Zheng, 1996). Studies suggest that Vav proteins specifically activate Rac1 and Cdc42 (Abe et al., 2000; Liu and Burridge, 2000; Marignani and Carpenter, 2001), Rho GTPases that promote spine formation and enlargement (Nakayama et al., 2000; Tashiro et

al., 2000). Furthermore, it has recently been demonstrated that Vav exhibits a preference for activating Rac1 over Cdc42 (Kawakatsu et al., 2005; Marignani and Carpenter, 2001).

Increasing evidence supports the coupling of functional synapse plasticity and dendritic spine structural dynamics, particularly in long-lasting forms of plasticity, including long-term potentiation (LTP) a widely hypothesized functional correlate of learning and memory. (Cingolani and Goda, 2008; Dillon and Goda, 2005; Yuste and Bonhoeffer, 2001). During LTP, dendritic spines undergo F-actin cytoskeletal remodeling and enlargement, which is hypothesized to facilitate the accumulation of α-amino-3-hydroxy-5-methyl-4-isoxazolepropionic (AMPA) receptors to strengthen synapses (Matsuzaki et al., 2004; Okamoto et al., 2004). Activation of Rac1 in neurons induces spine morphology changes associated with LTP, specifically dendritic spine enlargement (Tashiro and Yuste, 2004). Furthermore, its overexpression leads to synapse strengthening by promoting AMPA receptor clustering in spines (Wiens et al., 2005). Together, these studies suggest that Rac1 promotes dendritic spine cytoskeletal remodeling events to support the functional synapse changes underlying LTP.

BDNF and its cognate receptor, TrkB are well-established positive modulators of hippocampal LTP and dendritic spine growth, and increasing evidence demonstrates that BDNF/TrkB-induced Rac-GTP activation may

facilitate these plasticity events by stimulating F-actin remodeling and cytoskeletal dynamics. A recent study reported that BDNF promotes theta burst-induced increases in dendritic spine F-actin levels, and that sequestering BDNF impairs CA3-CA1 TBS-LTP, revealing that BDNF may facilitate LTP by enhancing F-actin remodeling in dendritic spines (Rex et al., 2007). Furthermore, a protocol pairing local glutamate uncaging with postsynaptic spikes results in increased dendritic spine head size, a long-lasting structural event demonstrated to require BDNF/TrkB kinase signaling (Tanaka et al., 2008).

Because Rac1 is the major effector of Vav GEFs, and Vav GEFs are tyrosine phosphorylated and activated by receptor tyrosine kinases, we previously speculated that Vav might be required for BDNF-dependent synapse plasticity events. In testing this hypothesis, we observed that Vav GEFs are tyrosine phosphorylated and activated by BDNF/TrkB stimulation in hippocampal slices, and are required for BDNF-induced Rac-GTP formation (Hale et al., 2011). Importantly, BDNF-dependent dendritic spine growth and CA3-CA1 TBS-LTP are impaired in Vav-deficient hippocampal slices (Hale et al., 2011), suggesting that Vav-dependent F-actin dynamics and regulation of dendritic spine morphology facilitates functional synapse plasticity.

Our findings propose the interesting possibility that Vav-dependent functional and structural synapse plasticity may control behavioral responses, and furthermore, that the GEFs may regulate behaviors mediated by BDNF/TrkB. One

of the most well-studied BDNF/TrkB-dependent behaviors is learning and memory, including hippocampal-dependent contextual fear conditioning and Morris water maze tests. BDNF heterozygote mice exhibit impaired context-dependent fear conditioning (Liu et al., 2004), without a change in cue-dependent fear conditioning, while TrkB conditional knockouts have deficits in contextual and cued fear conditioning (Minichiello et al., 1999). BDNF or TrkB conditional knockout mice also display deficits in the Morris water maze, a hippocampal-dependent spatial navigation task (Gorski et al., 2003; Minichiello et al., 1999). Numerous additional BDNF/TrkB-dependent behaviors in mice have been identified, including anxiety, depression, and in behaviors associated with addiction to drugs of abuse.

We report here that Vav GEFs are required for normal learning and memory, as well as anxiety behaviors in mice. We find that similar to BDNF-deficient mice, *Vav2*$^{-/-}$*3*$^{-/-}$ knockouts have deficits in context-, but not cue-, dependent fear conditioning, but exhibit no impairments in the Morris water maze. Additionally, Vav-deficient mice show reduced anxiety-like phenotypes in open field and elevated plus maze tests. Analysis of the contribution of the individual Vav genes indicates that both Vav2 and Vav3 are required for context-dependent fear conditioning, while only Vav2 supports normal anxiety responses. Together, these studies indicate that Vav GEFs, which are important regulators of hippocampal LTP and BDNF-induced dendritic spine growth, also mediate

normal hippocampal-dependent learning and memory, as well as anxiety behaviors in mice.

Materials and Methods

Behavior studies

Behavior studies were performed with adult male littermates between three and six months of age. All knockout mice used in this study were backcrossed to C57BL/6N (Charles River) for more than 10 generations. Mice were housed on a 12 hr light-dark cycle. Procedures were in accordance with the Institutional Animal Care and Use (IACUC) guidelines.

Locomotor activity

Mice were individually placed into new home cages with a thin layer of fresh bedding. Locomotor activity was measured for 2 hr using acquisition software linked to infrared beams evenly spaced across the length of each cage (San Diego Instruments). Activity was collected in five-minute bins.

Open field test

Mice were individually placed into a 72 cm-diameter square box and their activity was recorded for 6 minutes using Ethovision video-tracking (Noldus).

Overall locomotor activity, and time spent in the center and peripheries of the box were measured.

Elevated-plus maze

Mice were placed in the center of an elevated-plus maze (arms are 33 x 5 cm, opposing "closed" arms have 25 cm tall walls) and allowed to explore the maze for 5 min. Amount of time spent in the open arms, closed arms, and center of the maze was recorded using Ethovision video-tracking (Noldus).

Morris water maze

For MWM studies, we used a white, plastic, circular pool filled with opaque water (22 ± 1°C) in a room with extra-maze visual cues. During training, mice were given 8 trials per day for 5 consecutive days. The mice were placed in the pool at one of four start locations, with locations being randomized for each trial. Mice were allowed to swim until they reached a submerged platform, or until 60 s had elapsed. Time to reach the platform, distance traveled to reach the platform, swim speed, and thigmotaxis were measured using Ethovision video-tracking (Noldus). The probe trial (a 60 s free swim with the platform removed), was performed on Day 6, the day following the final training session. The amount of time spent in each quadrant of the pool, as well as the number of platform location crossings by the mouse were measured.

Fear conditioning

For training (Day 1), mice were individually placed into fear conditioning chambers (Med Associates) for 6 min, in which they were exposed to 3 30 s white noise tones that each co-terminated with a 2 s (0.5 mA) shock. The tone-shock pairings were separated by 1 min intervals. On Day 2, context-dependent fear conditioning was assessed by placing the mice into the same context as in Day 1, but without tone or shock. The mice remained in the chamber for 5 min, during which their movement was videotaped and the amount of time spent freezing was measured using FreezeFrame software. On Day 3, cue-dependent fear conditioning was assessed by placing the mice into the chamber in which various contextual alterations had been made. Time spent freezing was measured over 6 min, the first three minutes without tone and the last three minutes with continuous tone. Changes in context included introduction of vanilla scent, insertion of a smaller plastic box within the chamber, and placement of smooth plastic flooring over the shock-grid flooring. Following the conclusion of the tests, footshock sensitivity of the mice was determined. Mice were placed into the fear conditioning chamber and exposed to intermittent footshocks of increasing intensity (between 0 and 0.35 mA). The lowest shock intensities to elicit flinching, jumping, and vocalizations were measured.

Results

Vav GEFs are required for context-, but not cue-dependent fear conditioning

Vav-deficient mice have impaired BDNF-induced dendritic spine head growth and a concomitant deficiency in theta burst-induced hippocampal CA3-CA1 LTP, a widely hypothesized functional correlate of learning and memory (Hale et al., 2011). As a result of these findings, we speculated that Vav knockouts may exhibit impairments in behavioral learning and memory paradigms demonstrating dependence on BDNF/TrkB and intact hippocampal circuitry, including context-dependent fear conditioning, and the Morris water maze. Importantly, to minimize genetic and experimental variability, mice used in this and all subsequent behavioral assessments examined, were age-matched and had been backcrossed to the C57BL/6N strain in excess of 10 generations. We also tested all mice for alterations in locomotor activity, and observed no differences in activity levels of *Vav2*$^{-/-}$*3*$^{-/-}$, *Vav2*$^{-/-}$, and *Vav3*$^{-/-}$ mice in comparison to WT mice (Fig. 3.1 and 3.3).

Vav2$^{-/-}$*3*$^{-/-}$ mice were first examined for their performance in contextual and auditory cue fear conditioning. Lesion studies indicate that while cue-dependent conditioning relies primarily on the amygdala, the context-dependent counterpart also requires the hippocampus, as damage to the formation leads to impaired context-dependent but not auditory cue fear conditioning (Rudy et al., 2004; Rudy and O'Reilly, 1999). The fear conditioning assay was carried out over

three days, in which on the first day, mice were individually placed in a chamber and exposed to three tone-shock pairings. On the second day, the mice were returned to the chamber (same context as day 1) and freezing behavior was measured. We observed that Vav2/3 double knockouts (DKOs) spent significantly less time freezing in comparison to WT mice over a 5-minute observation period (Fig. 3.2A, left, $p<0.05$, Student's t-test). Importantly, footshock sensitivity tests revealed no difference between WT and Vav DKO mice in shock intensities required to elicit flinch, jump, and vocalization responses, suggesting that reduced freezing in the context was due to a deficit in learning and not differences in pain sensitivities (Fig. 3.2A, right).

On the third day, cue-dependent fear conditioning was assessed. Mice were placed into the fear conditioning box in which contextual modifications had been introduced (change in scent, appearance, and flooring texture), and freezing behavior was subsequently measured before and during presentation of tone. No difference was observed between WT and Vav DKO mice in time spent freezing in response to the cue (Fig. 3.2A, left, Cue test during tone). A significant difference emerged in baseline freezing in the "new" context, in which WT mice spent more time freezing than Vav DKOs before the tone was played ($p<0.05$, Student's t-test). This may indicate that despite changes to the context, sufficient similarities were present to provoke freezing responses in WTs, but not in the Vav-deficient mice, which were impaired in learning the tone-context association.

Overall, findings from the fear conditioning tests provide evidence that Vav2 and Vav3 are required for hippocampal-dependent contextual fear conditioning. In contrast, auditory cue fear conditioning remains intact in Vav-deficient mice.

$Vav2^{-/-}3^{-/-}$ mice are not impaired in spatial learning in the Morris water maze

Because Vav GEFs are necessary for normal hippocampal CA3-CA1 LTP and context-dependent fear conditioning, we speculated that they might also be required for performance in the Morris water maze, a well-described BNDF/TrkB- and hippocampal-dependent spatial learning and memory task. To examine this hypothesis, mice were trained to locate the hidden platform for five consecutive days, undergoing eight training sessions during each day. On the sixth day, a probe test was performed following removal of the platform, and various measurements were recorded, including percent time spent in each quadrant, and number of times the target platform was crossed. We found that Vav DKOs exhibited no differences in comparison with WTs in these examined measures (Fig. 3.2B), suggesting that while Vav GEFs are required for hippocampal-dependent contextual fear conditioning, they do not mediate hippocampal spatial learning and memory in the Morris water maze.

Deficiency of Vav2 or Vav3 leads to impaired context-dependent fear conditioning

Vav2$^{-/-}$*3*$^{-/-}$ mice have impaired context-dependent fear conditioning, but it remains unclear whether one or both genes are responsible for mediating the observed deficiency. Additionally, it might be reasonable to expect no differences to emerge between WT and *Vav2*$^{-/-}$ or *Vav3*$^{-/-}$ mice. This finding could indicate the existence of compensatory mechanisms, a potentially likely result since and Vav2 and Vav3 proteins have redundant GEF functions, and are also similarly regulated by BDNF/TrkB and other signaling pathways (Bustelo, 2000; Hale et al., 2011).

To probe these possibilities, responses of *Vav2*$^{-/-}$ and *Vav3*$^{-/-}$ mice were examined in the fear conditioning assay, executed as in Figure 3.2. Vav2- or Vav3-deficient mice have impaired context-dependent fear conditioning, both showing reductions in comparison to WT littermates in percent time spent freezing to the same context on day 2 of experimentation (Fig. 3.4A and B, Vav2 KO: $p<0.05$, Student's t-test; Vav3 KO: $p<0.05$, Student's t-test). Surprisingly, although we did not observe any differences in the cue-dependent task in Vav DKOs, a significant reduction was detected in percent time spent freezing during presentation of the tone in *Vav2*$^{-/-}$ but not *Vav3*$^{-/-}$ mice (Fig. 3.4A and B, Vav2 KO: $p<0.05$, Student's t-test). Despite the statistical significance of the Vav2 KO effect, the effect size is quite small and since it was not present in the Vav2/3 DKO, the confidence in this Vav2 KO finding is not high. Overall, results from

these studies demonstrate that both Vav2 and Vav3 individually contribute to hippocampal-dependent contextual fear conditioning.

Vav GEFs mediate anxiety-related behaviors

BDNF and TrkB have been implicated in anxiety-related behaviors, and because Vav GEFs are activated by BDNF/TrkB signaling, we speculated that Vav may also have a role in anxiety paradigms. *Vav2*$^{-/-}$*3*$^{-/-}$ mice exhibited reduced anxiety in the elevated plus maze, spending more time in the center and open arms of the maze (Fig. 3.5A, $p<0.05$, Student's t-test), while spending less time in the closed arms (Fig. 3.5A, $p<0.01$, Student's t-test). In the open field test, the mice spent an increased length of time in the non-periphery of the field (Fig. 3.5B, $p<0.05$, Student's t-test), and less time in the periphery over the 5-minute period (Fig. 3.5B, $p<0.05$, Student's t-test), indicative of an anxiolytic phenotype that is consistent with elevated plus maze results. Together, these findings illustrate that Vav GEFs are important in promoting behaviors associated with anxiety. In the future, it will be interesting to examine effects of Vav deficiency in responses of mice in depression-associated tasks, as anxiety and depression commonly exhibit comorbidity.

Vav2$^{-/-}$, but not Vav3$^{-/-}$ mice display reduced anxiety

Mice lacking Vav2 and Vav3 have reduced anxiety in the elevated plus maze and open field tests. To identify whether Vav2 or Vav3 mediates the anxiety-related phenotype in Vav DKO mice, or whether a compensatory mechanism is present, we measured performance of Vav single knockouts in these tasks. In the elevated plus maze, Vav2 KOs spent significantly more time in the center and open arms of the maze (Fig. 3.6A, $p<0.05$, Student's t-test), and conversely, spent less time in the closed arms (Fig. 3.6A, $p<0.001$). While no differences emerged in the open field test, the Vav2 KO mice exhibited a trend towards a reduced anxiety phenotype, and this effect may reach significance with an increased sample size (Fig. 3.6B). Unlike the *Vav2$^{-/-}$* mice, the Vav3-deficient mice revealed no differences in the elevated plus maze or open field test, suggesting that only Vav2 regulates the anxiety-associated behaviors in mice (Fig. 3.6C and D). Future experiments will be necessary to delineate the mechanisms by which Vav2 regulates anxiety-like behaviors in mice.

Discussion

In this study, we report an essential role for Vav GEFs in mediating normal hippocampal-dependent learning and memory, as well as anxiety-like behaviors, in mice. We find that *Vav2$^{-/-}$3$^{-/-}$* mice have reduced context-dependent fear conditioning and a reduced anxiety phenotype in open field and elevated plus

maze tests. Further investigation demonstrates that deficiency of Vav2 or Vav3 individually leads to impaired context-dependent fear conditioning, while only Vav2 facilitates normal anxiety behavior.

Recently published studies that describe roles for Vav in regulating cerebellar development, motor coordination, and visual circuit formation evoke the possibility that any reported behavioral impairments may occur as a consequence of these deficiencies. A recent study reported a role for Vav3 in cerebellar Purkinje and granule cell function, and motor coordination and gaiting (Quevedo et al., 2010). In the study, Purkinje cells from *Vav3*$^{-/-}$ mice were found to have deficient dendritic arborization *in vivo*, while granule cells in the internal and external granule layers of Vav3-deficient mice exhibited decreased survival and impaired migration, respectively. Importantly, analyses of motor coordination and gaiting in *Vav3*$^{-/-}$ mice at five weeks of age revealed impaired performance in the rotarod accelerating test and abnormal pattern of paw overlap (Quevedo et al., 2010). However, by four months of age, the approximate age in which we performed our behavioral studies, these problems were corrected or significantly ameliorated. Importantly, the Vav DKO mice used in our study were not hyper- or hypoactive, exhibited no gross motor coordination deficits, and displayed normal magnitudes of speed in all tasks assessed.

An additional concern for analyses of behavioral performance of the Vav KO mice is the potential for visual impairments, as a recent study reported

impaired ipsilateral axon projections from RGCs to the dLGN in *Vav2*$^{-/-}$*3*$^{-/-}$ mice (Cowan et al., 2005). However, our studies indicate that the Vav knockouts did not possess deficient vision, as overall, Vav single and double knockout mice exhibited learning of the platform location in the Morris water maze, and also easily located the escape platform when made visible.

The hippocampus is required for contextual fear conditioning, and is also highly implicated in anxiety and stress. Vav GEFs are required for BDNF-induced dendritic spine growth of CA1 pyramidal neurons and CA3-CA1 LTP (Hale et al., 2011), suggesting that Vav-dependent postsynaptic structural and functional synapse plasticity in the hippocampus may underlie or contribute to the learning and anxiety behaviors observed here. As total knockout mice were used in these studies, it is possible that Vav-dependent functions in other brain regions may account for or contribute to the observed behavioral effects in Vav-deficient mice. Furthermore, a developmental role for Vav GEFs that occurs prior to the reported deficits in dendritic spine and synapse plasticity may underlie or promote the behavioral responses. One potential experiment to investigate these concerns is to examine whether re-expressing and restoring Vav-dependent functions in the hippocampus is sufficient to rescue deficits in contextual fear conditioning and anxiety. Notably, the generation and analysis of Vav conditional knockout mice would be important to resolve these remaining questions and identify the specific circuitry by which Vav GEFs facilitate normal behavioral responses.

In this study, we hypothesized that Vav GEFs might mediate BDNF/TrkB-dependent behaviors, and therefore, that Vav KO mice would mimic behavior phenotypes that result from BDNF/TrkB deficiency. In learning tasks, heterozygous BDNF mice display reduced freezing to the context in fear conditioning, and BDNF conditional knockouts are impaired in the Morris water maze (Gorski et al., 2003; Liu et al., 2004). Furthermore, mice in which TrkB is knocked out in the forebrain exhibit deficits in the Morris water maze, as well as impaired contextual and cued fear conditioning (Minichiello et al., 1999). While BDNF's role in learning is well-established, a function for the neurotrophin in modulating anxiety has not been as extensively studied and results are often inconsistent. Heterozygous BDNF mice are reported to have increased anxiety in open field and elevated plus maze tests (Chen et al., 2006). A separate study describes that forebrain deletion of BDNF in mice leads to reduced anxiety in female mice in elevated plus maze and open field tests, with no differences observed in male mice (Monteggia et al., 2007). Here, we found that similar to BDNF- or TrkB-deficient mice, *Vav2*$^{-/-}$*3*$^{-/-}$ mice have impaired contextual fear conditioning; however, the behavior of Vav KOs in Morris water maze and anxiety tests are generally inconsistent with reports for BDNF and TrkB-deficient mice, suggesting that Vav GEFs may regulate a subset of behaviors controlled by BDNF/TrkB function.

Because hippocampal slices lacking Vav proteins display impaired CA3-CA1 TBS-LTP, we hypothesized that deficits in hippocampal-dependent learning and memory tasks may be present in Vav KO mice, and therefore assayed their responses in related behavioral paradigms. Interestingly, we observed that Vav-deficient mice have impairments in context-dependent fear conditioning, but not Morris water maze, learning and memory tasks that both rely on the intact hippocampal formation. While it may be expected that these tasks would yield similar concurrent deficits, recent work suggests that while place learning in the Morris water maze depends only on the hippocampus, corticohippocampal circuitry is required for the formation of an association between the context and the footshock in fear conditioning (Burwell et al., 2004). Specifically, a combination of perirhinal, postrhinal, and entorhinal lesions cause impaired contextual fear learning without impinging on learning in the Morris water maze. In contrast, the hippocampus is required for both, as hippocampal lesion alone resulted in deficient contextual fear conditioning and water maze navigation. Groups speculate that unlike exclusively spatial tasks, contextual tasks require higher-order processing of polymodal sensory information from the environment, and therefore, that spatial and contextual tasks require different brain systems. These findings may suggest that Vav function in cortical regions surrounding the hippocampus may be critical for associative fear conditioning, but is unnecessary for the Morris water maze spatial learning task.

In this study, we observe that *Vav2*$^{-/-}$*3*$^{-/-}$ have reduced anxiety, and further analysis of single knockouts indicates that Vav2, and not Vav3, mediates the anxiolytic phenotype in mice. In the future it will be interesting to investigate the mechanisms by which Vav2 specifically controls anxiety-related behavior. One possibility may be differences in expression levels of Vav2 and Vav3 in brain circuitry that underlies anxiety. To date, a detailed examination of Vav2 and Vav3 expression in specific brain regions has not been reported. It will thus be informative to investigate patterns of Vav2 and Vav3 expression in the brain from development through adulthood, which may have implications for cellular and behavioral functions for Vav proteins.

As additional functions for Vav GEFs in controlling development and plasticity continue in animal models continue to emerge, we may also expect future discoveries to implicate the GEF in regulating plasticity and behaviors associated with human disorders. It will therefore be critical to analyze a requirement for Vav GEFs in modulating additional behaviors, including in behaviors relevant to schizophrenia, addiction to drugs of abuse, and depression.

A recent genome wide association study (GWAS) of schizophrenia in a Japanese population was the first study to report a strong association signal in a region of *VAV3*, rs1410403 (Ikeda et al., 2011). Following this discovery, a separate study sought to examine whether rs1410403 is associated with altered brain structure in healthy and schizophrenic individuals, and also performed exon

resequencing for further mutation analysis (Aleksic et al., 2013). Previously published studies utilizing voxel-based morphometry (VBM) have reported the observation of smaller volumes in the temporal gyrus of schizophrenic individuals, a brain region that promotes the formation of language and semantic memory processing, visual perception, and multimodal sensory integration, cognitive processes that are deficient in patients with schizophrenia (Onitsuka et al., 2004). Interestingly, Vav3 is more highly expressed than Vav2 in the left superior and medial temporal gyri, suggesting that Vav3 may be more likely to impinge on region-specific functions that are deficient in individuals with schizophrenia, including formation of language and semantic memory processing, and multimodal sensory integration. Using VBM, it was discovered that rs1410403 is associated with a reduction in volume of the left superior and middle temporal gyri in patients with schizophrenia. As a result of mutation analysis, four rare novel missense mutations in *VAV3* were also detected, one of which, Glu741Gly was found to be significantly associated with schizophrenia in a large independent sample (P=0.02). Future experiments will be necessary to explore the mechanism by which Glu741Gly, located within the SH2 domain of Vav3, affects the pathogenesis of schizophrenia.

Regulation of actin-remodeling proteins has also been demonstrated to control behaviors associated with addiction to drugs of abuse, promoting speculation that GEFs may have a role in mediating behaviors induced by use of

illicit drugs. A recent study reported that repeated cocaine administration in mice negatively regulates Rac-GTP levels in the nucleus accumbens (NAc), a critical region in the brain reward pathway (Dietz et al., 2012). Down-regulation of Rac1 in mice promoted conditioned place preference to cocaine, and conversely, overexpression of active Rac1 blocked the reward to cocaine. This finding evokes that possibility that Vav or other Rho-family GEFs may contribute to activation of Rac1 in response to drugs of abuse to facilitate behavioral consequences. Indeed, a fellow Rho-family GEF, Kalirin-7, has already been implicated in controlling cocaine-dependent behaviors, as mice lacking Kalirin-7 show increased cocaine locomotor sensitization and have increased cocaine self-administration rates (Kiraly et al., 2013). These findings indicate that Kalirin-7, and suggestively increased Rac-GTP levels, may antagonize the rewarding effects of cocaine, a hypothesis that is consistent with findings from the Dietz *et al*. (2012) study.

The findings described here introduce a novel role for Vav GEFs in regulating learning and memory, as well as anxiety behaviors in mice. Specifically, we report that *Vav2*$^{-/-}$*3*$^{-/-}$ mice have impaired contextual, but not cued, fear conditioning, while displaying no deficits in the Morris water maze. *Vav2*$^{-/-}$*3*$^{-/-}$ mice also have an anxiolytic phenotype in elevated plus maze and open field tasks, suggesting that Vav GEFs promote normal anxiety behaviors in mice. Investigation of Vav single knockouts reveals that Vav2 and Vav3 individually contribute to context-dependent fear conditioning, but only Vav2 controls normal

anxiety responses in mice. Together, these studies describe that Vav GEFs mediate learning and memory and anxiety behaviors in mice, and suggest that their documented functions in neuronal development and synapse plasticity may contribute to these behaviors.

Figure 3.1. *Vav2/3 DKO* mice have normal locomotor activity.

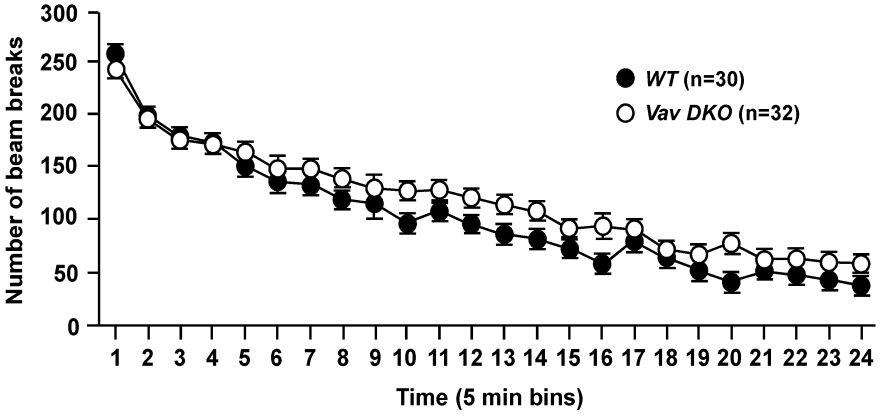

Figure 3.1. *Vav2/3 DKO* mice have normal locomotor activity. Locomotor activity was measured for 2 hr. Number of beam breaks collected in 5 min bins is indicated.

Figure 3.2. Vav2/3 GEFs are required for context-dependent fear conditioning.

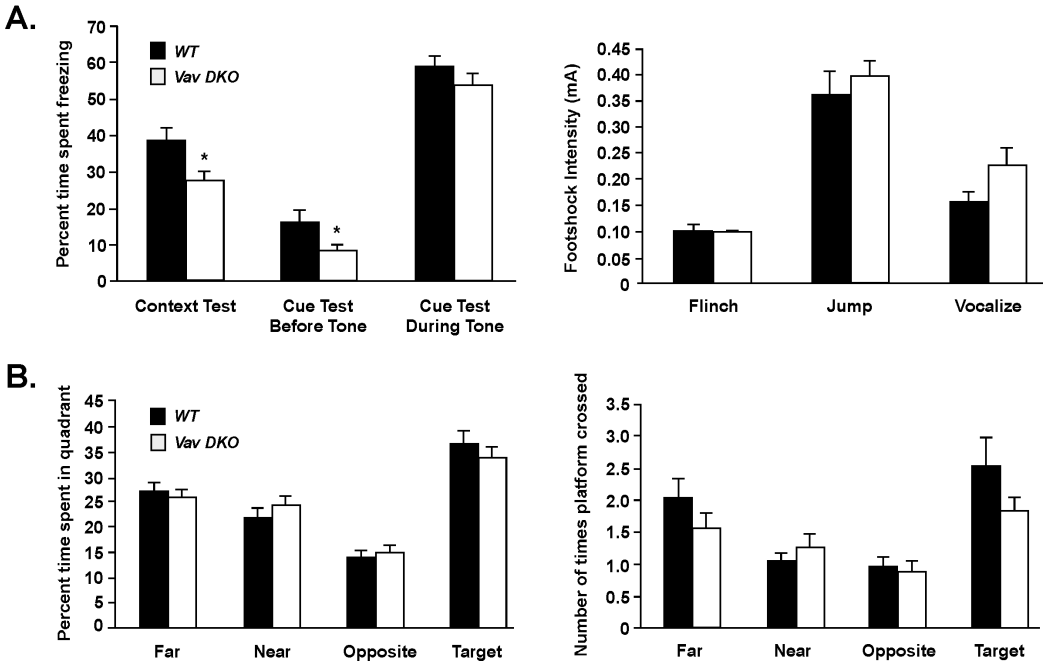

Figure 3.2. Vav2/3 GEFs are required for context-dependent fear conditioning. A, (Left) Context: Percent time spent freezing 24 hr after training. *Vav DKO* mice spent significantly less time freezing than *WT* mice (*p<0.05). Cue: Percent time spent freezing before and during tone. *Vav DKO* mice spent less time freezing than *WT* mice before tone (*p<0.05). No significant difference between *Vav DKO* and *WT* mice was observed in percent time spent freezing during tone. (Right) Footshock intensities required to elicit flinch, jump, and vocalization responses were not different between *Vav DKO* and *WT* mice. (*WT*: n=29; *Vav DKO*: n=32) **B**, *Vav DKO* mice are not impaired in the Morris water maze spatial learning task. (Left) Mice were trained in the Morris water maze for five consecutive days, with eight trials per day. On Day 6 (probe), percent time spent in quadrant, and number of platform crossings were measured. (*WT*: n=29; *Vav DKO*: n=32)

Figure 3.3. *Vav2* and *Vav3 KO* mice have normal locomotor activity.

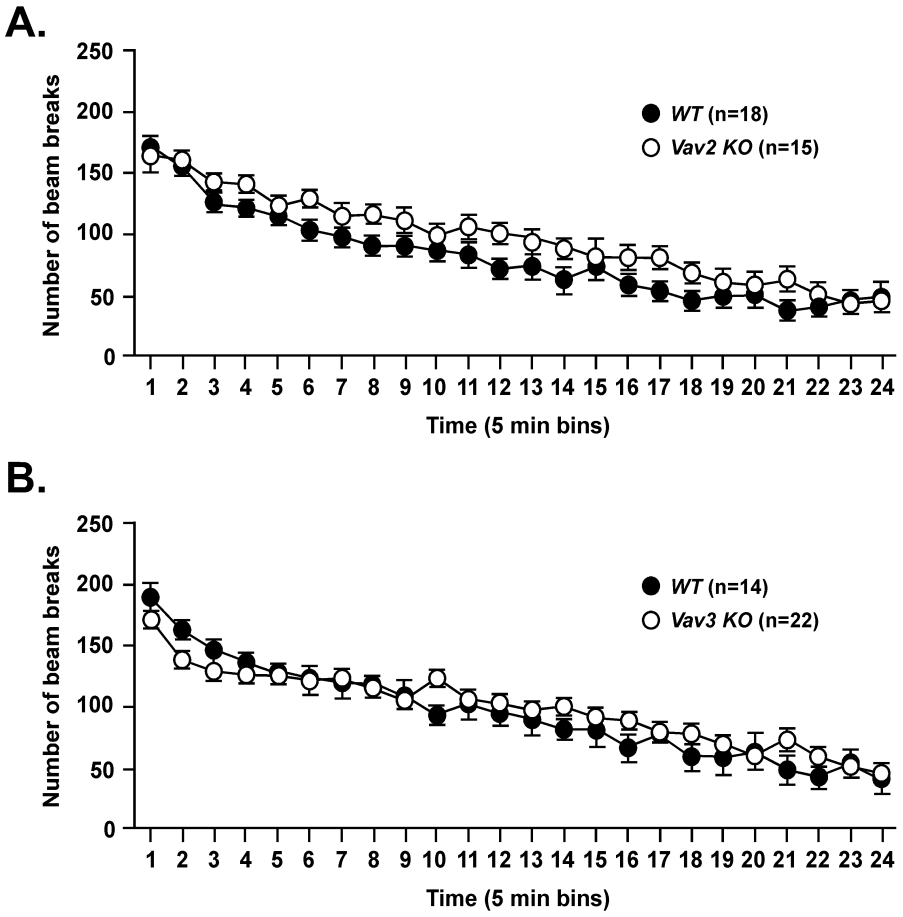

Figure 3.3. *Vav2* and *Vav3 KO* mice have normal locomotor activity. Locomotor activity was measured for 2 hr. Number of beam breaks collected in 5 min bins is indicated.

Figure 3.4. *Vav2* and *Vav3 KO* mice have impaired context-dependent fear conditioning.

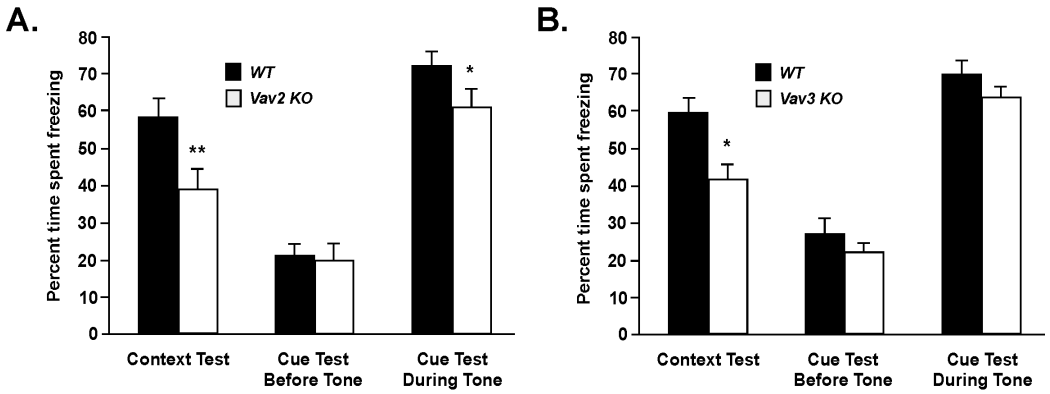

Figure 3.4. *Vav2* and *Vav3 KO* mice have impaired context-dependent fear conditioning. A, Context test: Percent time spent freezing 24 hr after training. *Vav2 KO* mice spent less time freezing than *WT* mice (**p<0.01). Cue test: Percent time spent freezing before and during tone. No significant difference between *Vav2 KO* and *WT* mice was observed in time spent freezing before tone. *Vav2 KO* mice spent less time freezing than *WT* mice during tone (*p<0.05). (*WT*: n=18; *Vav2 KO*: n=15) **B**, Context test: Percent time spent freezing 24 h after training. *Vav3 KO* mice spent less time freezing than *WT* mice (*p<0.05). Cue test: Percent time spent freezing before and during tone. No significant difference between *Vav3 KO* and *WT* mice was observed in percent time spent freezing before and during tone. (*WT*: n=14; *Vav3 KO*: n=22)

Figure 3.5. Vav2/3 GEFs are required for normal anxiety-like responses in mice.

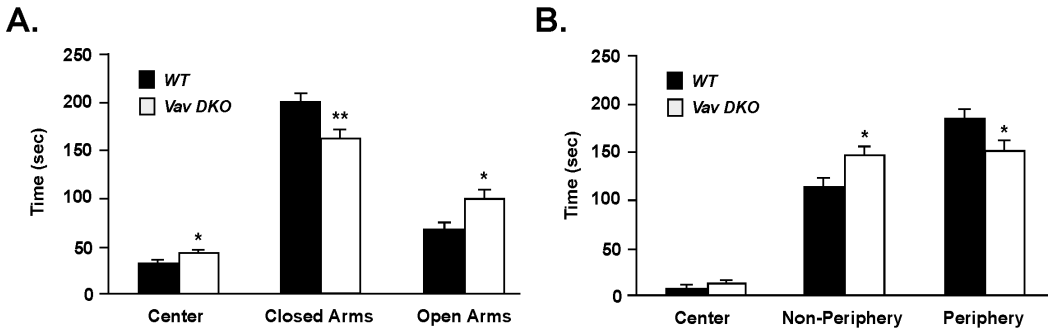

Figure 3.5. Vav2/3 GEFs are required for normal anxiety-like responses in mice. A, Elevated plus maze: Time spent in center, closed arms, and open arms of elevated plus maze are indicated. *Vav DKO* mice spent more time in center and open arms than *WT* mice (*p<0.05). *Vav DKO* mice spent less time in closed arms than *WT* mice (**p<0.01). (*WT*: n=15; *Vav DKO*: n=20) **B**, Open field test: Time spent in center, non-periphery, and periphery are shown. *Vav DKO* spent more time in non-periphery than *WT* mice (*p<0.05). *Vav DKO* spent less time in periphery than *WT* mice (*p<0.05). (*WT*: n=15; *Vav DKO*: n=20)

Figure 3.6. *Vav2*, but not *Vav3 KO* has reduced anxiety-like behavior.

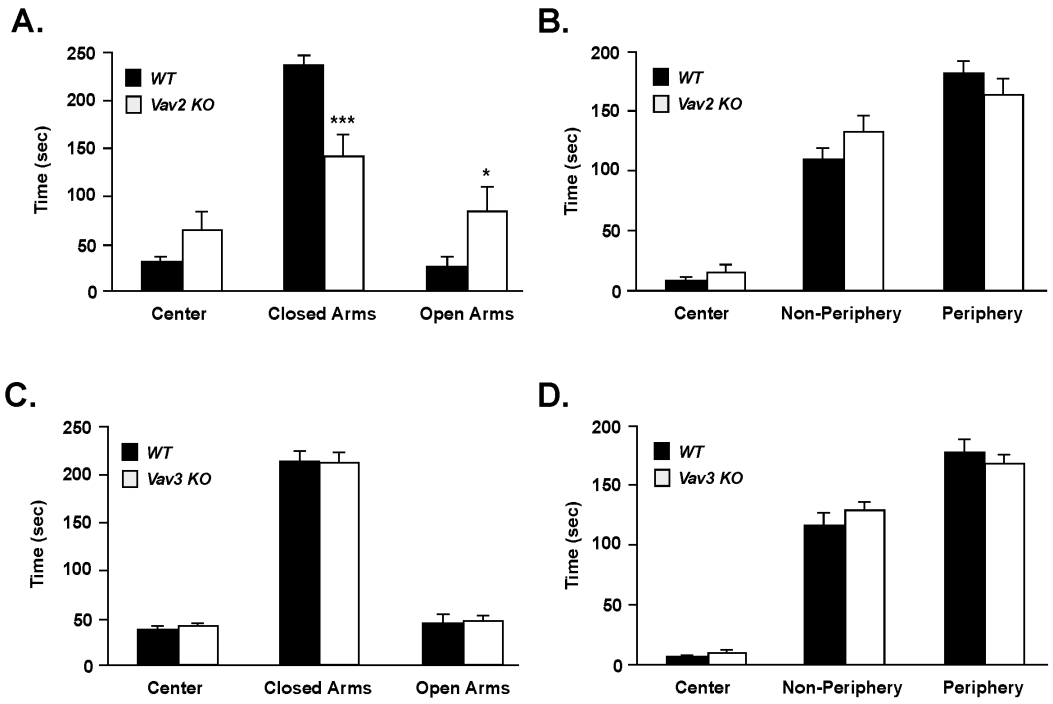

Figure 3.6. *Vav2*, but not *Vav3 KO* has reduced anxiety-like behavior. A, Elevated plus maze: Time spent in center, closed arms, and open arms are indicated. *Vav2 KO* spent less time in closed arms than *WT* mice (***p<0.001). *Vav2 KO* spent more time in open arms than *WT* mice (*p<0.05). (*WT*: n=18; *Vav2 KO*: n=15) **B**, Open field test: Time spent in center, non-periphery, and periphery are shown. No significant difference between *WT* and *Vav2 KO* mice was observed in time spent in each region. (*WT*: n=18; *Vav2 KO*: n=15) **C**, Elevated plus maze: Time spent in center, closed arms, and open arms are shown. No different between WT and Vav3 KO mice was observed in time spent in regions of maze. (*WT*: n=14; *Vav3 KO*: n=22) **D**, Open field test: Time spent in center, non-periphery, and periphery are indicated. No difference between *WT* and *Vav3 KO* mice was observed in time spent in each region. (*WT*: n=14; *Vav3 KO*: n=22)

CHAPTER FOUR: Pcdh17, a Common Target of MEF2 and FMRP, is Required for MEF2-induced Synapse Elimination

Summary

Synapses are formed during early brain development, but neuronal activity also promotes the elimination of synapses to either prune excess synapses or to homeostatically maintain a steady-state number of synaptic connections. The myocyte enhancer factor 2 (MEF2) transcription factors are important activity-dependent regulators of synapse elimination in the developing and adult brains, findings that have been correlated with a role for MEF2 in mediating various behaviors, including learning and memory. Fragile X mental retardation protein (FMRP) was recently found to be required for MEF2-dependent excitatory synapse elimination, suggesting that MEF2 and FMRP coordinate transcriptional and translational control of common mRNAs to confer proper experience-dependent synapse refinement. To pursue the identification of common MEF2 and FMRP targets, we utilized high-throughput sequencing of RNA isolated by cross-linking immunoprecipitation (HITS-CLIP) of FMRP to identify MEF2-regulated gene targets whose transcripts associate with FMRP in neurons. We identify a large overlap in MEF2 target genes and mRNAs associated with FMRP, consistent with their shared roles in synapse elimination. More specifically, we observe that the FMRP-associated mRNA coding for protocadherin 17 (Pcdh17)

is upregulated upon activation of MEF2, and it exhibits differential binding to FMRP following MEF2 activation. Pcdh17 is partially enriched at excitatory synapses in postnatal hippocampus. Reducing Pcdh17 alone did not alter basal structural or functional synapse number, but reducing Pcdh17 levels blocked MEF2-induced dendritic spine elimination of hippocampal CA1 pyramidal neurons. These data suggest that MEF2-induced synapse elimination requires Pcdh17 – a MEF2 target gene and FMRP associated transcript. Ongoing studies are examining the molecular and cellular mechanisms by which Pcdh17 mediates MEF2-dependent synapse elimination.

Introduction

The establishment and maintenance of proper synaptic connectivity within neural circuits is a dynamic process requiring the formation, elimination, stabilization, and plasticity of synapses (Hua and Smith, 2004). During early postnatal development, an excess of synapses are formed in many circuits, which undergo subsequent pruning during adolescence in a sensory- and activity-dependent mechanism, leading to fewer synapses in the adult (Hua and Smith, 2004; Rakic et al., 1986; Sanes and Lichtman, 1999; Zuo et al., 2005). While the molecular and cellular mechanisms that control the elimination of synapses remain poorly understood, the recent discovery that myocyte enhancer factor 2 (MEF2) transcription factors are important activity-dependent regulators of

synapse elimination provides a molecular link with the process of synapse removal (Barbosa et al., 2008; Flavell et al., 2006; Pfeiffer et al., 2010; Pulipparacharuvil et al., 2008).

The MEF2 family comprises four distinct genes (MEF2A-D), which are expressed in unique but overlapping patterns in the both the developing and adult brain (Leifer et al., 1993; Lin et al., 1996; Lyons et al., 1995; Lyons et al., 2012; Pulipparacharuvil et al., 2008). In neurons, glutamatergic synaptic activity and the resultant influx of calcium through voltage-sensitive calcium channels (VSCCs) leads to the activation of MEF2, which subsequently elicits a transcriptional program hypothesized to promote the elimination of synapses (Flavell et al., 2006; Flavell et al., 2008; McKinsey et al., 2002; Pulipparacharuvil et al., 2008). While numerous studies report that MEF2 is an important negative regulator of synapses, many questions remain regarding the mechanisms by which MEF2-dependent transcription regulates proper synapse number.

Fragile X mental retardation protein (FMRP) was recently demonstrated to be required for MEF2-dependent excitatory synapse elimination (Pfeiffer et al., 2010). Fragile X syndrome (FXS), the most prevalent inherited form of autism, results from the loss of FMRP, an RNA-binding protein with well-documented roles in the transport and translation of dendritic mRNAs (Bassell and Warren, 2008). Patients with FXS, as well as the mouse model of the disease, *Fmr1* knockout mice, exhibit an increased density of cortical dendritic spines (Comery

et al., 1997; Grossman et al., 2010; Grossman et al., 2006; Irwin et al., 2002; Irwin et al., 2001), prompting speculation that a deficit in synapse elimination may be present in FXS. In FMRP-deficient neurons, MEF2 fails to induce both structural and functional excitatory synapse elimination (Pfeiffer et al., 2010), suggesting that FMRP may function downstream of MEF2 to control synapse number by interacting with and regulating the translation of MEF2-induced transcripts that mediate the removal of synapses.

Here, we report the use of high throughput sequencing of RNA isolated by cross-linking immunoprecipitation (HITS-CLIP) of FMRP (Darnell et al., 2011) to identify common targets of MEF2 and FMRP in neurons. We find a strong overlap of MEF2-induced transcripts and RNAs associated with FMRP, and observe that a majority of one specific family of non-clustered protocadherins, the δ2 subfamily, are targets of both MEF2 and FMRP. The δ2 protocadherins are members of the superfamily of cadherins, calcium-dependent cell adhesion molecules with broad functions in neuronal and non-neuronal tissues (Kim et al., 2011). While δ2 protocadherins share many structural features with classical cadherins, they exhibit weaker homo- and heterophilic binding, and also possess a diverse C-terminal region with several hypothesized signaling-related motifs for which few effectors have yet been identified (Kim et al., 2011; Yasuda et al., 2007). Several δ2 protocadherins have established roles in regulating synapse number and function, and importantly, are being increasingly implicated in brain

disorders, including autism, schizophrenia, and cocaine abuse (Dean et al., 2007; Kim et al., 2011; Piton et al., 2011; Prasad et al., 2012; Tsai et al., 2012; Yasuda et al., 2007).

In this study, we find that Pcdh17 is a common target of both MEF2 and FMRP, and we investigate a role for this protocadherin in mediating MEF2-induced synapse pruning. Pcdh17 is highly expressed in the brain, and has been demonstrated to regulate presynaptic vesicle accumulation and synaptic transmission efficacy in corticobasal ganglia circuits in mice (Hoshina et al., 2013). Interestingly, a recent study links Pcdh17 with schizophrenia, reporting that Pcdh17 mRNA levels are increased in Brodmann area (BA) 46 in brains of individuals with schizophrenia (Dean et al., 2007). Importantly, these studies are beginning to provide insight into the poorly understood functions of Pcdh17, emphasizing the importance of additional studies investigating the protocadherin's regulatory roles in neurons.

Here, we report that Pcdh17 mRNA is 1) upregulated by MEF2, 2) a target of FMRP, and 3) differentially associated with FMRP following activation of MEF2 in neurons. We find that Pcdh17 is partially enriched with excitatory synaptic proteins, and that it is required for MEF2-induced dendritic spine elimination in the hippocampus. Furthermore, reducing Pcdh17 expression in CA1 neurons does not affect structural or functional synapse number, suggesting that Pcdh17 is necessary, but not sufficient, for MEF2-induced synapse pruning.

Materials and Methods

DNA constructs

Pcdh17 shRNA was purchased from Sigma (TRCN0000094739). The Pcdh17-EGFP plasmid was a gift from the Yamamoto Lab (Okinawa Institute of Science and Technology, Japan) and is described in (Hoshina et al., 2013).

Protein reagents

The following commercial antibodies were used in the study: anti-Pcdh17, 1:1000 (R&D Systems); anti-Pcdh10, 1:1000 (Sigma); anti-MEF2A, 1:1000 (Santa Cruz Biotechnology); anti-MEF2D, 1:1000 (BD Biosciences); anti-PSD95, 1:1000 (Santa Cruz Biotechnology); anti-synapsin I, 1:1000 (Abcam); anti-tubulin, 1:10,000 (Abcam).

Dissociated hippocampal and cortical cultures

Embryonic cortical neurons were cultured from embryonic day 16.5 (E16.5) mice. The cortices were dissected and treated with 100 U of papain (Worthington) for 3 min. The digestion was terminated by the addition of trypsin inhibitor (Sigma). The tissue was washed for a total of 3× with trypsin inhibitor, followed by 3 washes with plating medium consisting of DMEM (Life Technologies) supplemented with 10% fetal bovine serum (Life Technologies),

1% L-glutamine (Sigma), and 1% penicillin streptomycin (Sigma). Neurons were mechanically dissociated with a pipette and plated on polyornithine (Sigma)-coated 10 cm dishes at a density of 8 million cells per dish. The culture medium was replaced with Neurobasal medium (Life Technologies) supplemented with B-27 (Life Technologies), L-glutamine (Sigma), and 1% penicillin-streptomycin (Sigma) 24 h after plating. Postnatal hippocampal and cortical neurons were cultured from postnatal day 0 (P0) mice. Hippocampi or cortices were treated with 0.25% trypsin in HBSS (Life Technologies) for 10 min. The tissue was washed for a total of 3× with plating medium consisting of Neurobasal A medium (Life Technologies) supplemented with 10% fetal bovine serum (Life Technologies) and 1% L-glutamine (Sigma). Neurons were mechanically dissociated with a pipette and plated on poly-D-lysine (Sigma)-coated plates. One hr after plating, plates were washed 1× with Neurobasal A supplemented with B-27 (Life Technologies) and 1% L-glutamine, and replaced with glial conditioned medium.

Preparation of glial conditioned medium

Glia were cultured from postnatal day 0 (P0) mice. Cortices were treated with 0.25% trypsin in HBSS (Life Technologies) for 10 min. The tissue was washed for a total of 3× with plating medium consisting of Neurobasal A medium (Life Technologies) supplemented with 10% fetal bovine serum (Life

Technologies) and 1% L-glutamine (Sigma). The tissue was mechanically dissociated with a pipette and plated onto non-coated T75 flasks. Once glia reached confluence, pure astrocyte cultures were prepared by vigorously rotating flasks for 24 hr at room temperature. Twenty-four hr following rotation, glial conditioned medium was prepared by adding Neurobasal A supplemented with B-27 (Life Technologies) and 1% L-glutamine (Sigma) to glia for 48 hr.

Organotypic slice cultures

Hippocampal organotypic slices were culture from P6 mice of either sex following the protocol of (Stoppini et al., 1991). The mice were anesthetized with isoflurane and rapidly decapitated. The brains were extracted and placed in chilled dissection medium (10 mM HEPES, 1 mM $CaCl_2$, 5 mM $MgCl_2$, 10 mM dextrose, 4 mM Kcl, 26 mM $NaHCO_3$, and 248 mM sucrose) oxygenated with 95% O_2/5% CO_2. Hippocampi were dissected and sectioned coronally into 400-μM-thick sections using a McIlwain tissue chopper. Slices were transferred onto porous Millicell membranes in a six well plate with 750 μL of medium (MEM (Life Technologies) with 20% adult horse serum, 1 mM L-glutamine, 0.0012% ascorbic acid, 1 mM $CaCl_2$, 2 mM $MgSO_4$, 12.87 mM dextrose, 5.25 mM $NaHCO_3$, 30 mM HEPES, and 0.17 mM insulin, pH 7.28). Slices were maintained at this liquid-air interface at 37°C with 5% CO_2.

HEK293 cell transfections and preparation of lentivirus

To prepare lentivirus, HEK293T cells were transfected using Lipofectamine 2000 (Life Technologies). Cells were transfected with a lentiviral shRNA or overexpression plasmid and packaging vectors (MDLg, RSV-Rev, and VSVG). At 12 hr post-transfection, the medium was replaced with Neurobasal A (Life Technologies) supplemented with B-27 (Life Technologies) and 1% L-glutamine (Sigma). At 36-40 hr post-transfection, the virus-containing supernatant was harvested. Dissociated neuron cultures were treated with virus at 2-3 DIV for 12-16 hr.

FMRP HITS-CLIP

WT dissociated cortical neuron cultures were transfected with 4-hydroxy-tamoxifen (4OHT)-inducible, constitutively active MEF2 (MEF2-VP16-ER^{TM}) at 1 DIV using lentivirus. At 7 DIV, the neurons were treated with vehicle (0.1% EtOH) or 2.5 μM 4OHT for 3 or 6 hr to induce MEF2-dependent gene expression. Neurons were irradiated one time at 200 mJ/cm^2, and lysed in 1 mL PXL buffer (10 cm dish). FMRP HITS-CLIP was performed as described in (Darnell et al., 2011), with the following modifications. Prior to RNase treatment, lysates from crosslinked neurons were thawed on ice and homogenized using a Dounce homogenizer (three strokes). Samples were treated with RNAse cocktail (1:500 dilution), and lysates were precleared as described in Protocol 2 (Darnell et al.,

2011). The remaining steps were carried out as described in (Darnell et al., 2011). Sequencing was performed using an Illumina HiSeq 2000 platform by the Rockefeller University Genomics Resource Center. Raw sequences were filtered and analyzed as described in (Darnell et al., 2011).

RNA-seq

WT dissociated cortical neuron cultures were transfected with 4-hydroxy-tamoxifen (4OHT)-inducible, constitutively active MEF2 (MEF2-VP16-ER^{TM}) at 1 DIV using lentivirus. At 7 DIV, the neurons were treated with vehicle (0.1% EtOH) or 2.5 μM 4OHT for 3 or 6 hr to induce MEF2-dependent gene expression. Neurons were harvested in PXL buffer, and samples were diluted 1:1 with RNAse-free water. For RNA extraction, samples were lysed with TRIzol LS (Life Technologies), and the RNA was precipitated with chloroform. Samples were prepared for high throughput sequencing with the Illumina Tru-Seq V2 kit including RiboMinus removal of rRNA according to manufacturer's instructions. Samples were sequenced on an Illumina HiSeq 2000 platform.

RNA isolation and reverse transcription

Dissociated neuron cultures were lysed in TRIzol (Life Technologies), and the RNA was precipitated with chloroform (Sigma). The remaining steps were performed using the RNeasy Micro kit (Qiagen). The RNA concentration of each

sample was determined using a NanoDrop spectrophotometer and was reverse transcribed using the Superscript III First-Strand Synthesis System for RT-PCR (Life Technologies).

Quantitative real-time PCR

All primers were designed to amplify a 100-150 bp product. The primers used to amplify Pcdh17 RNA were 5'-GAACATCTGAAGTGCCCACA-3' (forward) and 5'-TCATCCTCCTTTTTGCGTCT-3' (reverse). The primers used to amplify Rgs2 RNA were 5'-GCAAGGGTGTTGACGTTCTT-3' (forward) and 5'-TTTGGCACTCGTAACAGACG-3' (reverse). The primers used to amplify Gapdh RNA were 5'-AGGTCGGTGTGAACGGATTTG-3' (forward) and 5'-TGTAGACCATGTAGTTGAGGTCA-3' (reverse). The reactions were performed using iTaq Universal SYBR Green Supermix (Bio-Rad) and the StepOnePlus Real-Time PCR System thermal cycler (Life Technologies). mRNA expression was determined by running reactions of 10 ng of cDNA. Fold changes relative to Gapdh were determined using the ΔΔCt method, in which the mean fold change ($2^{-\Delta\Delta CtAVE}$) and SEM ($abs(((2^{-\Delta\Delta CtAVE} \times 2^{-\Delta\Delta CtSEM}) - (2^{-\Delta\Delta CtAVE}/2^{-\Delta\Delta CtSEM}))/2)$) were determined.

Western blotting

Samples were run on SDS-PAGE gels and transferred to PVDF membrane (Millipore). The membranes were blocked in 10% milk for 1 hr and probed with 1° antibody for 2 hr at room temperature or overnight at 4°C. The membranes were then incubated with 2° antibody (1:10,000 G α R, G α M, or R α G, Jackson ImmunoResearch Laboratories) for 1 hr at room temperature and developed with a homemade enzymatic chemiluminescence (ECL) solution or SuperSignal West Femto Chemiluminescent Substrate (Thermo Scientific).

Synaptosome preparation

Whole hippocampi were dissected from P15 mice of either sex and homogenized in buffer consisting of 7 mM Tris-HCl, pH 7.5, 0.36 M sucrose, 0.5 mM EGTA, and 0.25 mM DTT using a Wheaton glass mortar and Teflon pestle homogenizer. The samples were spun at 3500 rpm for 2 min at 4°C to pellet nuclei. The supernatant was collected and spun at 23,000 × g for 6 min at 4°C, resulting in the formation of a membrane fraction-containing pellet. The pellet was resuspended in homogenization buffer and layered onto a 5%/13% discontinuous Ficoll gradient. The sample was spun at 45,000 × g for 45 min at 4°C. Synaptosomes were collected from the 5 and 13% Ficoll interface, washed in ice-cold PBS, spun at 23,000 × g for 20 min at 4°C, and resuspended in ice-cold PBS. The postsynaptic density (PSD) was collected by homogenizing an aliquot

of the synaptosome fraction in homogenization buffer with 0.5% Triton X-100. The sample was vortexed repeatedly during a 15 min incubation on ice, then spun at 33,000 × g for 20 min at 4°C. The pellet that formed during the centrifugation was PSD.

Biolistic transfection of organotypic slices

Organotypic hippocampal slices were biolistically transfected at 5-6 DIV. Preparation of gold bullets and biolistic transfection procedure were performed using the Helios Gene Gun system (Bio-Rad) according to the manufacturer's protocols.

Dendritic spine imaging

Organotypic hippocampal slice cultures were prepared from mice at P5-6, as described previously. At 5-6 DIV, slices were biolistically transfected with relevant constructs together with pAl-GFP, which expresses a myristoylated form of GFP to enhance filling of spines. After 48 hr, secondary apical dendrites (150-200 μM from soma) of transfected CA1 neurons were imaged using a Zeiss LSM 510 2-photon laser scanning microscope. Images were obtained using an excitation wavelength of 920 nm and a 63X 0.9 NA water immersion objective. An interval of 0.3 μM and pixel resolution of 2048×2048 was used to acquire Z-stacks, generating images with pixel dimensions of 0.07×0.07×0.3 μM. For each

neuron, 1-2 regions of interest were acquired. All imaging experiments were performed blind to treatment.

Intracellular recordings

Simultaneous whole-cell recordings were obtained from CA1 pyramidal neurons in slice cultures visualized using IR-DIC and GFP fluorescence to identify transfected and non-transfected neurons (Pfeiffer and Huber, 2007). Recordings were made at 34°C in a submersion chamber perfused at 3 ml/min with artificial cerebrospinal fluid (ACSF) containing (in mM): 119 NaCl, 2.5 KCl, 26 NaHCO3, 1 NaH2PO4, 11 D-Glucose, 3 CaCl2, 2 MgCl2, 0.1 picrotoxin, 0.002 2-chloro-adenosine; 0.1% DMSO pH 7.28, 300 mOsm and saturated with 95% O2/5%CO2. For evoked EPSC recordings, the ACSF was supplemented with 5 mM CPP as well. For evoked EPSC and mEPSC recordings, neurons were voltage clamped at -60 mV through whole cell recording pipettes (~4-6 MΩ) filled with an intracellular solution containing (in mM): 0.2 EGTA, 130 K-Gluconate, 6 KCl, 3 NaCl, 10 HEPES, 2 QX-314, 4 ATP-Mg, 0.4 GTP-Na, 14 phosphocreatine-Tris, pH7.2 adjusted by KOH, 290 mOsm.

For mEPSC measurements, the ACSF was supplemented with 1 μM TTX. Synaptic responses were evoked by single bipolar electrode placed in stratum radiatum of area CA1 (along the Schaffer collaterals) 50-100 μm from the recorded neurons with monophasic current pulses (10-100 μA, 0.05-1 ms). Series

and input resistance were measured in voltage clamp with a 400-ms, –10 mV step from a –60 mV holding potential (filtered at 30 kHz, sampled at 50 kHz). Cells were only used for analysis if the series resistance was less than 30 MΩ and was stable throughout the experiment. Input resistance ranged from 50-700 MΩ. Data were not corrected for junction potential. No significant difference was observed between transfected and untransfected neurons in resting membrane potential or input resistance, indicating that overall neuronal health and subthreshold membrane conductances were unaffected by expression of shRNA. Synaptic currents were filtered at 2 kHz, acquired and digitized at 10 kHz on a PC using custom software (Labview; National Instruments, Austin, TX). mEPSCs were detected off-line using an automatic detection program (MiniAnalysis; Synaptosoft Inc, Decatur, Ga.) with a detection threshold set at a value greater than at least 4 S.D. of the noise values, followed by a subsequent round of visual confirmation. The detection threshold remained constant for the duration of each experiment. For evoked EPSCs shown in figures the stimulation artifact has been digitally removed for clarity. Significant differences between transfected and nontransfected neurons were determined using a paired t-test.

Results

MEF2 and FMRP share a large overlap of targets

FMRP is required for MEF2-induced synapse elimination, suggesting that MEF2 and FMRP coordinate control of the transcription and translation of mRNA targets that promote synapse pruning (Pfeiffer et al., 2010). To identify common transcript targets of MEF2 and FMRP, we utilized HITS-CLIP of FMRP (Darnell et al., 2011) with cortical neurons expressing activated MEF2. Briefly, WT dissociated cortical neuron cultures were transfected with 4-hydroxy-tamoxifen (4OHT)-inducible, constitutively active MEF2 (MEF2-VP16-ER^{TM}) at 1 DIV using lentivirus. At 7 DIV, the neurons were treated with vehicle (0.1% EtOH) or 2.5 μM 4OHT for 3 or 6 hr to induce MEF2-dependent gene expression. We established these specific stimulation time-points for two reasons: 1) we observe robust induction of well-known MEF2 targets, including Nur77, Rgs2, Nurr1, and Nor1 at 3 and 6 hr (Fig. 2 and data not shown), and 2) MEF2-VP16-ER^{TM} causes a decrease in excitatory synapse number within 6-12 hr of 4OHT treatment, suggesting that the MEF2-induced transcripts that control the elimination of synapses are regulated in this time frame (Flavell et al., 2006).

Following cross-linking of live neurons by UV radiation, the FMRP-RNA complexes were immunoprecipitated, and cross-linked RNAs were amplified by RT-PCR. The RNA identities and abundances were determined using RNA sequencing, and FMRP targets were identified with a stringent false discovery

rate of less than 1%. Importantly, in parallel with the samples processed for HITS-CLIP, we also processed parallel lysates for RNA sequencing to identify genes regulated by MEF2. Three completely independent experiments were performed and combined to generate the final data sets for the HITS-CLIP and RNA-seq studies.

The HITS-CLIP experiment allowed us to discern two pieces of information: 1) identify if an mRNA was a significant target of FMRP, and 2) determine if the abundance of an mRNA associated with FMRP was altered upon activation of MEF2-dependent gene expression. Analysis of the HITS-CLIP studies revealed that 627 mRNAs were significant targets of FMRP in neuron cultures. Previously, Darnell *et al*. identified 842 FMRP targets in seven independent *in vivo* experiments using HITS-CLIP (Darnell et al., 2011). Comparison of results from the *in vitro* and *in vivo* HITS-CLIP studies described a large overlap of FMRP-associated mRNAs between the two preparations (Fig. 4.1A), and indicated that that we have successfully identified FMRP-associated mRNAs in neuron cultures. To identify the overlap of targets shared by MEF2 and FMRP, we compared results from the *in vitro* FMRP HITS-CLIP and RNA-seq studies. FMRP and MEF2 share a large overlap of targets, as approximately 25% of FMRP targets are induced >1.2-fold by MEF2 (Fig. 4.1B), supporting the hypothesis that MEF2 and FMRP function to co-regulate a large fraction of common transcripts.

Using a false discovery of less than 5%, 32 and 18 transcripts were differentially bound to FMRP following 3 and 6 hr of 4OHT-induced MEF2 transcription, respectively (Tables 4.1 and 4.2). Interestingly, the vast majority of these mRNAs exhibited reduced binding to FMRP, with only 5 of the 50 total regulated transcripts having an increased association with FMRP following MEF2 activation. As FMRP is hypothesized to translationally repress many of its targeted transcripts, these findings may suggest that FMRP is disassociating from these mRNAs to permit their translation. It also proposes the interesting possibility that MEF2 activation causes FMRP to release a subset of associated mRNAs, possibly to promote their conversion to new proteins. How MEF2 activation causes changes in FMRP binding to mRNAs, or the importance of this observed regulation, is not clear. Future studies will be necessary to probe these interesting questions.

Non-clustered protocadherins of the δ2 subfamily are common targets of MEF2 and FMRP

After discovering that MEF2 and FMRP share several common targets, we next sought to identify and examine requirement of specific candidates for MEF2-induced synapse elimination. In closely analyzing the HITS-CLIP data, we observed that several members of the δ2 subfamily of non-clustered protocadherins, including Pcdh10, 17, and 19, were targeted by FMRP. Of these,

Pcdh17 and Pcdh19 were also induced by MEF2, to 1.37- and 1.34-fold, respectively. These findings were particularly remarkable, as many δ2 non-clustered protocadherins have been linked with autism, schizophrenia, and drug abuse (Dean et al., 2007; Kim et al., 2011; Piton et al., 2011; Prasad et al., 2012; Tsai et al., 2012; Yasuda et al., 2007). Furthermore, members of the δ2 protocadherin subfamily, including Pcdh8 and Pcdh10, regulate activity-dependent synapse elimination (Tsai et al., 2012; Yasuda et al., 2007). In examining whether binding of these protocadherins to FMRP was regulated in the context of MEF2 activation, we observed that the abundance of Pcdh17 mRNA associated with FMRP following MEF2 activation began to decline at 3 hr of 4OHT stimulation, and was further reduced (0.73-fold) after 6 hr of 4OHT treatment. While statistical analysis of the abundance of Pcdh17 bound to FMRP following 4OHT stimulation (6 hr) did not reach significance, a strong trend was observed ($p=0.10$), which suggests that binding of Pcdh17 transcript to FMRP may be a MEF2-regulated association. Association of FMRP with Pcdh19 was not altered following MEF2 activation.

Pcdh17 colocalizes with excitatory synaptic proteins in the hippocampus

Pcdh17 is induced by MEF2 activation, is a target of FMRP, and may show a reduced association with FMRP following activation of MEF2. We therefore speculated that Pcdh17 might be required for MEF2-induced excitatory

synapse elimination in the hippocampus. To this end, we first analyzed protein levels of Pcdh17 over a time course of development, including the ages during which robust synaptogenesis and synapse remodeling are occurring. We found that Pcdh17 is expressed during early postnatal development (P4-P7), and that its levels increase at P14-P21 before beginning to decline at P28 (Fig. 4.2A). Interestingly, the time points in which Pcdh17 levels are increased coincide with the ages that MEF2A and MEF2D levels in the hippocampus are observed to elevate (P14-21). This is also a developmental time period during which neuronal activity is high, and we therefore might expect levels of MEF2 activity to be elevated. Overall, these data reveal that Pcdh17, as well as MEF2, are highly expressed in the developing hippocampus.

To examine whether Pcdh17 is localized near excitatory synapses, and therefore in a position to mediate the MEF2-induced effects on synapses, we performed a biochemical fractionation procedure to isolate synaptosomes, membranous fractions that are enriched for glutamatergic synaptic proteins. Synaptosomes were prepared from whole hippocampi of P15 mice, and western blotting was used to examine co-fractionation of Pcdh17 in the cellular fractions (Fig. 4.2B). Pcdh17 was strongly enriched in the P2 fraction containing non-nuclear cell membrane proteins, and was partially enriched in the synaptosome (syn) fraction. To examine whether Pcdh17 is a component of the post-synaptic density (PSD), we performed detergent extraction of the synaptosome fraction

using 0.5% Triton X-100. Pcdh17 was partially extracted from the synaptosome fraction, indicating that a large amount of Pcdh17 is associated with the PSD. Overall, these data suggest that Pcdh17 is localized in synapse-containing fractions and is partially enriched in the PSD, therefore in a position to exert structural and functional effects on excitatory synapse structure and/or function.

Pcdh17 expression is regulated by MEF2 and FMRP in hippocampal neurons

FMRP HITS-CLIP and RNA-sequencing experiments indicate that Pcdh17 mRNA is induced by MEF2, and also interacts with FMRP. However, it remains unclear whether Pcdh17 protein is increased resultant of the increase in MEF2-induced transcript abundance, and also whether Pcdh17 protein expression is modulated by FMRP. To more closely assess regulation of Pcdh17's mRNA and protein by MEF2 and FMRP in neurons, we transfected dissociated hippocampal neuron cultures from WT or *Fmr1* null mice (P0 + 2 DIV) with 4OHT-inducible MEF2-VP16-ER^{TM} using lentivirus. At 7-8 days following addition of virus, the neurons were treated with vehicle (0.1% EtOH) or 4OHT (2.5 μM) to induce MEF2-dependent gene transcription. For expression analyses described here comparing genotype and treatment conditions, all data are shown relative to the WT + vehicle (0.1% EtOH) condition.

Using reverse transcription and qRT-PCR, we found no changes in Pcdh17 mRNA levels in either WT or *Fmr1* KO mice upon a short 1 hr 4OHT

treatment (Fig. 4.3A), suggesting that longer stimulation lengths are required to observe regulation of MEF2-dependent gene transcription. However, a longer treatment length of 3 hr elicited a significant induction of Pcdh17 mRNA to 1.31-fold over vehicle-treated conditions in both WT and *Fmr1* KO neurons (Fig. 4.3A, WT: $p<0.05$, Two-way ANOVA; *Fmr1* KO: $p<0.05$, Two-way ANOVA). The magnitude of Pcdh17 mRNA induction observed here is consistent with a previously reported study examining regulation of genes by MEF2-VP16-ER^{TM} in hippocampal neuron cultures, which report a 44% increase in Pcdh17 mRNA expression following 2.5 hr 4OHT stimulation (Flavell et al., 2008). In our studies, Rgs2 served as a positive control, increasing by 53% and 58% with 3 hr of 4OHT treatment in WT and *Fmr1* null neurons, respectively, (Fig. 4.3A, WT: $p<0.01$, Two-way ANOVA; *Fmr1* KO: $p<0.01$, Two-way ANOVA). No differences were detected between WT and FMRP-deficient cultures in basal or MEF2-induced mRNA levels, indicating that FMRP does not regulate basal mRNA expression, mRNA stability, or MEF2's ability to induce gene transcription in cultured neurons. The MEF2-induced elevation in Pcdh17 mRNA levels persists through at least 6 hr of 4OHT treatment, with levels in WT neurons increased to 1.36-fold in comparison to the vehicle-stimulated condition (Fig. 4.3A, $p<0.05$, Two-way ANOVA). In contrast, the level of induced Rgs2 mRNA was reduced at this time point compared to a 3 hr 4OHT treatment. Together, these experiments show that Pcdh17 mRNA expression is stimulated by MEF2,

and is a simultaneously robust and long-lasting induction. Furthermore, both basal and MEF2-induced Pcdh17 and Rgs2 mRNA levels are not regulated in FMRP-deficient neurons, suggesting that FMRP does not modulate basal expression, or control the ability of MEF2 to induce expression of genes in dissociated neuron cultures, findings that are consistent with previously reported studies (Pfeiffer et al., 2010; Tsai et al., 2012).

Following the observation that Pcdh17 mRNA is induced by MEF2 activation in both WT and FMRP-deficient neurons, we next wanted to assess whether an increase in Pcdh17 protein levels can be detected. Additionally, because Pcdh17 mRNA is targeted by FMRP, and FMRP is widely hypothesized to regulate the translation of its associated transcripts, it is important to examine for any regulation of the basal or MEF2-induced protein levels by the RNA binding protein. As previously performed, dissociated WT and *Fmr1* null hippocampal neuron cultures were transfected with MEF2-VP16-ER^{TM} using lentivirus (P0 + 2 DIV), and stimulated with vehicle (0.1% EtOH) or 4OHT at 9-10 DIV. Since MEF2 stimulates increases in Pcdh17 mRNA with both 3 and 6 hr of 4OHT treatment, we hypothesized that elevations in Pcdh17 protein levels might be detected with a 4OHT treatment length of 3 or 6 hr. Western blot analyses revealed a trend towards a slight increase (~15%) in Pcdh17 protein levels following MEF2 activation ($p=0.09$) that may reach significance upon inclusion of more samples (Fig. 4.3B). Experiments are also underway to

determine whether an increased length of MEF2 activation (specifically, 9 hr 4OHT treatment) may yield further enhancement of Pcdh17 protein levels. Interestingly, a difference is detected between Pcdh17 protein expression in WT and *Fmr1* KO cultures in the 6 hr vehicle-treated control condition (Fig. 4.3B). Specifically, Pcdh17 protein was increased in FMRP-deficient neurons by 30% compared to WT, findings that may support a role for FMRP in the translational regulation of Pcdh17. However, in neuron cultures exposed to vehicle or 4OHT stimulation for 3 hr (Fig. 4.3B), there are no differences between Pcdh17 protein levels in WT and *Fmr1* KO cultures, suggesting that any regulation of Pcdh17 expression by FMRP may not be detected using these procedures and indicating the need for additional experiments.

Modulation of Pcdh17 protein expression by FMRP was also examined *in vivo*. Toward this end, whole hippocampal lysates were prepared from WT and *Fmr1* null mice of ages P12-P14 or P18-P20 and Western blot analysis was performed (Fig. 4.3C). No differences between Pcdh17 protein levels in WT and FMRP-deficient hippocampi were perceived at these ages, indicating that any FMRP-dependent regulation of Pcdh17 protein *in vivo* is not apparent using these experimental procedures. The possibility exists that we may be able to detect differences in specific subcellular fractions of the neuron that cannot be discerned in total cell lysates. Indeed, it has been previously reported that expression of Arc protein in *Fmr1* KO neurons is specifically enhanced in dendrites, an observation

that can be detected with immunocytochemistry (Niere et al., 2012). Experiments to investigate the possibility that Pcdh17 protein levels will be specifically controlled by FMRP at the synapse include the preparation of synaptosome fractions or immunostaining of dendrites.

Pcdh17 is not required for basal structural or functional glutamatergic synapse number in CA1 pyramidal neurons

MEF2 is a critical negative regulator of excitatory synapse number, eliciting a complex transcriptional program hypothesized to result in the pruning of synapses in neurons. FMRP was recently found to be required for MEF2-induced synapse elimination, suggesting that MEF2-induced transcripts specifically targeted and regulated by FMRP may be mediating the MEF2-dependent removal of synapses. Since (1) Pcdh17 mRNA is induced by MEF2 activation (2) Pcdh17 mRNA is targeted and may be regulated by FMRP, and (3) Pcdh17 is enriched in excitatory synaptic fractions, we hypothesized that Pcdh17 may be required for the pruning of excitatory synapses downstream of MEF2 activation.

To begin testing this idea, we first examined whether manipulation of Pcdh17 levels is sufficient to regulate synapse number in neurons. To determine the effect of Pcdh17 knockdown on dendritic spine density and functional synapse measures, we first test candidate shRNAs that were predicted to selectively target

Pcdh17 for RISC-mediated degradation. Five different shRNA constructs were evaluated for their efficacy and specificity in reducing Pcdh17 protein levels by preparing lentivirus for transfection of dissociated hippocampal neurons. After only 72 hr after addition of lentivirus-shRNA, three shRNAs reduced Pcdh17 protein levels, but only one shRNA reduced Pcdh17 protein (~80%) while not affecting protein levels of closely related family members, Pcdh10 (Fig. 4.4A) and Pcdh9 (data not shown).

The shRNA targeting Pcdh17 was introduced into hippocampal organotypic slices (P6 + 4-6 DIV) together with a myristoylated form of GFP using biolistic transfection. After 40-48 hr of expression, 2-photon live-cell imaging of dendritic spines or whole-cell patch clamp recordings was performed to assess changes in structural and functional synapse properties. For 2-photon studies, organotypic hippocampal slices were biolistically transfected with Pcdh17 shRNA and a myristoylated form of GFP, to allow for enhanced imaging of dendritic spines. After 40-48 hr, secondary apical dendrites of Pcdh17- and vector-expressing CA1 pyramidal neurons were imaged. Knockdown of Pcdh17 did not affect overall dendritic spine density, or density of specific spine subtypes (stubby, mushroom, and thin) in hippocampal CA1 pyramidal neurons (Fig. 4.4B).

In line with these findings, knocking down Pcdh17 did not elicit changes in mEPSC frequency or evoked AMPA receptor EPSC amplitude, measures of

functional synapse number (Fig. 4.4C). Further analyses revealed that reducing Pcdh17 did not alter mEPSC amplitude or paired pulse ratio (PPF), suggesting that no modifications in individual synapse strength or presynaptic release probability, respectively, were apparent (Fig. 4.4C). Overall, findings from the 2-photon imaging and electrophysiology studies provide evidence that Pcdh17 is not necessary for normal dendritic spine density, functional synapse number and strength, and presynaptic vesicle release probability in hippocampal pyramidal neurons.

Pcdh17 is required for MEF2-induced dendritic spine elimination in CA1 pyramidal neurons

Pcdh17 is not required for basal dendritic spine density or functional synapse number in hippocampus, but it may have a role in regulating MEF2-dependent structural synapse pruning. Toward this end, we co-expressed the Pcdh17 shRNA together with GFP and 4OHT-inducible MEF2-VP16, and assessed effects on dendritic spine density of transfected CA1 pyramidal neurons. While active MEF2 caused a reduction in the density of dendritic spines, reducing Pcdh17 levels blocked the MEF2-induced decrease in spine density, supporting a role for Pcdh17 in MEF2-induced elimination of synapses (Fig. 4.5). The next critical step is to validate that the synapse elimination phenotype can be rescued by expression of an shRNA-insensitive Pcdh17 construct. This will verify that the

Pcdh17 shRNA is mediating its effects by reducing Pcdh17 levels, and is not blocking synapse pruning through off-target effects. Additionally, we will examine whether Pcdh17 is also necessary for MEF2-induced elimination of functional synapses by obtaining electrophysiology responses in transfected CA1 hippocampal neurons.

Discussion

Together, the studies reported here identify a large overlap of shared MEF2 and FMRP mRNAs, supporting the hypothesis that MEF2 and FMRP coordinate the regulation of common mRNA targets to confer synapse refinement. Interestingly, we observe that many members the δ2 subfamily of non-clustered protocadherins, which have been linked with autism, schizophrenia, drug abuse, and language delay, are represented among all overlapping transcripts. Focusing attention on one specific protocadherin, we find that Pcdh17, a synaptically localized protein, is targeted for regulation by MEF2 and FMRP, and is necessary for MEF2-induced synapse pruning. Several key experiments remain to verify a role for Pcdh17 in MEF-triggered structural and functional synapse elimination, and to uncover the molecular and cellular mechanisms by which Pcdh17 controls MEF2-dependent synapse elimination.

Here, we report that expression of a shRNA targeting Pcdh17 in hippocampal CA1 neurons blocks MEF2-induced dendritic spine elimination,

suggesting that Pcdh17 is necessary for MEF2-dependent synapse pruning; however, key future experiments are necessary to support a role for Pcdh17 in this process. The initial immediate step will be to confirm that shRNA-mediated Pcdh17 knockdown, and not off-target effects of the short hairpin, is responsible for blocking MEF2-induced synapse elimination. This will be achieved by co-expressing an shRNA-insensitive Pcdh17 cDNA together with the inducible, constitutively active MEF2 and Pcdh17 shRNA constructs. A subsequent key step is to investigate whether in addition to its requirement in MEF2-dependent dendritic spine elimination, Pcdh17 is also necessary for MEF2-induced pruning of functional synapses. Toward this end, we will co-express the Pcdh17 shRNA together with constitutively active MEF2, following the protocols used for the structural spine studies. Effects on synapse number and function will be examined by obtaining spontaneous miniature EPSC and evoked EPSC responses. As with the dendritic spine experiments, we will rescue any effects observed with shRNA-insensitive Pcdh17. Finally, we will also perform experiments to examine whether overexpression of Pcdh17 is sufficient to induce synapse elimination in the presence or absence of basal MEF2 activity.

FMRP is required for MEF2-induced synapse elimination (Pfeiffer et al., 2010), suggesting that MEF2 and FMRP coordinate transcriptional and translational control of common mRNA targets that mediate MEF2-dependent synapse pruning. The comparison of the HITS-CLIP and RNA-seq experiments

support this hypothesis, as a large percentage of FMRP targets in cortical neuron cultures (approximately 25%) are induced to >1.2-fold by MEF2 activation. An interesting observation in the HITS-CLIP studies is that the majority (45/50 = 90%) of mRNA targets that showing altered binding to FMRP following MEF2 activation, specifically exhibited reduced binding to FMRP at both 3 and 6 hr 4OHT stimulation time points. As FMRP is hypothesized to suppress the translation of its associated target mRNAs, this finding lends evidence that FMRP might disassociate from specific transcripts to permit their translation. Furthermore, this finding generates speculation that MEF2 may somehow stimulate the disassociation of FMRP from its bound mRNA targets, therefore promoting the expression of FMRP targets. Future investigational studies are necessary to explore these intriguing questions.

Pcdh17 mRNA is 1) upregulated by MEF2 activity (Fig. 4.3 and Flavell et al., 2008), 2) targeted for association with FMRP, and 3) localized in CA1 dendrites (Cajigas et al., 2012), suggesting that FMRP may regulate the local dendritic translation of MEF2-induced Pcdh17 mRNA to mediate synapse elimination. Additional experiments are necessary to examine the specific regulation of Pcdh17 protein by MEF2 and FMRP. MEF2 activity increases Pcdh17 mRNA levels by approximately 35% in neuronal total cell lysates, but whether this generates an increase in Pcdh17 protein levels is not yet known. Preliminary experiments indicate a trend towards a slight increase (15%) in

MEF2-stimulated total levels of Pcdh17 protein, and this effect may reach significance with the inclusion of more replicates, or with longer lengths of MEF2 activation. Additionally, an enhancement of Pcdh17 protein levels may be more readily discerned in synaptic compartments, where we believe it is exerting its effects on synapses.

A well-established mechanism that stimulates FMRP-dependent translation is the activation of group 1 (Gp1) metabotropic glutamate receptors (mGluRs), mGluR1 and mGluR5 (Bassell and Warren, 2008; Dictenberg et al., 2008). Importantly, dendritic mGluR5 activity was recently reported to be necessary for MEF2-induced synapse elimination (Wilkerson et al., 2014). To determine if dendritic Pcdh17 translation is regulated by mGluR5 and FMRP, we will perfuse dendrites of MEF2-VP16-ER^{TM}-expressing WT and *Fmr1* KO hippocampal neurons in microfluidic culture chambers with inhibitors of translation or mGluR5, and examine effects on Pcdh17 protein levels. To examine if dendritic Pcdh17 is necessary for the removal of synapses triggered by MEF2, we will incubate the dendrites with a Pcdh17 siRNA or anti-sense oligo, and assess MEF2-induced decreases in synaptic markers using immunocytochemistry. An important note is that the specific regulation of Pcdh17 levels by MEF2 and FMRP may not be necessary for the MEF2-induced synapse elimination process. Rather, MEF2 may promote synapse elimination via a mechanism that requires

Pcdh17, but the regulation of Pcdh17 by MEF2 and FMRP may not be required for that function.

In the future, it will be crucial to delineate the molecular and cellular mechanisms by which Pcdh17 controls MEF2-induced elimination of synapses. Studies report that the autism-linked δ2 protocadherins Pcdh8 and Pcdh10 also mediate activity-dependent excitatory synapse removal, evoking the possibility that Pcdh17 may act as a negative regulator through similar processes. Yasuda and colleagues discovered that Pcdh8 interacts with and is required for the endocytosis of N-cadherin that occurs in response to depolarization or increased cAMP levels (Yasuda et al., 2007). Detailed analysis revealed that homophilic binding of Pcdh8, in *cis* or in *trans*, induces the recruitment of p38MAPK to its C-terminus, thereby stimulating N-cadherin endocytosis and subsequent synapse loss. Pcdh10 was also recently implicated in the process of activity-dependent synapse elimination, in a study reporting a requirement for Pcdh10 in MEF2-induced pruning of excitatory synapses (Tsai et al., 2012). Detailed experimental analyses indicated that MEF2 induces the ubiquitination and subsequent degradation of PSD-95, and that degradation of PSD-95 requires Pcdh10 to facilitate its delivery to the proteasome.

Insight into Pcdh17's functional mechanisms may be gained through a careful examination of its structure and binding motifs. Interestingly, recent studies reveal that two δ2 protocadherins, PCDH10 and PCDH19, interact with

the WAVE regulatory complex (WRC), a complex that controls actin cytoskeletal dynamics by inducing the actin-nucleating activity of the Arp2/3 complex (Chen et al., 2014). The study identified a novel conserved peptide motif, WRC interacting receptor sequence, that binds the WRC and is possessed by all δ2 protocadherins, revealing an intriguing mechanism through which δ2 protocadherins may regulate the actin cytoskeleton to effect changes in synapse plasticity.

Taken together, the studies described here support the coordinated efforts of MEF2 and FMRP in the regulation of mRNA targets that control synapse pruning. Findings specifically introduce a novel role for Pcdh17, a common target of MEF2 and FMRP, in MEF2-induced elimination of synapses. Ongoing experiments are examining the molecular and cellular processes by which Pcdh17 mediates this process.

Figure 4.1. MEF2 and FMRP share a large overlap of targets.

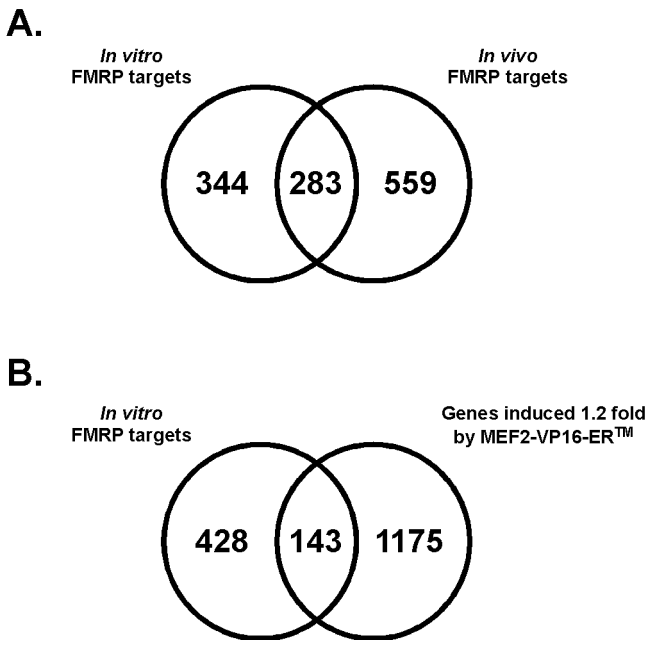

Figure 4.1. MEF2 and FMRP share a large overlap of targets. A, Venn diagram illustrating the overlap between FMRP targets identified with *in vitro* dissociated cortical neuron cultures and *in vivo* hippocampal tissue (Darnell et al., 2011). **B**, Venn diagram presenting the overlap between FMRP targets and genes whose expression is upregulated >1.2-fold following MEF2 activation.

Figure 4.2. Pcdh17 colozalizes with excitatory synaptic proteins in the hippocampus.

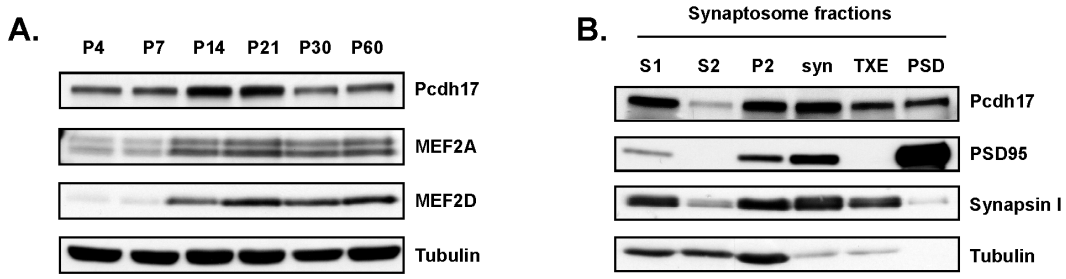

Figure 4.2. Pcdh17 colocalizes with excitatory synaptic proteins in the hippocampus. A, Timecourse of Pcdh17 protein expression in whole hippocampi from WT mice of ages ranging from P4 through P60. **B**, Synaptosomes were prepared from whole hippocampi of P15 mice. Pcdh17 colocalized to the membrane (P2) and synaptosome fractions. S1, total hippocampal homogenate with nuclei removed; S2, cytosol; P2, crude membrane fraction; syn, synaptosomes collected following Ficoll gradient fractionation; TXE, 1% Triton X-100-soluble fraction of syn; PSD, pellet after 0.5% Triton X-100 extraction. Synaptosome fractions were blotted with anti-Pcdh17, anti-PSD-95, anti-Synapsin1, and anti-Tubulin antibodies.

Figure 4.3. Analysis of Pcdh17 mRNA and protein regulation by MEF2 and FMRP in neurons.

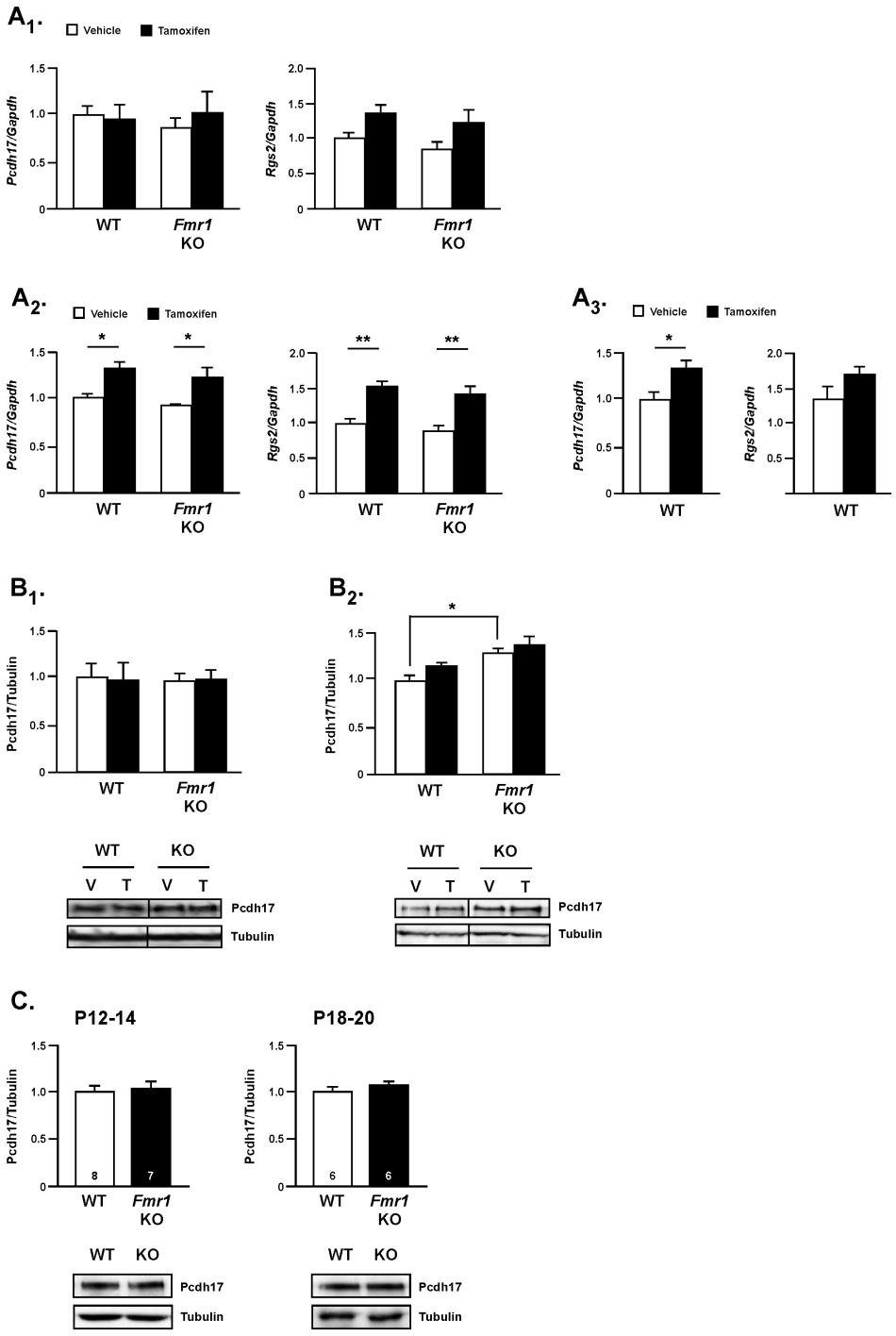

Figure 4.3. Analysis of Pcdh17 mRNA and protein regulation by MEF2 and FMRP in neurons. **A_1**, Dissociated WT or *Fmr1* KO hippocampal neurons cultured at P0 were transfected with MEF2-VP16-ER^{TM} using lentivirus at 2 DIV. At 9-10 DIV, neurons were stimulated with vehicle (0.1% EtOH) or 4OHT (2.5 μM) for 1 hr. Expression of *Pcdh10* and *Rgs2* mRNA was determined using real-time qPCR. Results were normalized to *Gapdh* mRNA levels. **A_2**, WT or *Fmr1* KO hippocampal neurons were cultured and transfected as in A_1. At 9-10 DIV, neurons were stimulated with vehicle (0.1% EtOH) or 4OHT (2.5 μM) for 3 hr. Expression of *Pcdh10* and *Rgs2* mRNA was determined using real-time qPCR. Results were normalized to *Gapdh* mRNA levels (*$p<0.05$, **$p<0.01$, Two-way ANOVA). **A_3**, WT or *Fmr1* KO hippocampal neurons were cultured and transfected as in A_1. At 9-10 DIV, neurons were stimulated with vehicle (0.1% EtOH) or 4OHT (2.5 μM) for 6 hr. Expression of *Pcdh10* and *Rgs2* mRNA was determined using real-time qPCR. Results were normalized to *Gapdh* mRNA levels (*$p<0.05$, Two-way ANOVA). **B_1**, WT or *Fmr1* KO hippocampal neurons were cultured and transfected as in A. At 9-10 DIV, neurons were stimulated with vehicle or 4OHT (2.5 μM) for 3 hr, and samples were lysed. Total cell lysates were blotted with anti-Pcdh17 and anti-Tubulin antibodies. **B_2**, WT or *Fmr1* KO hippocampal neurons were cultured and transfected as in A. At 9-10 DIV, neurons were stimulated with vehicle or 4OHT (2.5 μM) for 6 hr, and samples were lysed. Total cell lysates were blotted with anti-Pcdh17 and anti-Tubulin antibodies (*$p<0.05$, Two-way ANOVA). **C**, Western blots of whole hippocampi from P12-14 WT or *Fmr1* KO mice (left) and P18-20 WT or *Fmr1* KO mice (right). Lysates were blotted with anti-Pcdh17 and anti-Tubulin antibodies.

Figure 4.4. Pcdh17 knockdown does not affect excitatory synaptic number or function.

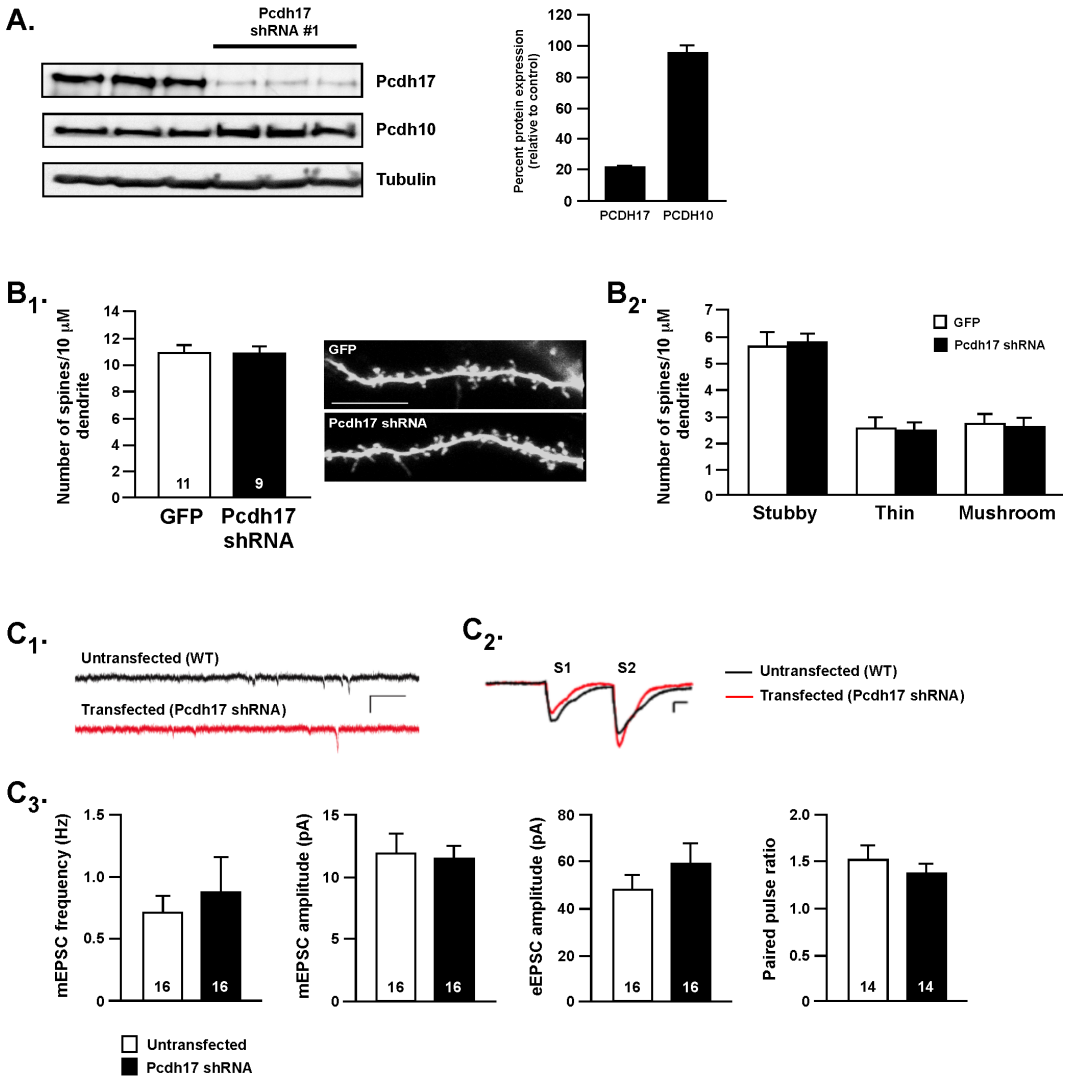

Figure 4.4. Pcdh17 knockdown does not affect excitatory synaptic number or function. A, Dissociated cortical neurons cultured at P0 were transfected with Pcdh17 shRNA using lentivirus at 3 DIV. Lysates were prepared 72 hr following addition of virus. Western blot analyses of Pcdh17 and Pcdh10 protein expression are shown (left). (Right) Quantification of Pcdh17 and Pcdh10 protein levels following expression of Pcdh17 shRNA. Pcdh17 and Pcdh10 protein levels are normalized to tubulin, and quantification of knockdown is indicated as percent

expression relative to control. The shRNA decreases Pcdh17 protein levels by 80%, without affecting levels of Pcdh10 protein. **B_1** and **B_2**, WT hippocampal organotypic slices were prepared at P6, and transfected with Pcdh17 shRNA at 5-6 DIV. **B_1**, Pcdh17 shRNA does not affect total dendritic spine density of CA1 pyramidal neurons. (Right) Representative images of apical dendrites from WT CA1 pyramdical neurons transfected with GFP alone or Pcdh17 + GFP for 48 hr. **B_2**, Pcdh17 shRNA does not affect density of dendritic spine subtypes (stubby, thin, mushroom). **C_1** and **C_2**, WT hippocampal organotypic slices were prepared at P6, and transfected with Pcdh17 shRNA at 5-6 DIV. Electrophysiology recordings from untransfected and transfected neurons in the same slice were performed at 48 hr post-transfection. Representative traces of mEPSCs (**C_1**) and evoked AMPAR-mediated EPSCs (**C_2**) are shown. **C_3**, Average mEPSC frequency, mEPSC amplitude, evoked AMPAR-mediated EPSC amplitude, and paired pulse ratio from untransfected WT neurons and neighboring neurons transfected with Pcdh17 shRNA.

Figure 4.5. Pcdh17 is required for MEF2-induced dendritic spine elimination.

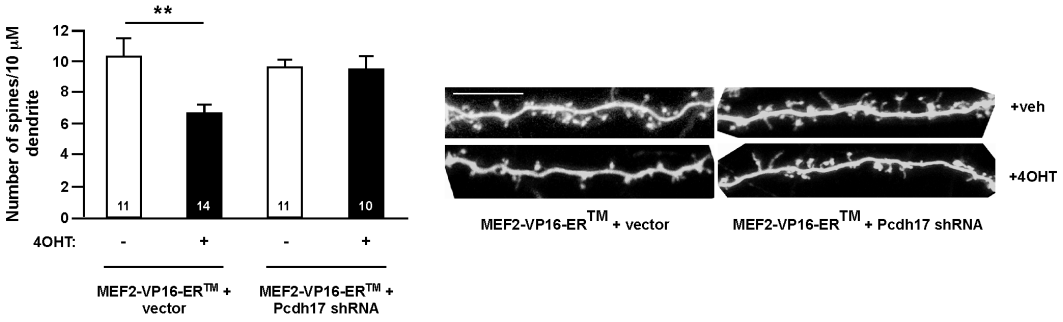

Figure 4.5. Pcdh17 is required for MEF2-induced dendritic spine elimination. WT organotypic hippocampal slices were prepared at P6, and transfected with Pcdh17 shRNA + vector or Pcdh17 shRNA + MEF2-VP16-ER^{TM} at 5-6 DIV. Slices were treated with vehicle or 4OHT (10 μM) 24 hr after transfection, and imaging was performed 24 hr later. Secondary apical dendrites from transfected CA1 pyramidal neurons were imaged (representative images shown, right).

Table 4.1. Results from HIT-CLIP studies (3 hr MEF2 activation).

FMRP binding order	Gene	Avg number of tags EtOH	Avg number of tags 4OHT	Fold change FMRP binding	t-test
548	Snx13	2108	2368	1.12	0.002
85	C330002I19Rik	7372	6186	0.84	0.005
573	St8sia1	1774	1049	0.59	0.008
16	Kif1b	17026	14895	0.87	0.011
114	Rfx3	6196	4792	0.77	0.012
546	Dchs1	2112	1406	0.67	0.014
537	Epb4.1l1	2167	1799	0.83	0.018
544	Auts2	2124	1219	0.57	0.018
202	Prkce	4307	3168	0.74	0.021
141	Mll1	5237	3965	0.76	0.021
218	Zfp238	4061	3324	0.82	0.021
589	Bclaf1	1856	2307	1.24	0.022
39	Sox11	10817	6424	0.59	0.024
58	Cugbp2	8255	6592	0.80	0.024
132	Trio	5547	4192	0.76	0.025
253	Smarca4	3623	2907	0.80	0.025
170	Mprip	4707	4002	0.85	0.026
516	Gnas	2235	1582	0.71	0.027
203	Ckap5	4289	3130	0.73	0.028
256	Lrp8	3590	2293	0.64	0.029
580	Angel2	789	2215	2.81	0.029
125	Zfp462	5747	3757	0.65	0.031
3	Macf1	31286	28075	0.90	0.032
494	Nucks1	2320	1521	0.66	0.034
50	Ncam1	9199	7203	0.78	0.038
40	Ccdc88a	10707	9026	0.84	0.040
121	Camsap1l1	5902	6548	1.11	0.043
468	Nufip2	2382	1949	0.82	0.046
603	Rapgef1	1579	2171	1.38	0.046
478	Lphn3	2387	1771	0.74	0.046
215	Pank3	4078	3258	0.80	0.046
562	Ccnd2	2055	1377	0.67	0.048

Table 4.1. Results from HITS-CLIP studies (3 hr MEF2 activation). Dissociated cortical neurons expressing MEF2-VP16-ER^{TM} were stimulated with 4OHT for 3 hr, and then exposed to UV radiation to crosslink FMRP-mRNA complexes. FMRP-mRNA complexes were immunoprecipitated, and RNA sequencing was performed to determine identities and abundances of FMRP-bound mRNAs. Transcripts that exhibited differential binding to FMRP following MEF2 activation are shown ($p<0.05$).

Table 4.2. Results from HITS-CLIP studies (6 hr MEF2 activation).

FMRP binding order	Gene	Avg number of tags EtOH	Avg number of tags 4OHT	Fold change FMRP binding	t-test
483	Nav2	3355	2518	0.75	0.002
445	Pcdhgc3	2502	1991	0.80	0.006
444	9030612M13Rik	2913	2199	0.76	0.010
435	Kif2a	3274	2347	0.72	0.021
440	Mapk6	3398	2336	0.69	0.021
495	Atp2b1	3084	2449	0.79	0.024
20	Spna2	17892	15030	0.84	0.025
557	Atp2a2	2468	1914	0.78	0.029
416	Mib1	3072	2074	0.68	0.031
526	Acvr2a	1998	1397	0.70	0.032
304	Brunol4	3466	2570	0.74	0.035
133	Matr3	6638	5400	0.81	0.037
11	Kif1a	20324	17840	0.88	0.039
91	Enc1	7536	6213	0.82	0.041
95	Mef2c	7004	5887	0.84	0.041
430	Prickle2	2767	2145	0.78	0.042
222	Rab6b	4828	4094	0.85	0.048
544	Auts2	1809	1499	0.83	0.048

Table 4.2. Results from HITS-CLIP studies (6 hr MEF2 activation). Dissociated cortical neurons expressing MEF2-VP16-ER^{TM} were stimulated with 4OHT for 6 hr, and then exposed to UV radiation to crosslink FMRP-mRNA complexes. FMRP-mRNA complexes were immunoprecipitated, and RNA sequencing was performed to determine identities and abundances of FMRP-bound mRNAs. Transcripts that exhibited differential binding to FMRP following MEF2 activation are shown ($p<0.05$).

CHAPTER FIVE: Concluding Remarks and Recommendations for Future Studies

The development of appropriate synaptic connections in the brain is a dynamic process involving synapse formation, elimination, maintenance, and plasticity. Early in postnatal development, many neural circuits form excess synapses that undergo pruning during adolescence in a sensory- and activity-dependent mechanism. Maintained synapses are also subject to experience-dependent modifications that can result in their strengthening or weakening. Deficits in synapse formation and function are hypothesized to underlie numerous neurological disorders; however, the molecular and cellular underpinnings of synaptic dysfunctions and their downstream consequences remain poorly understood.

BDNF and its high-affinity receptor, TrkB, are critical positive modulators of LTP, and emerging evidence suggests that BDNF/TrkB may facilitate LTP by inducing F-actin remodeling and morphological dynamics in dendritic spines. Indeed, BDNF-induced TrkB stimulates the activation of enzymes with well-documented roles in the regulation of F-actin cytoskeletal remodeling; however, additional studies are necessary to understand the molecular mechanisms that link BDNF/TrkB with this signaling event, and downstream consequences on synapse plasticity. In Chapters Two and Three of this manuscript, I describe the

identification of a novel, essential role for Vav GEFs in mediating BDNF-induced hippocampal dendritic spine growth and LTP, and furthermore, report that Vav promotes normal learning and memory, and anxiety-associated behaviors in mice.

More recently, the transcription factor MEF2 has emerged as a key regulator of synapse number and function. MEF2 proteins negatively regulate synapse number *in vitro* and *in vivo*, and recently, the RNA-binding protein FMRP was identified as an essential downstream component of MEF2-induced synapse pruning, revealing a common pathway through which MEF2 and FMRP promote the elimination of synapses. Critical experiments are necessary to delineate cellular and molecular mechanisms underlying this process. In Chapter Four, I investigate molecular mechanisms underlying MEF2- and FMRP-dependent elimination of synapses, applying a specific focus on the identification of shared MEF2 and FMRP mRNA targets that mediate synapse removal. I report that Pcdh17, a common target of MEF2 and FMRP that is enriched at excitatory synapses, is necessary for MEF2-induced dendritic spine elimination of hippocampal CA1 neurons.

Findings reported in this manuscript identify novel mechanisms underlying BDNF-dependent and MEF2-dependent regulation of synapses. However, future experiments remain to uncover the specific molecular and cellular processes through which Vav GEFs and MEF2 transcription factors control synapse plasticity.

Part One: Vav GEFs are Important Regulators of Synapse and Behavioral Plasticity

Increasing evidence suggests that functional synapse plasticity is highly correlated with structural spine dynamics, especially for durable plasticity events, including LTP and LTD, which are correlated with dendritic spine enlargement and contraction, respectively (Cingolani and Goda, 2008; Dillon and Goda, 2005; Yuste and Bonhoeffer, 2001). BDNF and its cognate receptor, TrkB, are positive modulators of hippocampal CA3-CA1 TBS-LTP, and studies reveal that BDNF/TrkB may facilitate LTP in part through the modulation of F-actin remodeling enzymes and dendritic spine dynamics. Lines of evidence supporting this hypothesis include (1) Rho-GTPases, critical regulators of F-actin formation and cytoskeletal dynamics, are activated by BDNF-stimulated TrkB signaling (Huang and Reichardt, 2003), (2) BDNF promotes the formation of TBS-induced F-actin assembly in dendritic spines (Rex et al., 2007), (3) F-actin polymerization is required for hippocampal CA3-CA1 TBS-LTP (Chen et al., 1999; Kim and Lisman, 1999; Krucker et al., 2000), and (4) pairing local glutamate uncaging with postsynaptic spikes leads to long-lasting increases in dendritic spine head size through a mechanism that requires TrkB kinase-dependent signaling (Tanaka et al., 2008).

BDNF/TrkB signaling is hypothesized to facilitate functional and structural synapse plasticity events, in part, through the activation of Rho-family GTPases, modulators of F-actin formation and cytoskeletal dynamics (Luo, 2002; Tashiro and Yuste, 2004). GTPases act as molecular switches, cycling between inactive and active states, in which they are bound to GDP and GTP, respectively. GEFs activate GTPases by facilitating the exchange of GDP for GTP, while GAPs render GTPases inactive by accelerating the hydrolysis of GTP. The BDNF/TrkB-induced activation of Rho GTPases is a well-established signaling event (Huang and Reichardt, 2003); however, the molecular events that link BDNF/TrkB with Rho GTPase activation, and subsequent downstream consequences on synapse plasticity have not been well studied.

Vav GEFs, which stimulate Rac1- and Cdc42-GTP formation, GTPases associated with dendritic spine formation and growth, are activated by several receptor tyrosine kinases, including Eph, FGF, and PDGF receptors (Abe et al., 2000; Cowan et al., 2005; Kawakatsu et al., 2005; Marignani and Carpenter, 2001). We speculated therefore that Vav GEFs might be activated by BDNF-induced TrkB receptor signaling, and that they might regulate BDNF/TrkB-dependent synaptic functions. In Chapter Two, we report that BDNF stimulates the transient tyrosine phosphorylation and activation of Vav in neurons, and that BDNF-induced Rac-GTP activation in hippocampal organotypic slices requires Vav GEFs. While Vav GEFs are not necessary for synapse number, they are

required for dendritic spine growth induced by stimulation with exogenous BDNF. Importantly, TBS-LTP is impaired in Vav-deficient hippocampal slices, suggesting that Vav-dependent F-actin remodeling may contribute to structural spine dynamics and functional plasticity. Experiments in HEK cells reveal that kinase-active TrkB activates Vav2 independently of the ERK/PI3-K- (Y490) and PLCγ (Y785)-interacting sites. A number of important questions remain regarding the role of Vav GEFs in BDNF-dependent structural and functional synapse plasticity.

In general, our findings are consistent with the large body of work generated by the BDNF/TrkB field. Zhou and colleagues recently reported that PI3-K activity is not required for BDNF-induced activation of Rac in cerebellar granule cell precursors, supporting the idea that Rac activation is not downstream of PI3-K activity, but is a parallel signaling process necessary for cell morphological changes (Zhou et al., 2007). Additional studies report that phosphorylation of TrkB's Y490 (ERK/PI3-K) is important for filopodial motility and hippocampal synaptogenesis (Luikart et al., 2008), but is dispensable for LTP induction (Gruart et al., 2007; Minichiello et al., 2002). Our findings are consistent with these observations, as TrkB Y490 is not necessary for BDNF/TrkB-dependent activation of Vav GEFs, which are required for LTP, but not synaptogenesis in the hippocampus. Interestingly, unlike TrkB knockout mice, CA1 neurons from brain-specific BDNF knockouts do not have a reduced

dendritic spine density. Rather, they exhibit fewer mushroom spines, more thin spines, and a concomitant impairment in CA3-CA1 LTP, indicating that TrkB may regulate dendritic spine number independently of BDNF *in vivo*, and furthermore, suggesting that BNDF-dependent LTP deficits do not result from dendritic spine and synapse loss (Rauskolb et al., 2010).

Our findings link Vav GEFs to F-actin dynamics in dendritic spines and functional synapses, and furthermore, suggest a potential mechanism by which BDNF/TrkB signaling may contribute to hippocampal LTP. In the future, it will be important to determine the downstream signaling events and cellular processes by which Vav GEFs elicit these changes. We speculate here that Vav mediates BDNF-induced dendritic spine growth and LTP by promoting F-actin dynamics in spines; however, no studies were performed to examine the specific involvement of Vav GEFs in BDNF- or LTP-induced F-actin formation. By staining hippocampal slices with phalloidin, a mushroom toxin that binds F-actin, it is possible to examine whether Vav GEFs promote the enhancement of F-actin levels induced by exogenous BDNF treatment or LTP stimulation protocols in neurons. Results from this experiment would implicate a clearer link between Vav GEFs and BDNF-induced F-actin polymerization. An additional note of interest is that in the absence of Vav GEFs, significant residual BDNF-induced Rac-GTP activation remains, suggesting the contribution of other GEFs to BDNF-enhanced Rac-GTP levels, F-actin formation, and possibly BDNF-dependent plasticities.

Two studies have recently reported that the Rho GEF Tiam1 is activated by BDNF/TrkB and is required for BDNF-stimulated Rac-GTP in cortical and cerebellar granule cell precursors (Miyamoto et al., 2006; Zhou et al., 2007). These studies link deficient Tiam1-dependent F-actin remodeling with impairments in neurite outgrowth and cell migration in cortical neurons and cerebellar granule cell precursors, respectively. In light of these findings, we believe that Tiam1 may also be contributing to BDNF-induced Rac-GTP levels in our experiments presented here.

BDNF induces transient Vav tyrosine phosphorylation and Rac-GTP production. As such, we hypothesize that Vav GEF signaling stimulates transient F-actin assembly, but that an independent, protein synthesis-dependent molecular process likely stabilizes the F-actin cytoskeleton and the maintenance of LTP. In line with these findings, we observe that treatment of hippocampal slices with exogenous BDNF induces rapid dendritic spine head growth, but that incubation with BDNF enhances, but is not sufficient to stimulate CA3-CA1 LTP. This observation lends evidence that BDNF-stimulated spine head enlargement may be permissive for LTP, but additional activity-dependent processes are necessary to induce and stabilize LTP.

Findings reported here suggest that Vav acts postsynaptically to induce F-actin dynamics and promote dendritic spine enlargement and hippocampal LTP. Because the mice used in these studies are total knockouts, we cannot rule out a

presynaptic contribution of the GEFs in the observed functional and structural synaptic deficits. An additional concern is that Vav2 and Vav3 mRNA and protein are expressed in glial astrocyte cultures, introducing the possibility that Vav-dependent functions in glia may contribute to the reported phenotypes. Also, any developmental aberrations formed prior to the synapse plasticities studied here at P15 may also impinge on or underlie these events. A potential experiment to address these concerns is to examine whether reducing Vav in the CA1 region of the hippocampus is sufficient to impair LTP. Notably, the development of a Vav conditional knockout mouse would be an important and invaluable tool to resolve the questions stated here, as well as address concerns relevant to Vav's roles in behavioral regulation, presented in Chapter Three.

On a mechanistic note, it is possible Vav GEFs may effect the synaptic events reported here by stimulating the endocytosis of the BDNF/TrkB receptor complex. Neuronal activity promotes BDNF-dependent TrkB receptor internalization, and unlike other receptors, in which endocytosis terminates growth factor signaling, the internalized TrkB receptor complex forms signaling endosomes with molecules such as PI3-K, MAPK, and PLCγ (Bhattacharyya et al., 1997; Riccio et al., 1997; Senger and Campenot, 1997; Sorkin and Waters, 1993). No evidence describing a requirement for endocytosis of BDNF/TrkB for TBS-LTP or dendritic spine plasticity has been reported. However, BDNF/TrkB endocytosis is critical for promoting forward-signaling processes necessary for

BDNF-dependent neuronal survival and migration of cerebellar granule cell precursors (Valdez et al., 2005; Zhou et al., 2007). As Vav GEFs are known to be required for internalization of the ephrinA1/Eph receptor complex in retinal ganglion cells to promote Eph receptor forward signaling during axon guidance (Cowan et al., 2005), this suggests that Vav GEFs may also regulate BDNF/TrkB endocytosis to stimulate downstream plasticity effects.

Findings described above link Vav GEFs with hippocampal dendritic spine enlargement and LTP, prompting speculation that Vav-dependent synaptic functions may facilitate normal behavioral responses. To investigate this possibility, we evaluated Vav2- and Vav3-deficient mice for performance in various behavioral paradigms. We hypothesized that because Vav knockouts have impaired hippocampal LTP, a cellular substrate of learning and memory, that they might exhibit deficits in hippocampal-dependent learning tasks, including contextual fear conditioning and Morris water maze tests. *Vav2*$^{-/-}$*3*$^{-/-}$ knockouts have impaired contextual but not cued fear conditioning, but demonstrate no changes in spatial navigation in the Morris water maze. Associative learning appears to be controlled by both *Vav2* and *Vav3* genes, as individual Vav GEF knockouts each displayed deficiencies in context-dependent fear conditioning. Vav GEFs are also necessary for behavioral responses related to anxiety, since *Vav2*$^{-/-}$*3*$^{-/-}$ knockout mice additionally exhibited an anxiolytic phenotype in elevated plus maze and open field tests. Vav2 specifically promotes normal

anxiety responses, as anxiolytic behaviors were observed only in Vav2 knockouts. These findings demonstrate that Vav GEFs facilitate associative fear conditioning and promote anxiety-like behaviors in mice.

Two recent studies linking Vav GEFs with proper visual and motor circuit formation raise concerns that the behavioral deficits arise from visual or motor impairments (Cowan et al., 2005; Quevedo et al., 2010). *Vav3*$^{-/-}$ mice at five weeks of age have impaired motor coordination in the rotarod accelerating test and an abnormal pattern of paw overlap (Quevedo et al., 2010). These deficits are a hypothesized consequence of deficient Purkinje cell dendritic arborization and impaired granule cell survival and migration. By four months of age, the approximate age in which we performed our behavioral studies, these problems were corrected or significantly ameliorated. Additionally, mice used in our study were not hyper- or hypoactive, exhibited no gross motor coordination deficits, and displayed normal magnitudes of speed in all tasks assessed. An additional concern for analyses of behavioral performance of the Vav knockout mice is the potential for visual impairments, as a recent study reported impaired ipsilateral axon projections from RGCs to the dLGN in *Vav2*$^{-/-}$*3*$^{-/-}$ mice (Cowan et al., 2005). However, our studies indicate that the Vav knockouts did not possess deficient vision, as overall, Vav single and double mutant mice exhibited learning of the platform location in the Morris water maze, and also easily located the escape platform when made visible.

The hippocampus is necessary for contextual fear conditioning and is also involved with anxiety and stress. Our findings suggest that Vav-dependent structural and functional synapse dynamics in the hippocampus may facilitate normal contextual fear conditioning and anxiety in mice. However, because total knockout mice were used in these studies, Vav-dependent functions in other brain regions may also be contributing to these behaviors. Additionally, there could be a developmental role for Vav GEFs occurring prior to the reported deficits in dendritic spine and synapse plasticity that underlies or promotes the behavioral responses. One potential experiment to investigate this concern is to examine whether re-expressing and restoring Vav-dependent functions in the hippocampus is sufficient to rescue deficits in contextual fear conditioning and anxiety. Also, the generation and analysis of Vav conditional knockout mice would be an important tool to resolve these remaining questions and identify the specific circuitry by which Vav GEFs facilitate normal behavioral responses.

An interesting finding in these studies is that Vav2, but not Vav3 promotes anxiety-related behaviors in mice. Specifically, we observe that *Vav2*$^{-/-}$*3*$^{-/-}$ mice have reduced anxiety, and further analysis of single knockouts indicates that Vav2, and not Vav3, mediates the anxiolytic phenotype. In the future it will be interesting to investigate the mechanisms by which Vav2 specifically controls anxiety-related behavior. One possibility may be differences in expression levels of Vav2 and Vav3 in brain circuitry that underlies anxiety. To date, a detailed

examination of Vav2 and Vav3 expression in specific brain regions has not been reported. It will thus be informative to investigate patterns of Vav2 and Vav3 expression in the brain from development through adulthood, which may have implications for cellular and behavioral functions for Vav proteins.

In this study, we hypothesized that Vav GEFs might mediate BDNF/TrkB-dependent behaviors, and therefore, that Vav knockout mice would mimic behavior phenotypes that result from BDNF/TrkB deficiency. Similar to BDNF or TrkB knockouts, Vav-deficient mice have impaired contextual fear conditioning; however, Vav knockouts do not present with deficits in spatial navigation in the Morris water maze, unlike BDNF- or TrkB-deficient mice. Functions for the neurotrophin in modulating anxiety has not been as extensively studied and results are often inconsistent. While one study reports that heterozygous BDNF mice have increased anxiety in open field and elevated plus maze tests (Chen et al., 2006), a separate study describes that forebrain deletion of BDNF in mice leads to reduced anxiety in female mice in elevated plus maze and open field tests, with no differences observed in male mice (Monteggia et al., 2007). Here, we found that *Vav2*$^{-/-}$*3*$^{-/-}$ mice have reduced anxiety in elevated plus maze and open field tests. Together, our results illustrate that Vav GEFs support a subset of behaviors controlled by BDNF/TrkB function, lending evidence that they may regulate these behaviors downstream of BDNF/TrkB signaling, but also indicating that they likely modulate other behaviors independently of BDNF/TrkB.

Here, we investigated a role for Vav GEFs in controlling learning and memory, as well as anxiety-related behaviors, but did not examine their involvement in other behavioral paradigms. As a recent GWAS links Vav3 with schizophrenia, it will interesting in the future to assess whether Vav GEFs control schizophrenia-related behaviors, including prepulse inhibition (PPI), latent inhibition, and social interaction. Regulation of Rac1 activation has also been demonstrated to control behaviors associated with addiction to cocaine, suggestive that GEFs may have a role in mediating behaviors induced by use of illicit drugs. Finally, analyses of depression-related behaviors in Vav-deficient mice may describe a role for the GEFs in regulating associated behaviors since anxiety and depression commonly exhibit comorbidity in human patients.

In conclusion, the data provided in this study describe a novel, essential role for Vav GEFs in controlling BDNF-induced dendritic spine enlargement and CA3-CA1 LTP. Specifically, our findings suggest that Vav GEFs promote BDNF-dependent structural and functional plasticity by facilitating BDNF-stimulated Rac-GTP activation and F-actin remodeling. Behavioral analysis of Vav knockout mice reveals that Vav deficiency leads to impaired hippocampal-dependent contextual fear conditioning and anxiolytic responses. These results support a role for Vav GEFs in controlling learning and memory, and anxiety behaviors in mice, and suggest that their functions in neuronal development and plasticity may underlie these behaviors.

Part Two: Pcdh17, a Common Target of MEF2 and FMRP, is Required for MEF2-induced Synapse Pruning

MEF2 transcription factors promote activity-dependent synapse elimination in neurons *in vitro* and *in vivo* in molecular and cellular processes that are poorly understood (Barbosa et al., 2008; Flavell et al., 2006; Pfeiffer et al., 2010; Pulipparacharuvil et al., 2008; Tsai et al., 2012; Wilkerson et al., 2014). The RNA binding protein FMRP was recently discovered to be required for MEF2-induced synapse pruning (Pfeiffer et al., 2010). Fragile X syndrome (FXS), the most prevalent inherited form of autism, results from loss-of-function mutations in FMRP and is characterized by several synaptic deficits, including increased excitatory synapse number (Bassell and Warren, 2008). FMRP controls synapse plasticity through translational regulation of its targeted transcripts, likely acting as a translational switch to suppress or permit mRNA translation (Bassell and Warren, 2008).

Studies indicate that one-third of the synaptic proteome are FMRP targets, and approximately 50% of identified autism gene candidates are targets of FMRP, supporting the hypothesis that dysfunction in FMRP-dependent translation increases the risk of synapse dysfunction and autism (Darnell et al., 2011). Molecular and behavioral studies also link MEF2 with autism and intellectual disability. MEF2 regulates numerous candidate autism genes, including *DIA1*

(deleted in autism-1) and *PCDH10* (protocadherin 10) (Flavell et al., 2008; Morrow et al., 2008). Importantly, several human patients with autism, mental retardation, and epilepsy are reported to have deletions in the *MEF2C* gene (Novara et al., 2010; Novara et al., 2013; Paciorkowski et al., 2013; Zweier et al., 2010; Zweier and Rauch, 2012).

Together, these studies suggest that MEF2 and FMRP coordinate transcriptional and translational control of common mRNAs to confer proper experience-dependent synapse refinement and brain function. To test this hypothesis, we utilized high throughput sequencing of RNA isolated by cross-linking immunoprecipitation (HITS-CLIP) of FMRP to identify common targets of MEF2 and FMRP in neurons. We find a large overlap of MEF2-induced transcripts and FMRP-associated mRNAs, consistent with their shared roles in synapse elimination. Interestingly, a majority of the δ2 subfamily of non-clustered protocadherins are targets of both MEF2 and FMRP. Several of the δ2 protocadherins, including *Pcdh8*, *9*, *10* and *19* have been linked with autism, and *Pcdh17* is implicated in schizophrenia and language delay (Dean et al., 2007; Kim et al., 2011; Morrow et al., 2008; Piton et al., 2011; Prasad et al., 2012). In our studies, we specifically observe that Pcdh17 mRNA is upregulated by MEF2, and that binding of the Pcdh17 transcript to FMRP is reduced following MEF2 activation. Using shRNA-mediated RNAi, we find that Pcdh17 is necessary for MEF2-dependent dendritic spine elimination of CA1 pyramidal neurons.

Reducing Pcdh17 in the absence of MEF2 activity does not alter structural or functional glutamatergic synapses, suggesting that Pcdh17 does not alter basal synapse numbers.

The studies presented here suggest a potential role for Pcdh17 in MEF2-dependent synaptic connectivity; however, several future experiments are necessary to support a requirement for Pcdh17 MEF2-triggered synapse pruning. The initial immediate step will be to confirm that shRNA-mediated Pcdh17 knockdown, and not off-target effects of the short hairpin, is responsible for blocking MEF2-induced synapse elimination. This will be achieved by co-expressing an shRNA-insensitive Pcdh17 cDNA together with the constitutively active MEF2 and Pcdh17 shRNA constructs. A subsequent key step is to examine whether Pcdh17 controls MEF2-mediated elimination of functional synapse number. To test this, the Pcdh17 shRNA will be co-expressed with constitutively active MEF2, and electrophysiology recordings will be obtained to ascertain effects on excitatory synapse number and function. As with the MEF2-induced structural dendritic spine elimination experiments, we will rescue any effects observed with the shRNA-insensitive Pcdh17.

FMRP is required for MEF2-triggered elimination of synapses (Pfeiffer et al., 2010), suggesting that MEF2 and FMRP coordinate transcriptional and translational control of common mRNA targets to promote appropriate synaptic refinement. Consistent with this idea, data from the HITS-CLIP and RNA-seq

experiments illustrate that MEF2 and FMRP share a large overlap of common gene transcript targets. Specifically, we observe that approximately 25% of FMRP's targets are induced to >1.2-fold by MEF2, supporting the hypothesis that MEF2 and FMRP function in the same pathway and regulate expression of common transcripts to produce synaptic changes. A particularly interesting finding in the FMRP HITS-CLIP analysis is that 90% (45/50) of mRNA targets that exhibited significantly changed binding to FMRP following MEF2 activation specifically showed reduced association with FMRP. Considering FMRP's widely hypothesized role as a translational suppressor, this observation suggests that FMRP is disassociating from the transcripts to allow their translation. Additionally, this finding raises the possibility that MEF2 may stimulate the disassociation of FMRP from its targets to promote expression of these transcripts. Future experiments are necessary to explore these interesting questions.

Pcdh17 mRNA is expressed in dendrites (Cajigas et al., 2012), is upregulated by MEF2 activity (Chapter 4 and (Flavell et al., 2008), and is targeted for association with FMRP. This suggests that FMRP may regulate the local dendritic translation of MEF2-induced transcripts that promote synapse removal. Additional experiments are necessary to examine the specific regulation of Pcdh17 protein by MEF2 activity and FMRP. MEF2 activity increases Pcdh17 mRNA levels by approximately 35% in neuronal total cell lysates, but whether

this generates an increase in Pcdh17 protein levels is not yet known. Preliminary experiments indicate a trend towards a slight increase (15%) in MEF2-stimulated total levels of Pcdh17 protein, and this effect may reach significance with the inclusion of more replicates, or with longer lengths of MEF2 activation. Additionally, an enhancement of Pcdh17 protein levels may be more readily discerned in synaptic compartments, where we believe it is exerting its effects on synapses. A well-established mechanism that stimulates FMRP-dependent translation is the activation of group 1 (Gp1) metabotropic glutamate receptors (mGluRs), mGluR1 and mGluR5 (Bassell and Warren, 2008; Dictenberg et al., 2008). Importantly, dendritic mGluR5 activity was recently reported to be necessary for MEF2-induced synapse elimination. It will therefore be interesting to determine if dendritic Pcdh17 translation is regulated by mGluR5 and FMRP, and if specific dendritic expression of Pcdh17 is necessary for the removal of synapses triggered by MEF2. An important note is that the specific regulation of Pcdh17 levels by MEF2 and FMRP may not be necessary for the MEF2-induced synapse elimination process. Rather, MEF2 may promote synapse elimination via a mechanism that requires Pcdh17, but the regulation of Pcdh17 by MEF2 and FMRP may not be required for that function.

Our findings suggest that Pcdh17 is required for MEF2-induced excitatory synapse pruning. Critical future experiments are necessary to examine key molecular and cellular mechanisms by which Pcdh17 mediates MEF2- and

FMRP-dependent synapse elimination. Previous studies report that fellow δ2 protocadherin family members Pcdh8 and Pcdh10 are necessary for activity-dependent synapse pruning, evoking the possibility that Pcdh17 may regulate MEF2-dependent synaptic connectivity through related mechanisms. Specifically, Pcdh8 stimulates p38MAPK-dependent endocytosis of N-cadherin in response to depolarization, resulting in dendritic spine loss (Yasuda et al., 2007). Pcdh10 promotes MEF2-triggered synapse pruning by facilitating the delivery of MEF2-induced ubiquitinated PSD-95 to the proteasome (Tsai et al., 2012). A structural analysis of Pcdh17 may lend insight into its mechanistic properties. For example, Tsai and colleagues identified a highly conserved region of approximately 100 amino acids in Pcdh10 that mediates an interaction with the proteasome. It will be interesting to determine whether the proteasome interacting region is conserved across δ2 protocadherins, including Pcdh17. Recently, a study identified a conserved perptide motif, the WAVE regulatory complex (WRC) interacting receptor sequence (WIRS), that is possessed by all δ2 protocadherins (Chen et al., 2014). The WIRS mediates binding to the WRC, a complex that regulates actin cytoskeletal dynamics by controlling activity of the Arp2/3 complex. Together, these studies reveal mechanisms of δ2 protocadherin-mediated synapse control involving N-cadherin internalization, PSD-95 degradation, and actin cytoskeletal dynamics, through which Pcdh17 may potentially control MEF2-induced synapse elimination.

Together, the findings described here support coordinated functions of MEF2 and FMRP in the transcriptional and translational regulation of shared mRNA targets that mediate synapse elimination, and specifically identify one gene transcript, Pcdh17, that is co-regulated by MEF2 and FMRP, and is necessary for MEF2-triggered pruning of synapses. Ongoing studies are examining the molecular and cellular mechanisms by which Pcdh17 mediates MEF2-dependent synapse elimination.

BIBLIOGRAPHY

(1994). Fmr1 knockout mice: a model to study fragile X mental retardation. The Dutch-Belgian Fragile X Consortium. Cell 78, 23-33.

Abe, K., Rossman, K.L., Liu, B., Ritola, K.D., Chiang, D., Campbell, S.L., Burridge, K., and Der, C.J. (2000). Vav2 is an activator of Cdc42, Rac1, and RhoA. J Biol Chem 275, 10141-10149.

Adachi, M., Barrot, M., Autry, A.E., Theobald, D., and Monteggia, L.M. (2008). Selective loss of brain-derived neurotrophic factor in the dentate gyrus attenuates antidepressant efficacy. Biol Psychiatry 63, 642-649.

Adams, J.P., and Sweatt, J.D. (2002). Molecular psychology: roles for the ERK MAP kinase cascade in memory. Annu Rev Pharmacol Toxicol 42, 135-163.

Aghazadeh, B., Lowry, W.E., Huang, X.Y., and Rosen, M.K. (2000). Structural basis for relief of autoinhibition of the Dbl homology domain of proto-oncogene Vav by tyrosine phosphorylation. Cell 102, 625-633.

Akhtar, M.W., Kim, M.S., Adachi, M., Morris, M.J., Qi, X., Richardson, J.A., Bassel-Duby, R., Olson, E.N., Kavalali, E.T., and Monteggia, L.M. (2012). In vivo analysis of MEF2 transcription factors in synapse regulation and neuronal survival. PLoS One 7, e34863.

Aleksic, B., Kushima, I., Hashimoto, R., Ohi, K., Ikeda, M., Yoshimi, A., Nakamura, Y., Ito, Y., Okochi, T., Fukuo, Y., et al. (2013). Analysis of the VAV3 as candidate gene for schizophrenia: evidences from voxel-based morphometry and mutation screening. Schizophr Bull 39, 720-728.

Aramburu, J., Heitman, J., and Crabtree, G.R. (2004). Calcineurin: a central controller of signalling in eukaryotes. EMBO Rep 5, 343-348.

Aramburu, J., Rao, A., and Klee, C.B. (2000). Calcineurin: from structure to function. Curr Top Cell Regul 36, 237-295.

Barbosa, A.C., Kim, M.S., Ertunc, M., Adachi, M., Nelson, E.D., McAnally, J., Richardson, J.A., Kavalali, E.T., Monteggia, L.M., Bassel-Duby, R., et al. (2008). MEF2C, a transcription factor that facilitates learning and memory

by negative regulation of synapse numbers and function. Proc Natl Acad Sci U S A 105, 9391-9396.

Bassell, G.J., and Warren, S.T. (2008). Fragile X syndrome: loss of local mRNA regulation alters synaptic development and function. Neuron 60, 201-214.

Berton, O., McClung, C.A., Dileone, R.J., Krishnan, V., Renthal, W., Russo, S.J., Graham, D., Tsankova, N.M., Bolanos, C.A., Rios, M., et al. (2006). Essential role of BDNF in the mesolimbic dopamine pathway in social defeat stress. Science 311, 864-868.

Bertos, N.R., Wang, A.H., and Yang, X.J. (2001). Class II histone deacetylases: structure, function, and regulation. Biochem Cell Biol 79, 243-252.

Bhattacharyya, A., Watson, F.L., Bradlee, T.A., Pomeroy, S.L., Stiles, C.D., and Segal, R.A. (1997). Trk receptors function as rapid retrograde signal carriers in the adult nervous system. J Neurosci 17, 7007-7016.

Black, B.L., and Olson, E.N. (1998). Transcriptional control of muscle development by myocyte enhancer factor-2 (MEF2) proteins. Annu Rev Cell Dev Biol 14, 167-196.

Bramham, C.R. (2008). Local protein synthesis, actin dynamics, and LTP consolidation. Curr Opin Neurobiol 18, 524-531.

Bremner, J.D., Narayan, M., Anderson, E.R., Staib, L.H., Miller, H.L., and Charney, D.S. (2000). Hippocampal volume reduction in major depression. Am J Psychiatry 157, 115-118.

Brown, V., Jin, P., Ceman, S., Darnell, J.C., O'Donnell, W.T., Tenenbaum, S.A., Jin, X., Feng, Y., Wilkinson, K.D., Keene, J.D., et al. (2001). Microarray identification of FMRP-associated brain mRNAs and altered mRNA translational profiles in fragile X syndrome. Cell 107, 477-487.

Burwell, R.D., Saddoris, M.P., Bucci, D.J., and Wiig, K.A. (2004). Corticohippocampal contributions to spatial and contextual learning. J Neurosci 24, 3826-3836.

Bustelo, X.R. (2000). Regulatory and signaling properties of the Vav family. Mol Cell Biol 20, 1461-1477.

Bustelo, X.R. (2001). Vav proteins, adaptors and cell signaling. Oncogene 20, 6372-6381.

Cajigas, I.J., Tushev, G., Will, T.J., tom Dieck, S., Fuerst, N., and Schuman, E.M. (2012). The local transcriptome in the synaptic neuropil revealed by deep sequencing and high-resolution imaging. Neuron 74, 453-466.

Caldeira, M.V., Melo, C.V., Pereira, D.B., Carvalho, R., Correia, S.S., Backos, D.S., Carvalho, A.L., Esteban, J.A., and Duarte, C.B. (2007). Brain-derived neurotrophic factor regulates the expression and synaptic delivery of alpha-amino-3-hydroxy-5-methyl-4-isoxazole propionic acid receptor subunits in hippocampal neurons. J Biol Chem 282, 12619-12628.

Castren, E. (2004). Neurotrophic effects of antidepressant drugs. Curr Opin Pharmacol 4, 58-64.

Castren, E., and Rantamaki, T. (2010). The role of BDNF and its receptors in depression and antidepressant drug action: Reactivation of developmental plasticity. Dev Neurobiol 70, 289-297.

Ceman, S., O'Donnell, W.T., Reed, M., Patton, S., Pohl, J., and Warren, S.T. (2003). Phosphorylation influences the translation state of FMRP-associated polyribosomes. Hum Mol Genet 12, 3295-3305.

Cerione, R.A., and Zheng, Y. (1996). The Dbl family of oncogenes. Curr Opin Cell Biol 8, 216-222.

Chahrour, M., Jung, S.Y., Shaw, C., Zhou, X., Wong, S.T., Qin, J., and Zoghbi, H.Y. (2008). MeCP2, a key contributor to neurological disease, activates and represses transcription. Science 320, 1224-1229.

Chan, J.K., Sun, L., Yang, X.J., Zhu, G., and Wu, Z. (2003). Functional characterization of an amino-terminal region of HDAC4 that possesses MEF2 binding and transcriptional repressive activity. J Biol Chem 278, 23515-23521.

Chang, Q., Khare, G., Dani, V., Nelson, S., and Jaenisch, R. (2006). The disease progression of Mecp2 mutant mice is affected by the level of BDNF expression. Neuron 49, 341-348.

Chen, B., Brinkmann, K., Chen, Z., Pak, C.W., Liao, Y., Shi, S., Henry, L., Grishin, N.V., Bogdan, S., and Rosen, M.K. (2014). The WAVE regulatory complex links diverse receptors to the actin cytoskeleton. Cell 156, 195-207.

Chen, G., Kolbeck, R., Barde, Y.A., Bonhoeffer, T., and Kossel, A. (1999). Relative contribution of endogenous neurotrophins in hippocampal long-term potentiation. J Neurosci 19, 7983-7990.

Chen, L., and Toth, M. (2001). Fragile X mice develop sensory hyperreactivity to auditory stimuli. Neuroscience 103, 1043-1050.

Chen, W.G., Chang, Q., Lin, Y., Meissner, A., West, A.E., Griffith, E.C., Jaenisch, R., and Greenberg, M.E. (2003). Derepression of BDNF transcription involves calcium-dependent phosphorylation of MeCP2. Science 302, 885-889.

Chen, Z.Y., Jing, D., Bath, K.G., Ieraci, A., Khan, T., Siao, C.J., Herrera, D.G., Toth, M., Yang, C., McEwen, B.S., et al. (2006). Genetic variant BDNF (Val66Met) polymorphism alters anxiety-related behavior. Science 314, 140-143.

Cingolani, L.A., and Goda, Y. (2008). Actin in action: the interplay between the actin cytoskeleton and synaptic efficacy. Nat Rev Neurosci 9, 344-356.

Citri, A., and Malenka, R.C. (2008). Synaptic plasticity: multiple forms, functions, and mechanisms. Neuropsychopharmacology 33, 18-41.

Cole, C.J., Mercaldo, V., Restivo, L., Yiu, A.P., Sekeres, M.J., Han, J.H., Vetere, G., Pekar, T., Ross, P.J., Neve, R.L., et al. (2012). MEF2 negatively regulates learning-induced structural plasticity and memory formation. Nat Neurosci 15, 1255-1264.

Comery, T.A., Harris, J.B., Willems, P.J., Oostra, B.A., Irwin, S.A., Weiler, I.J., and Greenough, W.T. (1997). Abnormal dendritic spines in fragile X knockout mice: maturation and pruning deficits. Proc Natl Acad Sci U S A 94, 5401-5404.

Cowan, C.W., Shao, Y.R., Sahin, M., Shamah, S.M., Lin, M.Z., Greer, P.L., Gao, S., Griffith, E.C., Brugge, J.S., and Greenberg, M.E. (2005). Vav family GEFs link activated Ephs to endocytosis and axon guidance. Neuron 46, 205-217.

Crespo, P., Schuebel, K.E., Ostrom, A.A., Gutkind, J.S., and Bustelo, X.R. (1997). Phosphotyrosine-dependent activation of Rac-1 GDP/GTP exchange by the vav proto-oncogene product. Nature 385, 169-172.

Cunningham, M.E., and Greene, L.A. (1998). A function-structure model for NGF-activated TRK. EMBO J 17, 7282-7293.

Darnell, J.C., Jensen, K.B., Jin, P., Brown, V., Warren, S.T., and Darnell, R.B. (2001). Fragile X mental retardation protein targets G quartet mRNAs important for neuronal function. Cell 107, 489-499.

Darnell, J.C., Van Driesche, S.J., Zhang, C., Hung, K.Y., Mele, A., Fraser, C.E., Stone, E.F., Chen, C., Fak, J.J., Chi, S.W., et al. (2011). FMRP stalls ribosomal translocation on mRNAs linked to synaptic function and autism. Cell 146, 247-261.

De Boulle, K., Verkerk, A.J., Reyniers, E., Vits, L., Hendrickx, J., Van Roy, B., Van den Bos, F., de Graaff, E., Oostra, B.A., and Willems, P.J. (1993). A point mutation in the FMR-1 gene associated with fragile X mental retardation. Nat Genet 3, 31-35.

Dean, B., Keriakous, D., Scarr, E., and Thomas, E.A. (2007). Gene expression profiling in Brodmann's area 46 from subjects with schizophrenia. Aust N Z J Psychiatry 41, 308-320.

Dictenberg, J.B., Swanger, S.A., Antar, L.N., Singer, R.H., and Bassell, G.J. (2008). A direct role for FMRP in activity-dependent dendritic mRNA transport links filopodial-spine morphogenesis to fragile X syndrome. Dev Cell 14, 926-939.

Dietz, D.M., Sun, H., Lobo, M.K., Cahill, M.E., Chadwick, B., Gao, V., Koo, J.W., Mazei-Robison, M.S., Dias, C., Maze, I., et al. (2012). Rac1 is essential in cocaine-induced structural plasticity of nucleus accumbens neurons. Nat Neurosci 15, 891-896.

Dillon, C., and Goda, Y. (2005). The actin cytoskeleton: integrating form and function at the synapse. Annu Rev Neurosci 28, 25-55.

Dluzen, D.E., Gao, X., Story, G.M., Anderson, L.I., Kucera, J., and Walro, J.M. (2001). Evaluation of nigrostriatal dopaminergic function in adult +/+ and +/- BDNF mutant mice. Exp Neurol 170, 121-128.

Dolen, G., Osterweil, E., Rao, B.S., Smith, G.B., Auerbach, B.D., Chattarji, S., and Bear, M.F. (2007). Correction of fragile X syndrome in mice. Neuron 56, 955-962.

Dressel, U., Bailey, P.J., Wang, S.C., Downes, M., Evans, R.M., and Muscat, G.E. (2001). A dynamic role for HDAC7 in MEF2-mediated muscle differentiation. J Biol Chem 276, 17007-17013.

Eadie, B.D., Zhang, W.N., Boehme, F., Gil-Mohapel, J., Kainer, L., Simpson, J.M., and Christie, B.R. (2009). Fmr1 knockout mice show reduced anxiety and alterations in neurogenesis that are specific to the ventral dentate gyrus. Neurobiol Dis 36, 361-373.

Ehler, E., van Leeuwen, F., Collard, J.G., and Salinas, P.C. (1997). Expression of Tiam-1 in the developing brain suggests a role for the Tiam-1-Rac signaling pathway in cell migration and neurite outgrowth. Mol Cell Neurosci 9, 1-12.

Figurov, A., Pozzo-Miller, L.D., Olafsson, P., Wang, T., and Lu, B. (1996). Regulation of synaptic responses to high-frequency stimulation and LTP by neurotrophins in the hippocampus. Nature 381, 706-709.

Flavell, S.W., Cowan, C.W., Kim, T.K., Greer, P.L., Lin, Y., Paradis, S., Griffith, E.C., Hu, L.S., Chen, C., and Greenberg, M.E. (2006). Activity-dependent regulation of MEF2 transcription factors suppresses excitatory synapse number. Science 311, 1008-1012.

Flavell, S.W., Kim, T.K., Gray, J.M., Harmin, D.A., Hemberg, M., Hong, E.J., Markenscoff-Papadimitriou, E., Bear, D.M., and Greenberg, M.E. (2008). Genome-wide analysis of MEF2 transcriptional program reveals synaptic target genes and neuronal activity-dependent polyadenylation site selection. Neuron 60, 1022-1038.

Fukazawa, Y., Saitoh, Y., Ozawa, F., Ohta, Y., Mizuno, K., and Inokuchi, K. (2003). Hippocampal LTP is accompanied by enhanced F-actin content within the dendritic spine that is essential for late LTP maintenance in vivo. Neuron 38, 447-460.

Gao, Y., Dickerson, J.B., Guo, F., Zheng, J., and Zheng, Y. (2004). Rational design and characterization of a Rac GTPase-specific small molecule inhibitor. Proc Natl Acad Sci U S A 101, 7618-7623.

Garber, K.B., Visootsak, J., and Warren, S.T. (2008). Fragile X syndrome. Eur J Hum Genet 16, 666-672.

Garrett, T.A., Van Buul, J.D., and Burridge, K. (2007). VEGF-induced Rac1 activation in endothelial cells is regulated by the guanine nucleotide exchange factor Vav2. Exp Cell Res 313, 3285-3297.

Gartner, A., and Staiger, V. (2002). Neurotrophin secretion from hippocampal neurons evoked by long-term-potentiation-inducing electrical stimulation patterns. Proc Natl Acad Sci U S A 99, 6386-6391.

Gartner, A., Polnau, D.G., Staiger, V., Sciarretta, C., Minichiello, L., Thoenen, H., Bonhoeffer, T., and Korte, M. (2006). Hippocampal long-term potentiation is supported by presynaptic and postsynaptic tyrosine receptor kinase B-mediated phospholipase Cgamma signaling. J Neurosci 26, 3496-3504.

Gaudilliere, B., Shi, Y., and Bonni, A. (2002). RNA interference reveals a requirement for myocyte enhancer factor 2A in activity-dependent neuronal survival. J Biol Chem 277, 46442-46446.

Gong, X., Tang, X., Wiedmann, M., Wang, X., Peng, J., Zheng, D., Blair, L.A., Marshall, J., and Mao, Z. (2003). Cdk5-mediated inhibition of the protective effects of transcription factor MEF2 in neurotoxicity-induced apoptosis. Neuron 38, 33-46.

Gorski, J.A., Balogh, S.A., Wehner, J.M., and Jones, K.R. (2003). Learning deficits in forebrain-restricted brain-derived neurotrophic factor mutant mice. Neuroscience 121, 341-354.

Graham, D.L., Edwards, S., Bachtell, R.K., DiLeone, R.J., Rios, M., and Self, D.W. (2007). Dynamic BDNF activity in nucleus accumbens with cocaine use increases self-administration and relapse. Nat Neurosci 10, 1029-1037.

Graham, D.L., Krishnan, V., Larson, E.B., Graham, A., Edwards, S., Bachtell, R.K., Simmons, D., Gent, L.M., Berton, O., Bolanos, C.A., et al. (2009). Tropomyosin-related kinase B in the mesolimbic dopamine system: region-specific effects on cocaine reward. Biol Psychiatry 65, 696-701.

Grossman, A.W., Aldridge, G.M., Lee, K.J., Zeman, M.K., Jun, C.S., Azam, H.S., Arii, T., Imoto, K., Greenough, W.T., and Rhyu, I.J. (2010). Developmental characteristics of dendritic spines in the dentate gyrus of Fmr1 knockout mice. Brain Res 1355, 221-227.

Grossman, A.W., Elisseou, N.M., McKinney, B.C., and Greenough, W.T. (2006). Hippocampal pyramidal cells in adult Fmr1 knockout mice exhibit an immature-appearing profile of dendritic spines. Brain Res 1084, 158-164.

Grozinger, C.M., and Schreiber, S.L. (2000). Regulation of histone deacetylase 4 and 5 and transcriptional activity by 14-3-3-dependent cellular localization. Proc Natl Acad Sci U S A 97, 7835-7840.

Gruart, A., Sciarretta, C., Valenzuela-Harrington, M., Delgado-Garcia, J.M., and Minichiello, L. (2007). Mutation at the TrkB PLC{gamma}-docking site affects hippocampal LTP and associative learning in conscious mice. Learn Mem 14, 54-62.

Hagerman, R.J., Ono, M.Y., and Hagerman, P.J. (2005). Recent advances in fragile X: a model for autism and neurodegeneration. Curr Opin Psychiatry 18, 490-496.

Hale, C.F., Dietz, K.C., Varela, J.A., Wood, C.B., Zirlin, B.C., Leverich, L.S., Greene, R.W., and Cowan, C.W. (2011). Essential role for vav Guanine nucleotide exchange factors in brain-derived neurotrophic factor-induced dendritic spine growth and synapse plasticity. J Neurosci 31, 12426-12436.

Hale, C.F., Dietz, K.C., Varela, J.A., Wood, C.B., Zirlin, B.C., Leverich, L.S., Greene, R.W., and Cowan, C.W. (2011). Essential role for vav Guanine nucleotide exchange factors in brain-derived neurotrophic factor-induced dendritic spine growth and synapse plasticity. J Neurosci 31, 12426-12436.

Han, J., Das, B., Wei, W., Van Aelst, L., Mosteller, R.D., Khosravi-Far, R., Westwick, J.K., Der, C.J., and Broek, D. (1997). Lck regulates Vav activation of members of the Rho family of GTPases. Mol Cell Biol 17, 1346-1353.

Han, J., Jiang, Y., Li, Z., Kravchenko, V.V., and Ulevitch, R.J. (1997). Activation of the transcription factor MEF2C by the MAP kinase p38 in inflammation. Nature 386, 296-299.

Harris, K.M., and Kater, S.B. (1994). Dendritic spines: cellular specializations imparting both stability and flexibility to synaptic function. Annu Rev Neurosci 17, 341-371.

Hashimoto, T., Bergen, S.E., Nguyen, Q.L., Xu, B., Monteggia, L.M., Pierri, J.N., Sun, Z., Sampson, A.R., and Lewis, D.A. (2005). Relationship of brain-derived neurotrophic factor and its receptor TrkB to altered inhibitory prefrontal circuitry in schizophrenia. J Neurosci 25, 372-383.

Hays, S.A., Huber, K.M., and Gibson, J.R. (2011). Altered neocortical rhythmic activity states in Fmr1 KO mice are due to enhanced mGluR5 signaling and involve changes in excitatory circuitry. J Neurosci 31, 14223-14234.

Heidenreich, K.A., and Linseman, D.A. (2004). Myocyte enhancer factor-2 transcription factors in neuronal differentiation and survival. Mol Neurobiol 29, 155-166.

Heo, J., Thapar, R., and Campbell S.L. (2005). Recognition and activation of Rho GTPases by Vav1 and Vav2 guanine nucleotide exchange factors. Biochemistry 44, 6573-6585.

Honkura, N., Matsuzaki, M., Noguchi, J., Ellis-Davies, G.C., and Kasai, H. (2008). The subspine organization of actin fibers regulates the structure and plasticity of dendritic spines. Neuron 57, 719-729.

Hoshina, N., Tanimura, A., Yamasaki, M., Inoue, T., Fukabori, R., Kuroda, T., Yokoyama, K., Tezuka, T., Sagara, H., Hirano, S., et al. (2013). Protocadherin 17 regulates presynaptic assembly in topographic corticobasal Ganglia circuits. Neuron 78, 839-854.

Hua, J.Y., and Smith, S.J. (2004). Neural activity and the dynamics of central nervous system development. Nat Neurosci 7, 327-332.

Huang, E.J., and Reichardt, L.F. (2003). Trk receptors: roles in neuronal signal transduction. Annu Rev Biochem 72, 609-642.

Huang, Y.Y., Zakharenko, S.S., Schoch, S., Kaeser, P.S., Janz, R., Sudhof, T.C., Siegelbaum, S.A., and Kandel, E.R. (2005). Genetic evidence for a protein-kinase-A-mediated presynaptic component in NMDA-receptor-dependent forms of long-term synaptic potentiation. Proc Natl Acad Sci U S A 102, 9365-9370.

Huber, K.M., Gallagher, S.M., Warren, S.T., and Bear, M.F. (2002). Altered synaptic plasticity in a mouse model of fragile X mental retardation. Proc Natl Acad Sci U S A 99, 7746-7750.

Huber, K.M., Kayser, M.S., and Bear, M.F. (2000). Role for rapid dendritic protein synthesis in hippocampal mGluR-dependent long-term depression. Science 288, 1254-1257.

Hunter, S.G., Zhuang, G., Brantley-Sieders, D., Swat, W., Cowan, C.W., and Chen, J. (2006). Essential role of Vav family guanine nucleotide exchange factors in EphA receptor-mediated angiogenesis. Mol Cell Biol 26, 4830-4842.

Ikeda, M., Aleksic, B., Kinoshita, Y., Okochi, T., Kawashima, K., Kushima, I., Ito, Y., Nakamura, Y., Kishi, T., Okumura, T., et al. (2011). Genome-wide association study of schizophrenia in a Japanese population. Biol Psychiatry 69, 472-478.

Ikeshima, H., Imai, S., Shimoda, K., Hata, J., and Takano, T. (1995). Expression of a MADS box gene, MEF2D, in neurons of the mouse central nervous system: implication of its binary function in myogenic and neurogenic cell lineages. Neurosci Lett 200, 117-120.

Irwin, S.A., Idupulapati, M., Gilbert, M.E., Harris, J.B., Chakravarti, A.B., Rogers, E.J., Crisostomo, R.A., Larsen, B.P., Mehta, A., Alcantara, C.J., et al. (2002). Dendritic spine and dendritic field characteristics of layer V pyramidal neurons in the visual cortex of fragile-X knockout mice. Am J Med Genet 111, 140-146.

Irwin, S.A., Idupulapati, M., Gilbert, M.E., Harris, J.B., Chakravarti, A.B., Rogers, E.J., Crisostomo, R.A., Larsen, B.P., Mehta, A., Alcantara, C.J., et al. (2002). Dendritic spine and dendritic field characteristics of layer V pyramidal neurons in the visual cortex of fragile-X knockout mice. Am J Med Genet 111, 140-146.

Irwin, S.A., Patel, B., Idupulapati, M., Harris, J.B., Crisostomo, R.A., Larsen, B.P., Kooy, F., Willems, P.J., Cras, P., Kozlowski, P.B., et al. (2001). Abnormal dendritic spine characteristics in the temporal and visual cortices of patients with fragile-X syndrome: a quantitative examination. Am J Med Genet 98, 161-167.

Jovanovic, J.N., Benfenati, F., Siow, Y.L., Sihra, T.S., Sanghera, J.S., Pelech, S.L., Greengard, P., and Czernik, A.J. (1996). Neurotrophins stimulate phosphorylation of synapsin I by MAP kinase and regulate synapsin I-actin interactions. Proc Natl Acad Sci U S A 93, 3679-3683.

Jovanovic, J.N., Czernik, A.J., Fienberg, A.A., Greengard, P., and Sihra, T.S. (2000). Synapsins as mediators of BDNF-enhanced neurotransmitter release. Nat Neurosci 3, 323-329.

Kang, H., and Schuman, E.M. (1996). A requirement for local protein synthesis in neurotrophin-induced hippocampal synaptic plasticity. Science 273, 1402-1406.

Kanhema, T., Dagestad, G., Panja, D., Tiron, A., Messaoudi, E., Havik, B., Ying, S.W., Nairn, A.C., Sonenberg, N., and Bramham, C.R. (2006). Dual regulation of translation initiation and peptide chain elongation during BDNF-induced LTP in vivo: evidence for compartment-specific translation control. J Neurochem 99, 1328-1337.

Kao, H.Y., Verdel, A., Tsai, C.C., Simon, C., Juguilon, H., and Khochbin, S. (2001). Mechanism for nucleocytoplasmic shuttling of histone deacetylase 7. J Biol Chem 276, 47496-47507.

Kaplan, D.R., and Miller, F.D. (2000). Neurotrophin signal transduction in the nervous system. Curr Opin Neurobiol 10, 381-391.

Kasai, H., Fukuda, M., Watanabe, S., Hayashi-Takagi, A., and Noguchi, J. (2010). Structural dynamics of dendritic spines in memory and cognition. Trends Neurosci 33, 121-129.

Kaufmann, W.E., Cortell, R., Kau, A.S., Bukelis, I., Tierney, E., Gray, R.M., Cox, C., Capone, G.T., and Stanard, P. (2004). Autism spectrum disorder in fragile X syndrome: communication, social interaction, and specific behaviors. Am J Med Genet A 129A, 225-234.

Kawakatsu, T., Ogita, H., Fukuhara, T., Fukuyama, T., Minami, Y., Shimizu, K., and Takai, Y. (2005). Vav2 as a Rac-GDP/GTP exchange factor responsible for the nectin-induced, c-Src- and Cdc42-mediated activation of Rac. J Biol Chem 280, 4940-4947.

Kim, C.H., and Lisman, J.E. (1999). A role of actin filament in synaptic transmission and long-term potentiation. J Neurosci 19, 4314-4324.

Kim, S.Y., Yasuda, S., Tanaka, H., Yamagata, K., and Kim, H. (2011). Non-clustered protocadherin. Cell Adh Migr 5, 97-105.

Kiraly, D.D., Nemirovsky, N.E., LaRese, T.P., Tomek, S.E., Yahn, S.L., Olive, M.F., Eipper, B.A., and Mains, R.E. (2013). Constitutive knockout of

kalirin-7 leads to increased rates of cocaine self-administration. Mol Pharmacol 84, 582-590.

Korte, M., Carroll, P., Wolf, E., Brem, G., Thoenen, H., and Bonhoeffer, T. (1995). Hippocampal long-term potentiation is impaired in mice lacking brain-derived neurotrophic factor. Proc Natl Acad Sci U S A 92, 8856-8860.

Korte, M., Griesbeck, O., Gravel, C., Carroll, P., Staiger, V., Thoenen, H., and Bonhoeffer, T. (1996). Virus-mediated gene transfer into hippocampal CA1 region restores long-term potentiation in brain-derived neurotrophic factor mutant mice. Proc Natl Acad Sci U S A 93, 12547-12552.

Kossel, A.H., Cambridge, S.B., Wagner, U., and Bonhoeffer, T. (2001). A caged Ab reveals an immediate/instructive effect of BDNF during hippocampal synaptic potentiation. Proc Natl Acad Sci U S A 98, 14702-14707.

Krishnan, V., Han, M.H., Graham, D.L., Berton, O., Renthal, W., Russo, S.J., Laplant, Q., Graham, A., Lutter, M., Lagace, D.C., et al. (2007). Molecular adaptations underlying susceptibility and resistance to social defeat in brain reward regions. Cell 131, 391-404.

Krucker, T., Siggins, G.R., and Halpain, S. (2000). Dynamic actin filaments are required for stable long-term potentiation (LTP) in area CA1 of the hippocampus. Proc Natl Acad Sci U S A 97, 6856-6861.

Krueger, D.D., Osterweil, E.K., Chen, S.P., Tye, L.D., and Bear, M.F. (2011). Cognitive dysfunction and prefrontal synaptic abnormalities in a mouse model of fragile X syndrome. Proc Natl Acad Sci U S A 108, 2587-2592.

Lauterborn, J.C., Rex, C.S., Kramar, E., Chen, L.Y., Pandyarajan, V., Lynch, G., and Gall, C.M. (2007). Brain-derived neurotrophic factor rescues synaptic plasticity in a mouse model of fragile X syndrome. J Neurosci 27, 10685-10694.

Leifer, D., Krainc, D., Yu, Y.T., McDermott, J., Breitbart, R.E., Heng, J., Neve, R.L., Kosofsky, B., Nadal-Ginard, B., and Lipton, S.A. (1993). MEF2C, a MADS/MEF2-family transcription factor expressed in a laminar distribution in cerebral cortex. Proc Natl Acad Sci U S A 90, 1546-1550.

Li, H., Radford, J.C., Ragusa, M.J., Shea, K.L., McKercher, S.R., Zaremba, J.D., Soussou, W., Nie, Z., Kang, Y.J., Nakanishi, N., et al. (2008).

Transcription factor MEF2C influences neural stem/progenitor cell differentiation and maturation in vivo. Proc Natl Acad Sci U S A 105, 9397-9402.

Lin, X., Shah, S., and Bulleit, R.F. (1996). The expression of MEF2 genes is implicated in CNS neuronal differentiation. Brain Res Mol Brain Res 42, 307-316.

Lisman, J., Yasuda, R., and Raghavachari, S. (2012). Mechanisms of CaMKII action in long-term potentiation. Nat Rev Neurosci 13, 169-182.

Liu, B.P., and Burridge, K. (2000). Vav2 activates Rac1, Cdc42, and RhoA downstream from growth factor receptors but not beta1 integrins. Mol Cell Biol 20, 7160-7169.

Liu, I.Y., Lyons, W.E., Mamounas, L.A., and Thompson, R.F. (2004). Brain-derived neurotrophic factor plays a critical role in contextual fear conditioning. J Neurosci 24, 7958-7963.

Luikart, B.W., Nef, S., Virmani, T., Lush, M.E., Liu, Y., Kavalali, E.T., and Parada, L.F. (2005). TrkB has a cell-autonomous role in the establishment of hippocampal Schaffer collateral synapses. J Neurosci 25, 3774-3786.

Luikart, B.W., Zhang, W., Wayman, G.A., Kwon, C.H., Westbrook, G.L., and Parada, L.F. (2008). Neurotrophin-dependent dendritic filopodial motility: a convergence on PI3K signaling. J Neurosci 28, 7006-7012.

Luo, L. (2002). Actin cytoskeleton regulation in neuronal morphogenesis and structural plasticity. Annu Rev Cell Dev Biol 18, 601-635.

Lyons, G.E., Micales, B.K., Schwarz, J., Martin, J.F., and Olson, E.N. (1995). Expression of mef2 genes in the mouse central nervous system suggests a role in neuronal maturation. J Neurosci 15, 5727-5738.

Lyons, M.R., Schwarz, C.M., and West, A.E. (2012). Members of the myocyte enhancer factor 2 transcription factor family differentially regulate Bdnf transcription in response to neuronal depolarization. J Neurosci 32, 12780-12785.

Mao, Z., and Wiedmann, M. (1999). Calcineurin enhances MEF2 DNA binding activity in calcium-dependent survival of cerebellar granule neurons. J Biol Chem 274, 31102-31107.

Marignani, P.A., and Carpenter, C.L. (2001). Vav2 is required for cell spreading. J Cell Biol 154, 177-186.

Marinissen, M.J., Chiariello, M., Pallante, M., and Gutkind, J.S. (1999). A network of mitogen-activated protein kinases links G protein-coupled receptors to the c-jun promoter: a role for c-Jun NH2-terminal kinase, p38s, and extracellular signal-regulated kinase 5. Mol Cell Biol 19, 4289-4301.

Matsutani, S., and Yamamoto, N. (2004). Brain-derived neurotrophic factor induces rapid morphological changes in dendritic spines of olfactory bulb granule cells in cultured slices through the modulation of glutamatergic signaling. Neuroscience 123, 695-702.

Matsuzaki, M., Honkura, N., Ellis-Davies, G.C., and Kasai, H. (2004). Structural basis of long-term potentiation in single dendritic spines. Nature 429, 761-766.

McKinsey, T.A., Zhang, C.L., and Olson, E.N. (2002). MEF2: a calcium-dependent regulator of cell division, differentiation and death. Trends Biochem Sci 27, 40-47.

Merenstein, S.A., Sobesky, W.E., Taylor, A.K., Riddle, J.E., Tran, H.X., and Hagerman, R.J. (1996). Molecular-clinical correlations in males with an expanded FMR1 mutation. Am J Med Genet 64, 388-394.

Minichiello, L. (2009). TrkB signalling pathways in LTP and learning. Nat Rev Neurosci 10, 850-860.

Minichiello, L., Calella, A.M., Medina, D.L., Bonhoeffer, T., Klein, R., and Korte, M. (2002). Mechanism of TrkB-mediated hippocampal long-term potentiation. Neuron 36, 121-137.

Minichiello, L., Korte, M., Wolfer, D., Kuhn, R., Unsicker, K., Cestari, V., Rossi-Arnaud, C., Lipp, H.P., Bonhoeffer, T., and Klein, R. (1999). Essential role for TrkB receptors in hippocampus-mediated learning. Neuron 24, 401-414.

Miyamoto, Y., Yamauchi, J., Tanoue, A., Wu, C., and Mobley, W.C. (2006). TrkB binds and tyrosine-phosphorylates Tiam1, leading to activation of Rac1 and induction of changes in cellular morphology. Proc Natl Acad Sci U S A 103, 10444-10449.

Molkentin, J.D., Black, B.L., Martin, J.F., and Olson, E.N. (1996). Mutational analysis of the DNA binding, dimerization, and transcriptional activation domains of MEF2C. Mol Cell Biol 16, 2627-2636.

Montag, C., Basten, U., Stelzel, C., Fiebach, C.J., and Reuter, M. (2010). The BDNF Val66Met polymorphism and anxiety: support for animal knock-in studies from a genetic association study in humans. Psychiatry Res 179, 86-90.

Monteggia, L.M., Barrot, M., Powell, C.M., Berton, O., Galanis, V., Gemelli, T., Meuth, S., Nagy, A., Greene, R.W., and Nestler, E.J. (2004). Essential role of brain-derived neurotrophic factor in adult hippocampal function. Proc Natl Acad Sci U S A 101, 10827-10832.

Monteggia, L.M., Luikart, B., Barrot, M., Theobold, D., Malkovska, I., Nef, S., Parada, L.F., and Nestler, E.J. (2007). Brain-derived neurotrophic factor conditional knockouts show gender differences in depression-related behaviors. Biol Psychiatry 61, 187-197.

Moon, M.S., and Gomez, T.M. (2010). Balanced Vav2 GEF activity regulates neurite outgrowth and branching in vitro and in vivo. Mol Cell Neurosci 44, 118-128.

Morrow, E.M., Yoo, S.Y., Flavell, S.W., Kim, T.K., Lin, Y., Hill, R.S., Mukaddes, N.M., Balkhy, S., Gascon, G., Hashmi, A., et al. (2008). Identifying autism loci and genes by tracing recent shared ancestry. Science 321, 218-223.

Musumeci, S.A., Bosco, P., Calabrese, G., Bakker, C., De Sarro, G.B., Elia, M., Ferri, R., and Oostra, B.A. (2000). Audiogenic seizures susceptibility in transgenic mice with fragile X syndrome. Epilepsia 41, 19-23.

Nakao, S., Platek, A., Hirano, S., and Takeichi, M. (2008). Contact-dependent promotion of cell migration by the OL-protocadherin-Nap1 interaction. J Cell Biol 182, 395-410.

Nakayama, A.Y., Harms, M.B., and Luo, L. (2000). Small GTPases Rac and Rho in the maintenance of dendritic spines and branches in hippocampal pyramidal neurons. J Neurosci 20, 5329-5338.

Niere, F., Wilkerson, J.R., and Huber, K.M. (2012). Evidence for a fragile X mental retardation protein-mediated translational switch in metabotropic

glutamate receptor-triggered Arc translation and long-term depression. J Neurosci 32, 5924-5936.

Novara, F., Beri, S., Giorda, R., Ortibus, E., Nageshappa, S., Darra, F., Dalla Bernardina, B., Zuffardi, O., and Van Esch, H. (2010). Refining the phenotype associated with MEF2C haploinsufficiency. Clin Genet 78, 471-477.

Novara, F., Rizzo, A., Bedini, G., Girgenti, V., Esposito, S., Pantaleoni, C., Ciccone, R., Sciacca, F.L., Achille, V., Della Mina, E., et al. (2013). MEF2C deletions and mutations versus duplications: a clinical comparison. Eur J Med Genet 56, 260-265.

O'Donnell, W.T., and Warren, S.T. (2002). A decade of molecular studies of fragile X syndrome. Annu Rev Neurosci 25, 315-338.

Okamoto, K., Nagai, T., Miyawaki, A., and Hayashi, Y. (2004). Rapid and persistent modulation of actin dynamics regulates postsynaptic reorganization underlying bidirectional plasticity. Nat Neurosci 7, 1104-1112.

Okamoto, S., Li, Z., Ju, C., Scholzke, M.N., Mathews, E., Cui, J., Salvesen, G.S., Bossy-Wetzel, E., and Lipton, S.A. (2002). Dominant-interfering forms of MEF2 generated by caspase cleavage contribute to NMDA-induced neuronal apoptosis. Proc Natl Acad Sci U S A 99, 3974-3979.

Onitsuka, T., Shenton, M.E., Salisbury, D.F., Dickey, C.C., Kasai, K., Toner, S.K., Frumin, M., Kikinis, R., Jolesz, F.A., and McCarley, R.W. (2004). Middle and inferior temporal gyrus gray matter volume abnormalities in chronic schizophrenia: an MRI study. Am J Psychiatry 161, 1603-1611.

Paciorkowski, A.R., Traylor, R.N., Rosenfeld, J.A., Hoover, J.M., Harris, C.J., Winter, S., Lacassie, Y., Bialer, M., Lamb, A.N., Schultz, R.A., et al. (2013). MEF2C Haploinsufficiency features consistent hyperkinesis, variable epilepsy, and has a role in dorsal and ventral neuronal developmental pathways. Neurogenetics 14, 99-111.

Pandey, A., Podtelejnikov, A.V., Blagoev, B., Bustelo, X.R., Mann, M., and Lodish, H.F. (2000). Analysis of receptor signaling pathways by mass spectrometry: identification of vav-2 as a substrate of the epidermal and platelet-derived growth factor receptors. Proc Natl Acad Sci U S A 97, 179-184.

Paradee, W., Melikian, H.E., Rasmussen, D.L., Kenneson, A., Conn, P.J., and Warren, S.T. (1999). Fragile X mouse: strain effects of knockout phenotype and evidence suggesting deficient amygdala function. Neuroscience 94, 185-192.

Patel, A.B., Loerwald, K.W., Huber, K.M., and Gibson, J.R. (2013). Postsynaptic FMRP promotes the pruning of cell-to-cell connections among pyramidal neurons in the L5A neocortical network. J Neurosci 34, 3413-3418.

Patterson, S.L., Abel, T., Deuel, T.A., Martin, K.C., Rose, J.C., and Kandel, E.R. (1996). Recombinant BDNF rescues deficits in basal synaptic transmission and hippocampal LTP in BDNF knockout mice. Neuron 16, 1137-1145.

Peier, A.M., McIlwain, K.L., Kenneson, A., Warren, S.T., Paylor, R., and Nelson, D.L. (2000). (Over)correction of FMR1 deficiency with YAC transgenics: behavioral and physical features. Hum Mol Genet 9, 1145-1159.

Pfeiffer, B.E., and Huber, K.M. (2007). Fragile X mental retardation protein induces synapse loss through acute postsynaptic translational regulation. J Neurosci 27, 3120-3130.

Pfeiffer, B.E., Zang, T., Wilkerson, J.R., Taniguchi, M., Maksimova, M.A., Smith, L.N., Cowan, C.W., and Huber, K.M. (2010). Fragile X mental retardation protein is required for synapse elimination by the activity-dependent transcription factor MEF2. Neuron 66, 191-197.

Pietropaolo, S., Guilleminot, A., Martin, B., D'Amato, F.R., and Crusio, W.E. (2011). Genetic-background modulation of core and variable autistic-like symptoms in Fmr1 knock-out mice. PLoS One 6, e17073.

Piton, A., Gauthier, J., Hamdan, F.F., Lafreniere, R.G., Yang, Y., Henrion, E., Laurent, S., Noreau, A., Thibodeau, P., Karemera, L., et al. (2011). Systematic resequencing of X-chromosome synaptic genes in autism spectrum disorder and schizophrenia. Mol Psychiatry 16, 867-880.

Pozzo-Miller, L.D., Gottschalk, W., Zhang, L., McDermott, K., Du, J., Gopalakrishnan, R., Oho, C., Sheng, Z.H., and Lu, B. (1999). Impairments in high-frequency transmission, synaptic vesicle docking, and synaptic protein distribution in the hippocampus of BDNF knockout mice. J Neurosci 19, 4972-4983.

Prasad, A., Merico, D., Thiruvahindrapuram, B., Wei, J., Lionel, A.C., Sato, D., Rickaby, J., Lu, C., Szatmari, P., Roberts, W., et al. (2012). A discovery resource of rare copy number variations in individuals with autism spectrum disorder. G3 (Bethesda) 2, 1665-1685.

Pulipparacharuvil, S., Renthal, W., Hale, C.F., Taniguchi, M., Xiao, G., Kumar, A., Russo, S.J., Sikder, D., Dewey, C.M., Davis, M.M., et al. (2008). Cocaine regulates MEF2 to control synaptic and behavioral plasticity. Neuron 59, 621-633.

Qiu, L.F., Lu, T.J., Hu, X.L., Yi, Y.H., Liao, W.P., and Xiong, Z.Q. (2009). Limbic epileptogenesis in a mouse model of fragile X syndrome. Cereb Cortex 19, 1504-1514.

Quevedo, C., Sauzeau, V., Menacho-Marquez, M., Castro-Castro, A., and Bustelo, X.R. (2010). Vav3-deficient mice exhibit a transient delay in cerebellar development. Mol Biol Cell 21, 1125-1139.

Rakic, P., Bourgeois, J.P., Eckenhoff, M.F., Zecevic, N., and Goldman-Rakic, P.S. (1986). Concurrent overproduction of synapses in diverse regions of the primate cerebral cortex. Science 232, 232-235.

Rao, A., and Steward, O. (1991). Evidence that protein constituents of postsynaptic membrane specializations are locally synthesized: analysis of proteins synthesized within synaptosomes. J Neurosci 11, 2881-2895.

Rauskolb, S., Zagrebelsky, M., Dreznjak, A., Deogracias, R., Matsumoto, T., Wiese, S., Erne, B., Sendtner, M., Schaeren-Wiemers, N., Korte, M., et al. (2010). Global deprivation of brain-derived neurotrophic factor in the CNS reveals an area-specific requirement for dendritic growth. J Neurosci 30, 1739-1749.

Rex, C.S., Chen, L.Y., Sharma, A., Liu, J., Babayan, A.H., Gall, C.M., and Lynch, G. (2009). Different Rho GTPase-dependent signaling pathways initiate sequential steps in the consolidation of long-term potentiation. J Cell Biol 186, 85-97.

Rex, C.S., Lin, C.Y., Kramar, E.A., Chen, L.Y., Gall, C.M., and Lynch, G. (2007). Brain-derived neurotrophic factor promotes long-term potentiation-related cytoskeletal changes in adult hippocampus. J Neurosci 27, 3017-3029.

Riccio, A., Pierchala, B.A., Ciarallo, C.L., and Ginty, D.D. (1997). An NGF-TrkA-mediated retrograde signal to transcription factor CREB in sympathetic neurons. Science 277, 1097-1100.

Righi, M., Tongiorgi, E., and Cattaneo, A. (2000). Brain-derived neurotrophic factor (BDNF) induces dendritic targeting of BDNF and tyrosine kinase B mRNAs in hippocampal neurons through a phosphatidylinositol-3 kinase-dependent pathway. J Neurosci 20, 3165-3174.

Robinson, T.E., and Kolb, B. (1999). Alterations in the morphology of dendrites and dendritic spines in the nucleus accumbens and prefrontal cortex following repeated treatment with amphetamine or cocaine. Eur J Neurosci 11, 1598-1604.

Ronesi, J.A., Collins, K.A., Hays, S.A., Tsai, N.P., Guo, W., Birnbaum, S.G., Hu, J.H., Worley, P.F., Gibson, J.R., and Huber, K.M. (2012). Disrupted Homer scaffolds mediate abnormal mGluR5 function in a mouse model of fragile X syndrome. Nat Neurosci 15, 431-440, S431.

Rudy, J.W., and O'Reilly, R.C. (1999). Contextual fear conditioning, conjunctive representations, pattern completion, and the hippocampus. Behav Neurosci 113, 867-880.

Rudy, J.W., Huff, N.C., and Matus-Amat, P. (2004). Understanding contextual fear conditioning: insights from a two-process model. Neurosci Biobehav Rev 28, 675-685.

Russo, S.J., Mazei-Robison, M.S., Ables, J.L., and Nestler, E.J. (2009). Neurotrophic factors and structural plasticity in addiction. Neuropharmacology 56 Suppl 1, 73-82.

Saarelainen, T., Hendolin, P., Lucas, G., Koponen, E., Sairanen, M., MacDonald, E., Agerman, K., Haapasalo, A., Nawa, H., Aloyz, R., et al. (2003). Activation of the TrkB neurotrophin receptor is induced by antidepressant drugs and is required for antidepressant-induced behavioral effects. J Neurosci 23, 349-357.

Sahin, M., Greer, P.L., Lin, M.Z., Poucher, H., Eberhart, J., Schmidt, S., Wright, T.M., Shamah, S.M., O'Connell, S., Cowan, C.W., Hu, L., Goldberg, J.L., Debant, A., Corfas, G., Krull, C.E., and Greenberg, M.E. (2005). Eph-dependent tyrosine phosphorylation of ephexin1 modulates growth cone collapse. Neuron 46, 191-204.

Sanes, J.R., and Lichtman, J.W. (1999). Development of the vertebrate neuromuscular junction. Annu Rev Neurosci 22, 389-442.

Saylor, A.J., and McGinty, J.F. (2008). Amphetamine-induced locomotion and gene expression are altered in BDNF heterozygous mice. Genes Brain Behav 7, 906-914.

Schratt, G.M., Tuebing, F., Nigh, E.A., Kane, C.G., Sabatini, M.E., Kiebler, M., and Greenberg, M.E. (2006). A brain-specific microRNA regulates dendritic spine development. Nature 439, 283-289.

Schuebel, K.E., Movilla, N., Rosa, J.L., and Bustelo, X.R. (1998). Phosphorylation-dependent and constitutive activation of Rho proteins by wild-type and oncogenic Vav-2. EMBO J 17, 6608-6621.

Schwechter, B., and Tolias, K.F. (2013). Cytoskeletal mechanisms for synaptic potentiation. Commun Integr Biol 6, e27343.

Senger, D.L., and Campenot, R.B. (1997). Rapid retrograde tyrosine phosphorylation of trkA and other proteins in rat sympathetic neurons in compartmented cultures. J Cell Biol 138, 411-421.

Servitja, J.M., Marinissen, M.J., Sodhi, A., Bustelo, X.R., and Gutkind, J.S. (2003). Rac1 function is required for Src-induced transformation. Evidence of a role for Tiam1 and Vav2 in Rac activation by Src. J Biol Chem 278, 34339-34346.

Shalizi, A., Gaudilliere, B., Yuan, Z., Stegmuller, J., Shirogane, T., Ge, Q., Tan, Y., Schulman, B., Harper, J.W., and Bonni, A. (2006). A calcium-regulated MEF2 sumoylation switch controls postsynaptic differentiation. Science 311, 1012-1017.

Shamah, S.M., Lin, M.Z., Goldberg, J.L., Estrach, S., Sahin, M., Hu, L., Bazalakova, M., Neve, R.L., Corfas, G., Debant, A., and Greenberg, M.E. (2001). EphA receptors regulate growth cone dynamics through the novel guanine nucleotide exchange factor ephexin. Cell 105, 233-244.

Shen, K., and Cowan, C.W. (2010). Guidance molecules in synapse formation and plasticity. Cold Spring Harb Perspect Biol 2:a001842.

Shiina, N., Shinkura, K., and Tokunaga, M. (2005). A novel RNA-binding protein in neuronal RNA granules: regulatory machinery for local translation. J Neurosci 25, 4420-4434.

Simsek-Duran, F., and Lonart, G. (2008). The role of RIM1alpha in BDNF-enhanced glutamate release. Neuropharmacology 55, 27-34.

Siomi, H., Choi, M., Siomi, M.C., Nussbaum, R.L., and Dreyfuss, G. (1994). Essential role for KH domains in RNA binding: impaired RNA binding by a mutation in the KH domain of FMR1 that causes fragile X syndrome. Cell 77, 33-39.

Smith, L.N., Jedynak, J.P., Fontenot, M.R., Hale, C.F., Dietz, K.C., Taniguchi, M., Thomas, F.S., Zirlin, B.C., Birnbaum, S.G., Huber, K.M., et al. (2014). Fragile x mental retardation protein regulates synaptic and behavioral plasticity to repeated cocaine administration. Neuron 82, 645-658.

Soliman, F., Glatt, C.E., Bath, K.G., Levita, L., Jones, R.M., Pattwell, S.S., Jing, D., Tottenham, N., Amso, D., Somerville, L.H., et al. (2010). A genetic variant BDNF polymorphism alters extinction learning in both mouse and human. Science 327, 863-866.

Sorkin, A., and Waters, C.M. (1993). Endocytosis of growth factor receptors. Bioessays 15, 375-382.

Stoppini, L., Buchs, P.A., and Muller, D. (1991). A simple method for organotypic cultures of nervous tissue. J Neurosci Methods 37, 173-182.

Suen, P.C., Wu, K., Levine, E.S., Mount, H.T., Xu, J.L., Lin, S.Y., and Black, I.B. (1997). Brain-derived neurotrophic factor rapidly enhances phosphorylation of the postsynaptic N-methyl-D-aspartate receptor subunit 1. Proc Natl Acad Sci U S A 94, 8191-8195.

Suzaki, Y., Yoshizumi, M., Kagami, S., Koyama, A.H., Taketani, Y., Houchi, H., Tsuchiya, K., Takeda, E., and Tamaki, T. (2002). Hydrogen peroxide stimulates c-Src-mediated big mitogen-activated protein kinase 1 (BMK1) and the MEF2C signaling pathway in PC12 cells: potential role in cell survival following oxidative insults. J Biol Chem 277, 9614-9621.

Tai, K., Kubota, M., Shiono, K., Tokutsu, H., and Suzuki, S.T. (2010). Adhesion properties and retinofugal expression of chicken protocadherin-19. Brain Res 1344, 13-24.

Takahashi, M., Shirakawa, O., Toyooka, K., Kitamura, N., Hashimoto, T., Maeda, K., Koizumi, S., Wakabayashi, K., Takahashi, H., Someya, T., et al.

(2000). Abnormal expression of brain-derived neurotrophic factor and its receptor in the corticolimbic system of schizophrenic patients. Mol Psychiatry 5, 293-300.

Takei, N., Kawamura, M., Hara, K., Yonezawa, K., and Nawa, H. (2001). Brain-derived neurotrophic factor enhances neuronal translation by activating multiple initiation processes: comparison with the effects of insulin. J Biol Chem 276, 42818-42825.

Takumi, Y., Ramirez-Leon, V., Laake, P., Rinvik, E., and Ottersen, O.P. (1999). Different modes of expression of AMPA and NMDA receptors in hippocampal synapses. Nat Neurosci 2, 618-624.

Tamas, P., Solti, Z., Bauer, P., Illes, A., Sipeki, S., Bauer, A., Farago, A., Downward, J., and Buday, L. (2003). Mechanism of epidermal growth factor regulation of Vav2, a guanine nucleotide exchange factor for Rac. J Biol Chem 278, 5163-5171.

Tanaka, J., Horiike, Y., Matsuzaki, M., Miyazaki, T., Ellis-Davies, G.C., and Kasai, H. (2008). Protein synthesis and neurotrophin-dependent structural plasticity of single dendritic spines. Science 319, 1683-1687.

Tashiro, A., and Yuste, R. (2004). Regulation of dendritic spine motility and stability by Rac1 and Rho kinase: evidence for two forms of spine motility. Mol Cell Neurosci 26, 429-440.

Tashiro, A., Minden, A., and Yuste, R. (2000). Regulation of dendritic spine morphology by the rho family of small GTPases: antagonistic roles of Rac and Rho. Cereb Cortex 10, 927-938.

Tebartz van Elst, L., Woermann, F., Lemieux, L., and Trimble, M.R. (2000). Increased amygdala volumes in female and depressed humans. A quantitative magnetic resonance imaging study. Neurosci Lett 281, 103-106.

Thompson Ray, M., Weickert, C.S., Wyatt, E., and Webster, M.J. (2011). Decreased BDNF, trkB-TK+ and GAD67 mRNA expression in the hippocampus of individuals with schizophrenia and mood disorders. J Psychiatry Neurosci 36, 195-203.

Tolias, K.F., Bikoff, J.B., Burette, A., Paradis, S., Harrar, D., Tavazoie, S., Weinberg, R.J., and Greenberg, M.E. (2005). The Rac1-GEF Tiam1

couples the NMDA receptor to the activity-dependent development of dendritic arbors and spines. Neuron 45, 525-538.

Tsai, N.P., Wilkerson, J.R., Guo, W., Maksimova, M.A., DeMartino, G.N., Cowan, C.W., and Huber, K.M. (2012). Multiple autism-linked genes mediate synapse elimination via proteasomal degradation of a synaptic scaffold PSD-95. Cell 151, 1581-1594.

Tsai, N.P., Wilkerson, J.R., Guo, W., Maksimova, M.A., DeMartino, G.N., Cowan, C.W., and Huber, K.M. (2012). Multiple autism-linked genes mediate synapse elimination via proteasomal degradation of a synaptic scaffold PSD-95. Cell 151, 1581-1594.

Turner, M., and Billadeau, D.D. (2002). VAV proteins as signal integrators for multi-subunit immune-recognition receptors. Nat Rev Immunol 2, 476-486.

Tyler, W.J., and Pozzo-Miller, L. (2003). Miniature synaptic transmission and BDNF modulate dendritic spine growth and form in rat CA1 neurones. J Physiol 553, 497-509.

Tyler, W.J., and Pozzo-Miller, L.D. (2001). BDNF enhances quantal neurotransmitter release and increases the number of docked vesicles at the active zones of hippocampal excitatory synapses. J Neurosci 21, 4249-4258.

Uutela, M., Lindholm, J., Louhivuori, V., Wei, H., Louhivuori, L.M., Pertovaara, A., Akerman, K., Castren, E., and Castren, M.L. (2012). Reduction of BDNF expression in Fmr1 knockout mice worsens cognitive deficits but improves hyperactivity and sensorimotor deficits. Genes Brain Behav 11, 513-523.

Valdez, G., Akmentin, W., Philippidou, P., Kuruvilla, R., Ginty, D.D., and Halegoua, S. (2005). Pincher-mediated macroendocytosis underlies retrograde signaling by neurotrophin receptors. J Neurosci 25, 5236-5247.

Van Dam, D., D'Hooge, R., Hauben, E., Reyniers, E., Gantois, I., Bakker, C.E., Oostra, B.A., Kooy, R.F., and De Deyn, P.P. (2000). Spatial learning, contextual fear conditioning and conditioned emotional response in Fmr1 knockout mice. Behav Brain Res 117, 127-136.

Verdin, E., Dequiedt, F., and Kasler, H.G. (2003). Class II histone deacetylases: versatile regulators. Trends Genet 19, 286-293.

Wang, A.H., and Yang, X.J. (2001). Histone deacetylase 4 possesses intrinsic nuclear import and export signals. Mol Cell Biol 21, 5992-6005.

Wang, Y.T., and Salter, M.W. (1994). Regulation of NMDA receptors by tyrosine kinases and phosphatases. Nature 369, 233-235.

Weickert, C.S., Hyde, T.M., Lipska, B.K., Herman, M.M., Weinberger, D.R., and Kleinman, J.E. (2003). Reduced brain-derived neurotrophic factor in prefrontal cortex of patients with schizophrenia. Mol Psychiatry 8, 592-610.

West, A.G., Shore, P., and Sharrocks, A.D. (1997). DNA binding by MADS-box transcription factors: a molecular mechanism for differential DNA bending. Mol Cell Biol 17, 2876-2887.

Wiens, K.M., Lin, H., and Liao, D. (2005). Rac1 induces the clustering of AMPA receptors during spinogenesis. J Neurosci 25, 10627-10636.

Wilkerson, J.R., Tsai, N.P., Maksimova, M.A., Wu, H., Cabalo, N.P., Loerwald, K.W., Dictenberg, J.B., Gibson, J.R., and Huber, K.M. (2014). A Role for Dendritic mGluR5-Mediated Local Translation of Arc/Arg3.1 in MEF2-Dependent Synapse Elimination. Cell Rep.

Xie, Z., Srivastava, D.P., Photowala, H., Kai, L., Cahill, M.E., Woolfrey, K.M., Shum, C.Y., Surmeier, D.J., and Penzes, P. (2007). Kalirin-7 controls activity-dependent structural and functional plasticity of dendritic spines. Neuron 56, 640-656.

Yan, Q.J., Rammal, M., Tranfaglia, M., and Bauchwitz, R.P. (2005). Suppression of two major Fragile X Syndrome mouse model phenotypes by the mGluR5 antagonist MPEP. Neuropharmacology 49, 1053-1066.

Yang, Y., Wang, X.B., Frerking, M., and Zhou, Q. (2008). Spine expansion and stabilization associated with long-term potentiation. J Neurosci 28, 5740-5751.

Yasuda, S., Sugiura, H., Tanaka, H., Takigami, S., and Yamagata, K. (2011). p38 MAP kinase inhibitors as potential therapeutic drugs for neural diseases. Cent Nerv Syst Agents Med Chem 11, 45-59.

Yasuda, S., Tanaka, H., Sugiura, H., Okamura, K., Sakaguchi, T., Tran, U., Takemiya, T., Mizoguchi, A., Yagita, Y., Sakurai, T., et al. (2007). Activity-induced protocadherin arcadlin regulates dendritic spine number by triggering N-cadherin endocytosis via TAO2beta and p38 MAP kinases. Neuron 56, 456-471.

Yin, Y., Edelman, G.M., and Vanderklish, P.W. (2002). The brain-derived neurotrophic factor enhances synthesis of Arc in synaptoneurosomes. Proc Natl Acad Sci U S A 99, 2368-2373.

Ying, S.W., Futter, M., Rosenblum, K., Webber, M.J., Hunt, S.P., Bliss, T.V., and Bramham, C.R. (2002). Brain-derived neurotrophic factor induces long-term potentiation in intact adult hippocampus: requirement for ERK activation coupled to CREB and upregulation of Arc synthesis. J Neurosci 22, 1532-1540.

Yu, Y.T., Breitbart, R.E., Smoot, L.B., Lee, Y., Mahdavi, V., and Nadal-Ginard, B. (1992). Human myocyte-specific enhancer factor 2 comprises a group of tissue-restricted MADS box transcription factors. Genes Dev 6, 1783-1798.

Yuste, R., and Bonhoeffer, T. (2001). Morphological changes in dendritic spines associated with long-term synaptic plasticity. Annu Rev Neurosci 24, 1071-1089.

Zeitelhofer, M., Karra, D., Macchi, P., Tolino, M., Thomas, S., Schwarz, M., Kiebler, M., and Dahm, R. (2008). Dynamic interaction between P-bodies and transport ribonucleoprotein particles in dendrites of mature hippocampal neurons. J Neurosci 28, 7555-7562.

Zeng, L., Sachdev, P., Yan, L., Chan, J.L., Trenkle, T., McClelland, M., Welsh, J., and Wang, L.H. (2000). Vav3 mediates receptor protein tyrosine kinase signaling, regulates GTPase activity, modulates cell morphology, and induces cell transformation. Mol Cell Biol 20, 9212-9224.

Zhang, Y., Sawada, T., Jing, X., Yokote, H., Yan, X., and Sakaguchi, K. (2007). Regulation of ephexin1, a guanine nucleotide exchange factor of Rho family GTPases, by fibroblast growth factor receptor-mediated tyrosine phosphorylation. J Biol Chem 282, 31103-31112.

Zhang, C.L., McKinsey, T.A., and Olson, E.N. (2001). The transcriptional corepressor MITR is a signal-responsive inhibitor of myogenesis. Proc Natl Acad Sci U S A 98, 7354-7359.

Zhang, C.L., McKinsey, T.A., and Olson, E.N. (2002). Association of class II histone deacetylases with heterochromatin protein 1: potential role for histone methylation in control of muscle differentiation. Mol Cell Biol 22, 7302-7312.

Zhao, X., Ito, A., Kane, C.D., Liao, T.S., Bolger, T.A., Lemrow, S.M., Means, A.R., and Yao, T.P. (2001). The modular nature of histone deacetylase HDAC4 confers phosphorylation-dependent intracellular trafficking. J Biol Chem 276, 35042-35048.

Zhou, P., Porcionatto, M., Pilapil, M., Chen, Y., Choi, Y., Tolias, K.F., Bikoff, J.B., Hong, E.J., Greenberg, M.E., and Segal, R.A. (2007). Polarized signaling endosomes coordinate BDNF-induced chemotaxis of cerebellar precursors. Neuron 55, 53-68.

Zhu, B., and Gulick, T. (2004). Phosphorylation and alternative pre-mRNA splicing converge to regulate myocyte enhancer factor 2C activity. Mol Cell Biol 24, 8264-8275.

Zuo, Y., Yang, G., Kwon, E., and Gan, W.B. (2005). Long-term sensory deprivation prevents dendritic spine loss in primary somatosensory cortex. Nature 436, 261-265.

Zweier, M., and Rauch, A. (2012). The MEF2C-Related and 5q14.3q15 Microdeletion Syndrome. Mol Syndromol 2, 164-170.

Zweier, M., Gregor, A., Zweier, C., Engels, H., Sticht, H., Wohlleber, E., Bijlsma, E.K., Holder, S.E., Zenker, M., Rossier, E., et al. (2010). Mutations in MEF2C from the 5q14.3q15 microdeletion syndrome region are a frequent cause of severe mental retardation and diminish MECP2 and CDKL5 expression. Hum Mutat 31, 722-733.